DYSREGULATION of PROTEIN QUALITY CONTROL IMPAIRS FUNCTION of PRIMARY CARDIOMYOCYTES

A Dissertation
Submitted to
the Temple University Graduate Board

In Partial Fulfillment
of the Requirements for the Degree
DOCTOR OF PHILOSOPHY
OF BIOENGINEERING

by
Farzaneh Ghasemi Tahrir
August 2018

Examining Committee Members:

Dr. Kamel Khalili, Department of Neuroscience, Center for Neurovirology, Temple University
Dr. Peter I. Lelkes, Department of Bioengineering, Temple University
Dr. Cezary Marcinkiewicz, Department of Bioengineering, Temple University
Dr. Evangelia Bellas, Department of Bioengineering, Temple University
Dr. Ilker K. Sariyer, Department of Neuroscience, Center for Neurovirology, Temple University

ABSTRACT

Mitochondria provide the main energy required for cardiac excitation-contraction coupling via aerobic oxidative phosphorylation (OXPHOS) process. Accumulation of reactive oxygen species (ROS), by-products of mitochondrial respiration, within dysfunctional mitochondria results in the activation of cardiac cell death pathways and has been associated with heart failure development. Therefore, maintaining mitochondrial homeostasis as a balance between mitochondrial biogenesis and degradation is of great importance toward cardiac proper functioning. In addition to the importance of mitochondrial energy supply, gap junctions, intercellular channels which connect plasma membrane of adjacent cardiomyocytes, by propagating action potential throughout the myocardium maintain cardiac synchronous beating and rhythm. Gap junctions have a rapid turnover and impair of gap junction quality control impacts cell-to-cell communication; resulting in electrical conduction abnormalities and arrhythmogenesis. Therefore, understanding the underlying mechanism the quality control of mitochondria and gap junctions profoundly contributes toward understating the genesis of cardiomyopathy. Furthermore, cardiovascular problems in HIV (Human immunodeficiency virus) positive patients whose viral load is controlled via antiretroviral therapy remains a problem while the underlying mechanism remains elusive. The current study has used an *in vitro* model of primary neonatal rat ventricular cardiomyocytes (NRVCs) to discover the molecular mechanisms of mitochondrial as well as gap junction quality control under normal and stress conditions. Furthermore, electrical activities of the primary cardiomyocytes were recorded using microelectrode array (MEA) system and important electrophysiological components such as impulse propagation pattern and

conduction velocity were extracted from the complex signal recordings. Overall, we have pursued four main aims; Aim 1. Dysregulation of mitochondrial quality control machinery leads to cardiac death; Aim 2. HIV-1 Tat (transcriptional transactivator) dysregulates cardiac homeostasis via mitochondrial pathway; Aim 3. Impairment of protein quality control impacts the quality of gap junction; Aim 4. Inhibition of gap junction quality dysregulates electrical signal propagation within the culture.

STATEMENT OF SIGNIFICANCE

Cardiovascular problems are the leading cause of morbidity and mortality as they contribute to the human death of more than 610,000 in the United States every year. Despite controlling the viral load via antiretroviral therapies, patients infected by Human Immunodeficiency Virus-1 (HIV-1) carry a high risk of cardiac complications such as hypertrophy, vasculopathy and valvular heart disease. Furthermore, the current antiretroviral therapies may even lead to the development of other cardiovascular complications such as ischemic heart disease. Therefore, understanding the precise mechanisms and key molecular players underlying heart diseases contributes toward development of more effective clinical therapies for cardiac complications emerged either under HIV infection or other cardiac stress conditions such as ischemia/reperfusion in case of cardiopulmonary bypass. Genetic or pharmacologic modulation of these molecular players plays an important role in switching the stress-activated pathways toward cardioprotective pathways. Considering the role of mitochondria in supplying more than 90% of energy required for cardiac excitation-contraction coupling as well as the role of gap junctions in regulating cell-to-cell communication in the myocardium, dysregulation of their quality has been associated with development of various cardiovascular problems and heart failure. Therefore, this study investigates the underlying mechanisms and key molecular players regulating the function of mitochondria and gap junctions in primary cardiomyocytes.

DEDICATION

To my mom and dad for all their sacrifices

and

To my dear Taha for always being there for me

ACKNOWLEDGEMENTS

Last, but not least, I would like to thank my beloved husband, loving parents, my dearest sister and brothers for all the good times in my life. Their endless love and unconditional support has always encouraged me to reach my dreams.

TABLE OF CONTENTS:

LIST OF FIGURES

CHAPTER 1

LITERATURE REVIEW AND SUMMARY OF SPECIFIC AIMS

Abstract

Mitochondria are dynamic organelles and are highly abundant in cardiomyocytes. By supplying the major energy required for cardiac excitation-contraction coupling as well as controlling the key intracellular survival and death pathways, mitochondria play an important role in maintaining cardiac homeostasis and proper functioning. Healthy mitochondria generate ATP molecules through an aerobic process known as oxidative phosphorylation (OXPHOS). Mitochondrial injury under myocardial infarction impairs OXPHOS and results in the excessive production of reactive oxygen species (ROS), bioenergetics insufficiency and contributes toward development of cardiovascular problems. Therefore, presence of proper mitochondrial quality control machinery which removes unhealthy mitochondria along with mitochondrial biogenesis is pivotal for mitochondrial homeostasis and cardiac health. Upon damage to mitochondrial network, mitochondrial quality control components are employed to segregate the unhealthy mitochondria or mitochondrial proteins for further degradation and elimination. Impair of mitochondrial quality control and accumulation of abnormal mitochondria have been reported in pathogenesis of various cardiac problems and heart failure. This review provides an overview of recent studies describing various mechanistic pathways underlying the mitochondrial homeostasis with the main focus on cardiac cells. In addition, this review demonstrates the potential role of mitochondrial quality control dysregulation in development of cardiovascular disease.

Keywords: Mitochondrial quality control, Mitophagy, Proteasome, Cardiomyopathy, BAG3, Ischemia/Reperfusion Injury. Fission, Fusion

Introduction

Mitochondria by generating energy and controlling key signaling of cell death play an important role in maintaining cellular homeostasis and mitochondrial disorders have been associated with the development of a large number of cardiovascular diseases such as atherosclerosis, ischemic heart disease, cardiac hypertrophy and heart failure [Chistiakov et al., 2017]. Mitochondria synthesize a large amount of energy via oxidation of carbohydrates, fats and amino acids through oxidative phosphorylation (OXPHOS) respiratory chain in which electron transport chain across the mitochondrial inner membrane results in the reduction of oxygen and subsequent production of ATP molecules [Narendra et al., 2011, Koene et al., 2009, Joncheere et al., 2012]. Patients with mitochondrial defects show deficiencies in ATP synthesis and energy metabolism [Koene et al., 2009]. Considering the high energy demand of cardiac excitation-contraction cycle and the role of OXPHOS in supplying the highest energy of cardiac muscle, patients with mitochondrial abnormalities carry a high risk of heart disease development which is a leading cause of mortality in those patients [Holmgren et al., 2003, Rosca et al., 2013]. For example, hypertrophic cardiomyopathy was found in children with cytochrome *c* deficiency which led to their death before the age of 13 years [Holmgren et al., 2003].

Dysfunctional mitochondria have diminished capacity for ATP synthesis and generate excessive amounts of ROS. ROS are highly reactive by-products of mitochondrial respiration and their accumulation within the cells damages cellular components such as DNA, carbohydrates, proteins and lipids leading to aging acceleration and cell death [Narendra et al., 2011, Koene et al., 2011]. Considering the abundance of mitochondria in cardiac muscle, elevated levels of ROS results in chronic oxidative damage and contributes toward development of cardiovascular disease and potentially heart failure

[Drummomd et al., 2011, Billia et al., 2011]. In this regard, mitochondrial quality control machinery which targets the unhealthy mitochondria or mitochondrial proteins for degradation and removal plays a vital role toward maintaining myocardial homeostasis [Chistiakov et al., 2017]. Accumulation of abnormal, enlarged mitochondria has been reported in myocardial tissue of patients with hypertrophic and dilated cardiomyopathy [Holmgren et al., 2003, Rosca et al., 2013].

The quality of mitochondria is ensured via different intracellular pathways. Degradation of mitochondrial damaged proteins usually occurs via ubiquitin-proteasome system (UPS); whereas under chronic pathological condition whole mitochondrion is degraded by autophagy-lysosome [Hammerling et al., 2014]. In these two pathways, substrates are covalently conjugated with a small protein known as ubiquitin in an ubiquitination process mediated by ubiquitin-handling enzymes and targeted for further degradation and removal either by proteasome or lysosome [Bragoszewski et al., 2017]. Impair of mitochondrial quality control components has been associated with contractile dysfunction and cardiovascular disease [Nakai et al., 2007]. Within this review, we describe recent discoveries about the mechanisms underlying the quality control of mitochondria in cardiac cells. Furthermore, we discuss how impairment in the function of mitochondrial quality control components may impact cardiac homeostasis leading to development of cardiovascular complications.

Mitochondrial metabolism in heart

OXPHOS is an aerobic metabolic pathway in which electrons are transferred through an electron transport chain (ETC) along with the mitochondrial inner membrane to reduce oxygen into water molecules and simultaneously protons are pumped into intermembrane space against their concentration gradient (ΔpH_m) [Perry et al., 2011, Koene et al., 2009]. The movement of electrons in this respiratory chain creates a

negative charge inside the mitochondrial matrix known as mitochondrial membrane potential ($\Delta\Psi_m$) [Logan et al., 2016]. Then by F1/F0 ATPase, complex V, protons move down their electrochemical gradient ($\Delta\Psi_m$ and ΔpH_m) into the matrix resulting in the synthesis of ATP molecules [Holmgren et al., 2003, Perry et al., 2011, Jonckeere et al., 2012]. Alterations in mitochondrial respiratory chain have been associated with development of cardiovascular disorders which can potentially advance to heart failure [Doenst et al., 2013]. For example, mitochondrial ETC defects have been implicated in the pathogenesis of diabetic cardiomyopathy in patients with diabetes mellitus [Berthiaume et al., 2017]. Furthermore, oxidative stress as a consequence of respiratory chain dysfunction is accompanied with development of cardiac hypertrophy [Maulik et al., 2012].

$\Delta\Psi_m$ functions as a crucial driving force for ATP synthesis. Considering the abundance of mitochondria in the heart and role of mitochondria in supplying the major ATP requiredfor excitation-contraction coupling of cardiac cells [Griffiths et al., 2009], therefore $\Delta\Psi_m$ serves as an important indicator of cardiomyocyte health [Logan et al., 2016]. Pathological stress damaging mitochondria results in $\Delta\Psi_m$ collapse and energetic deficit leading to activation of cell death pathways and potential cardiovascular problems [Perry et al., 2011, Jonckeere et al., 2012, Kuzmicic et al., 2011]. The extent of mitochondrial damage has been reported as a key determinant factor of myocardial injury under ischemia-reperfusion toward progression to heart failure [Doenst et al., 2013, Niemann et al., 2017]. Ischemia-reperfusion injury as a consequence of coronary heart disease dramatically increases mitochondrial permeability leading to dissipation of electron and proton gradients, dysregulation of mitochondrial calcium homeostasis and release of superoxide and apoptosis inducing factors which give rise to myocardial cell death [Kang et al., 2017, Lesnefsky et al., 2017, Zhang et al., 2018]. Furthermore,

mitochondrial super complexes lose their integrity as ETC subunits degrade under IR which leads to impair of mitochondrial metabolism and enhanced ROS generation [Jang et al., 2017, Sepuri et al., 2017] (Figure 1.1).
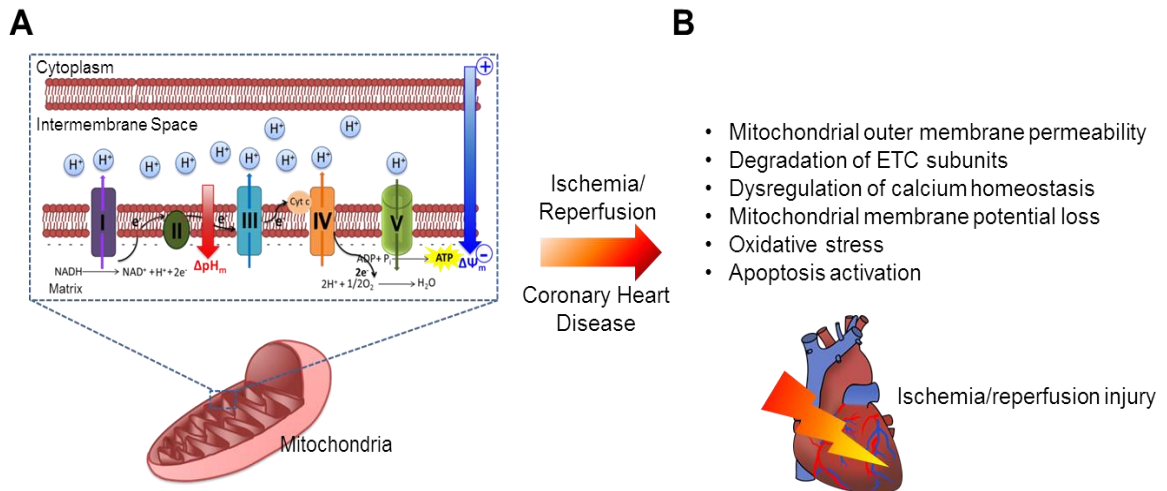
Figure 1.1. Schematic of mitochondrial oxidative phosphorylation process. (A) Movement of electrons through the complexes embedded in mitochondrial inner membrane creates an electrical gradient ($\Delta\Psi_m$) and simultaneously protons are pumped into the intermembrane space creating a proton gradient (ΔpH_m). Electrical and proton gradients together create an electrochemical motive force leading to the synthesis of ATP by F_1/F_0 ATP-synthase. **(B)** Ischemia/reperfusion damages mitochondrial respiration and leads to myocardial injury.

Mitochondrial dynamism in heart

Mitochondria account for over 30% of myocardial mass [Chen et al., 2011]. In neonatal cardiomyocytes, mitochondria are located throughout the cytosol; whereas in adult heart, mitochondria are arranged within three subpopulations of subsarcolemmal, myofibrillarand perinuclear mitochondria [Ong et al., 2017]. Upon damage to mitochondrial network, mitochondria undergo structural and functional remodeling to replenish the damaged mtDNA and dysfunctional units [Gegg et al., 2011, Niemann et al., 2017]. To this end, mitochondria undergo fission and divide into two daughter mitochondria, one with increased $\Delta\Psi_m$ and high fusion affinity while the other one bears

diminished $\Delta\Psi_m$ and low fusion affinity [Ashrafi et al., 2013]. The damaged units with major loss of functionality are then targeted by mitochondrial quality control machinery for degradation and clearance; while the bioenergetically active units go under further regeneration and repair to maintain membrane potential [Narendra et al., 2011, Song et al., 2015].

Fission and fusion proteins function in a network to maintain mitochondrial homeostasis and play an important role in regulating cardiac response under pathological conditions such as ischemia-reperfusion, cardiomyopathy and heart failure [Kuzmicic et al., 2011]. Alterations of mitochondrial dynamic play a key role in pathophysiology of various cardiac complications [Niemann et al., 2017]. Mice with deficiency of fission protein, Drp1 (Dynamin-related protein 1), indicated lethal dilated cardiomyopathy with ventricular wall thinning and reduced ejection fraction [Song et al., 2015]. Drp1 is highly expressed in the heart, upregulates under stress [Chan et al., 2011] and translocates from cytosol to the outer mitochondrial membrane to regulate mitochondrial dynamism [Ikeda et al., 2015]. Drp1 deletion led to the mitochondrial enlargement and excessive activation of mitophagy machinery [Song et al., 2015, Song et al., 2015]; and Drp1-deleted mice developed heart failure 6 to 7 weeks after deletion [Song et al., 2015]. Mitochondrial fission by promoting autophagic degradation of damaged mitochondria plays a protective role; however, excessive fission leads to mitochondrial mass loss, ATP deficit and apoptosis activation [Zhou et al., 2017, Jin et al., 2018]. Drp1 functions with the Bcl-2 family proteins, BAX and BAK, and promotes mitochondrial fragmentation, mitochondrial outer membrane permeabilization and cytochrome *c* release in response to apoptosis stimulation [Große et al., 2016]. Inhibition of Drp1 by hindering excessive fission at the onset of reperfusion, maintained mitochondrial integrity and played a cardiprotective role under cardiac stress circumstances such as IR and cardiac arrest in

cell [Ong et al., 2010, Sharp et al., 2014], murine [Ong et al., 2010, Sharp et al., 2015] and rat models [Tian et al., 2017, Disatnik et al., 2013]. Furthermore, reducing the levels of mitochondrial fission factor, Mff, under hypoxia/reoxygenation resulted in enhanced mitochondrial homeostasis as mitochondrial membrane potential loss was recovered and apoptosis induction reduced [Jin et al., 2018].

Mitochondrial fusion proteins, Mfn1 and Mfn2, reside on the outer mitochondrial membrane and ensure health of mitochondrial network by regulating fusion process [Ikeda et al., 2015]. Considering the enormous amount of energy required for myocardial contractility, presence of a fused mitochondrial network is of great importance toward cardiac proper functioning [Kuzmicic et al., 2011]. In neonatal cardiac cells, mitochondria are mobile; whereas, in adult cardiac cells mitochondria are relatively static and have limited motility [Ong et al., 2017]. Fission and fusion occurrence in post mitotic myocytes of adult hearts remains controversial; however these proteins are essential for mitochondria to adjust their metabolism to meet the energy demands of cardiac muscle and their disruption causes cardiovascular complications [Chen et al., 2011, Song et al., 2015]. Suppression of fusion proteins in Drosophila model led to dilated cardiomyopathy as well as contractile abnormality [Dorn et al., 2011]. Deletion of fusion proteins, Mfn1/Mfn2, in mice heart resulted in abnormal mitochondrial morphology and mitochondrial fragmentation leading to ventricular wall thickening and increase in cardiac mass (>30%) accompanied with the symptoms of eccentric hypertrophy [Song et al., 2015].

Mitochondrial quality control in heart

Autophagy-lysosome and ubiquitin-proteasome system (UPS) are two major proteolytic machineries which degrade intracellular substrates to maintain protein homeostasis [Minoia et al., 2014]. Deficiency or dysregulation of protein quality control pathways have

been implicated in muscle degeneration in dystrophic patients [Wattin et al., 2018]. Clearance of misfolded proteins mostly occurs by UPS, while protein aggregates and damaged organelles degrade mostly by autophagy pathway [Liu et al., 2013]. Mitochondrial damaged proteins degrade via UPS; while elimination of entire mitochondrion under chronic stress selectively occurs via mitochondrial autophagy known as mitophagy [Hammerling et al., 2014]. Failure in the function of mitochondrial quality control machinery has been described in pathogenesis of heart failure [Doenst et al., 2013].

Mitochondrial degradation via proteasome

Degradation of mitochondrial damaged proteins mostly occurs via proteasome. UPS components are localized on mitochondria and are key regulators of mitochondrial dynamism. Inhibition of proteasome activity can cause mitochondrial function abnormalities [Bragoszewski et al., 2017]. For this purpose, damaged proteins are tagged with ubiquitin protein through the action of an E1 ubiquitin-activating enzyme, an E2 ubiquitin-conjugating enzyme, and an E3 ubiquitin ligase and targeted for elimination via the proteasome [Ciechanover et al., 2017]. Accumulation of poly-ubiquitinated substrates has been observed in heart tissue of patients with cardiac manifestations such as cardiomyopathy and heart failure [Nishida et al., 2017]. Furthermore, impair of UPS function has been detected in heart tissues of patients with hypertrophic cardiomyopathy and human failing hearts; while no changes in protein content of the UPS subunits were detected in those patients [Predmore et al., 2009]. Enhancement of cardiac proteasome proteolytic function has been demonstrated to play a protective role against pathophysiology of proteinopathy and ischemia-reperfusion injury in mice [Li et al., 2011].

Proteasome-dependent degradation is an important pathway for the quality control of mitochondrial fission and fusion proteins [Bragoszewski et al., 2017]. In this regard, parkin-mediated degradation of mitochondrial proteins via proteasome has been reported in several research studies [Chan et al., 2011, Yoshii et al., 2011]. Upon mitochondrial membrane potential loss, parkin translocates to mitochondria, ubiquitinates mitochondrial outer membrane proteins [Narendra et al., 2008, Bragoszewski et al., 2017], and by recruiting proteasome components to mitochondria activates UPS [Chan et al., 2011, Hammerling et al., 2014]. For example, fission protein, Drp1, was indicated to be ubiquitinated by Parkin and targeted for degradation through proteasome in neurons. Parkin suppression resulted in the accumulation of Drp1 and mitochondrial fragmentation [Wang et al., 2011]. However, fewer studies have been performed regarding the role of proteasome in degradation of mitochondrial proteins in cardiac cells.

Autophagy-lysosome and UPS pathways have been reported to be interrelated; such that inhibition of proteasome activity leads to activation of autophagy-lysosome pathway [Liu et al., 2013, Tahrir et al., 2017]. Under pressure overload, inhibition of proteasome activity by preventing cardiac remodeling played a protective role and inhibited heart failure progression in mice model [Hedhi et al., 2009]. In addition, proteasome inhibition reduced the size of myocardial infarction after reperfusion injury [Pye et al., 2003]. However, whether protective effects of proteasome inhibition under stress conditions arise from activation of autophagy-lysosome remains to be determined.

Mitochondrial degradation via mitophagy

Autophagy is a catabolism mechanism which by degrading non-essential or dysfunctional cytoplasmic constituents preserves cellular ATP level and allows cells to survive longer under adverse nutritional condition [Yoshii et al., 2011, Zhang et al.,

2014]. Under pathological conditions cells protect themselves by activating survival pathways such as autophagy; however, chronic pathological conditions trigger apoptotic and necrotic pathways [Scherz-Shouval et al., 2007]. Autophagy upregulation in mouse atrial HL-1 cardiomyocytes and human AC16 cells under mitochondrial stress restored $\Delta\Psi_m$ and mitochondrial respiration [Dutta et al., 2013]. Mitochondrial autophagy is selective degradation of mitochondria via autophagy which is known as mitophagy. In this process, defective mitochondria are marked with ubiquitin chains and engulfed into double-layered vesicles, autophagosomes, and ultimately delivered to lysosome for further degradation and removal [Padman et al., 2013, Yoshii et al., 2011, Matsuda et al., 2015]. Accumulation of damaged mitochondria when mitophagy is impaired is associated with oxidative stress, reduced respiration and death activation in cardiomyocytes [Tahrir et al., 2018]. Mitophagy-mediated degradation of mitochondria has been extensively studied in cardiac cells; suggesting the importance of mitophagy pathway in maintaining mitochondrial quality control in the heart [Song et al., 2015, Chen et al., 2013, McWilliams et al., 2018]. Various mechanisms of mitophagy-mediated degradation of mitochondria in cardiac cells are overviewed below.

Parkin-mediated mitophagy

Parkin gene encodes an E3 ubiquitin ligase composed of 465 amino acids [Truban et al., 2017]. Parkin through interaction with E2 ubiquitin-conjugating enzymes promotes ubiquitination of mitochondrial proteins and targets them for degradation and removal [Chan et al., 2011, Lee et al., 2010]. Parkin translocation to mitochondria is pink1 (PTEN-induced putative kinase 1) dependent [Vives-Bauza et al., 2010]; such that PINK1 promotes phosphorylation events on depolarized mitochondria and phosphorylation acts as a signal for Parkin recruitment and subsequent ubiquitination [Chen et al., 2013, Lazarou et al., 2015, Kane et al., 2014, Kazlauskaite et al., 2014,

Koyano et al., 2014]. Ubiquitination then allows for binding of mitophagy proteins such as p62/SQSTM1 and LC3 followed by cargo sequestration within autophagosome and elimination of dysfunctional mitochondria via lysosome [Hammerling et al., 2014, Narendra et al., 2011, Gegg et al., 2011]. Parkin deficiency in mice did not alter mitochondrial respiration or cardiac function under basal condition; suggesting that Parkin-mediated mitophagy may not be essential for cardiac function [Kubli et al., 2013, Song et al., 2015]. However, parkin-deficient hearts indicated declined cardiac function and larger infarct size compare to control mice after myocardial infarction [Kubli et al., 2013]. Parkin-mediated mitophagy by maintaining mitochondrial homeostasis prevented heart failure progression in mice with transverse aortic constriction (TAC) [Wang et al., 2018] and in rats with injured hearts post MI [Qiao et al., 2018].

Mitochondrial outer membrane protein, Mfn2 functions as a substrate for Pink1 phosphorylation and phosphorylated Mfn2 is ubiquitinated by Parkin and subsequently mitophagy is activated [Chen et al., 2013]. Mutated Mfn2 lacking Pink1 phosphorylation site inhibited recruitment of Parkin to depolarized mitochondria and activation of mitophagy in mouse hearts [Gong et al., 2015]. Mfn2 deletion in mouse hearts inhibited Parkin-mediated mitophagy [Song et al., 2014] and caused mitochondrial enlargement with impaired respiration [Chen et al., 2013] and higher ROS production; leading to heart failure development [Song et al., 2014]. Mfn2 deficiency in mouse cardiac myocytes inhibited Parkin translocation to mitochondria and reduced ubiquitination when mitochondria were depolarized. Furthermore, Mitophagy activation and p62 recruitment reduced in Mfn2-deficient mouse cardiomyocytes in response to mitochondrial damage [Chen et al., 2013] (Figure 1.2). Additionally, Mfn1/Mfn2 deficiency in mouse hearts led to mitochondrial fragmentation and mitochondrial morphology abnormalities without mitophagy activation [Song et al., 2015] followed by lethal cardiomyopathy and heart

failure progression by 7 to 8 weeks of age [Chen et al., 2011]. However, Mfn1 deficiency did not impair Parkin translocation and mitochondrial ubiquitination [Chen et al., 2013].
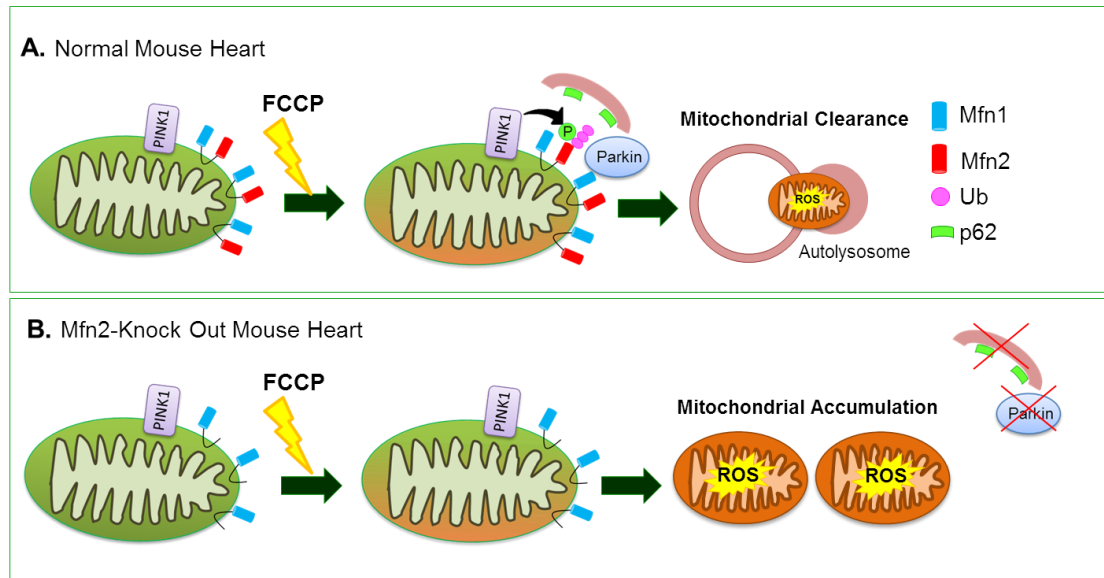
Figure 1.2. Mfn2 functions as a substrate for Parkin ubiquitination in mitophagy process. **(A)** Parkin ubiquitinates Mfn2 in a PINK1-dependent manner in depolarized cardiac myocytes. **(B)** Mfn2 ablation inhibited Parkin translocation and recruitment of p62 to depolarized mitochondria; leading to mitophagy impairment and accumulation of damaged mitochondria.

In drosophila model, Parkin-deleted hearts were detected with the accumulation of enlarged, depolarized mitochondria with abnormal morphology and high ROS content which advanced to development of dilated cardiomyopathy [Bhandari et al., 2014] (Figure 1.3A). Furthermore, Mitofusin ortholog, MARF (mitochondrial assembly regulatory factor), deficiency in drosophila heart resulted in enhanced levels of ROS and mitochondrial depolarization leading to development of dilated cardiomyopathy [Bhandari et al., 2014]. Interestingly, MARF knockout in Parkin-deficient drosophila hearts rescued cardiomyopathy by correcting heart tube contraction and mitochondrial dysfunction; whereas mitochondrial dysmorphology was not normalized [Bhandari et al., 2014] (Figure 1.3B). Parkin deficiency impairs mitophagy and presence of fusion proteins may lead to contamination of healthy mitochondria with the unhealthy ones;

while simultaneous suppression of Parkin and fusion proteins prevents that event [Bhandari et al., 2014].

In mice undergoing pressure overload, mitophagy was upregulated in a Drp1-dependent manner. Prolonged pressure overload led to mitophagy suppression and heart failure development [Shirakabe et al., 2016]. Deficiency of cardiac Drp1 impaired mitochondrial degradation and resulted in the accumulation of enlarged mitochondria surrounded in vacuolar compartments, impaired mitochondrial respiration and development of lethal cardiomyopathy in mice [Kageyama et al., 2014]. Parkin deletion led to increased levels of Drp1 and simultaneous deficiency of Drp1 and Parkin exacerbated cardiomyopathy [Kageyama et al., 2014]. Controversial results were published by another group; demonstrating that Parkin deficiency rescued Drp1 ablation effect in adult mouse hearts by improving cardiac function and survival [Song et al., 2015]. They demonstrated that Drp1 deficiency led to Parkin upregulation and elevated mitophagy resulting in mitochondrial mass loss and lethal cardiomyopathy. Therefore, simultaneous deficiency of Parkin and Drp1 reduced mitophagy and ventricular remodeling and improved cardiac contractility and diminished cardiac myocyte necrosis [Song et al., 2015].

However, whether dysregulation of cardiac function under pathological conditions such as ischemia/reperfusion occurs via direct effect on cardiomyocytes or impairing the function of neighboring cells such as endothelial cells may contribute toward pathogenesis of cardiomyocyte complications remains elusive. Recent study in mouse hearts has described that excessive Drp1-mediated fission and subsequent Parkin-mediated mitophagy triggers endothelial cell death pathways; leading to microvascular injury and barrier permeability under reperfusion injury [Zhou et al., 2017]. Suppression of Drp1-meditade mitochondrial fission inhibited apoptosis and protected cardiac microvascular system [Zhou et al., 2017].
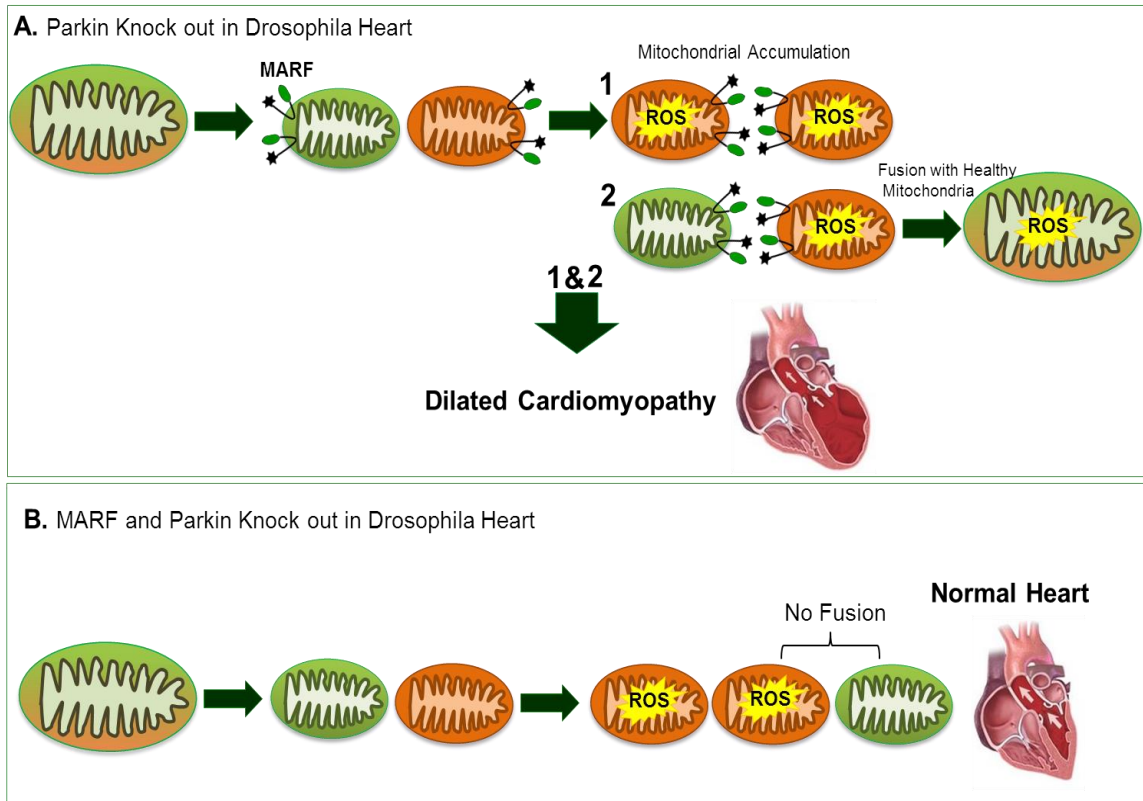
Figure 1.3. Parkin-mediated mitophagy in drosophila heart. (A) Parkin deficiency in drosophila heart impaired mitophagy and led to development of dilated cardiomyopathy. **(B)** Simultaneous deletion of MARF and Parkin rescued cardiomyopathy.

Receptor-mediated mitophagy

Mitophagy receptors such as Bnip3l, BCL2/adenovirus E1B, also known as Nix (Nip3-like protein X), and FUNDC1 (FUN14 domain containing 1) reside on mitochondrial outer membrane and by regulating mitophgay pathway play an important role under I/R [Hammerling et al., 2014, Nishida et al., 2017, Yuan et al., 2017]. FUNDC1 is highly expressed in the heart and mediates mitochondrial fragmentation and mitophagy under hypoxia [Liu et al., 2012, Zhang et al., 2017]. FUNDC1 interacts with LC3 on autophagosome membrane and impair of LC3-interacting domain of FUNDC1 impairs mitophagy [Liu et al., 2012]. Under cardiac I/R, activation of FUNDC1-mediated mitophagy during ischemia blocks apoptosis; whereas, in reperfusion phase FUNDC1-

mediated mitophagy is impaired which leads to apoptosis activation [Zhou et al., 2017]. Cardiomyocytes have been reported as major targets of I/R injury, however; recent findings have demonstrated that circulating platelets play a crucial role in determining cardiac dysfunction as a consequence of I/R injury [Zhang et al., 2018]. Mice lacking FUNDC1 in their platelets had smaller infarct size with improved cardiac function compare to control mice under I/R [Zhang et al., 2017]. Mitophgay improves energy metabolism of platelets; therefore, activated platelets form thrombi and occlude coronary artery leading to secondary ischemia and contribute toward cardiac IR injury [Zhang et al., 2018]. In this regard, pharmacological or genetic manipulation of FUNDC1-mediated mitophagy in platelets which suppresses their hyperactivity can protect heart against I/R injury [Zhang et al., 2017, Zhou et al., 2017, Zhang et al., 2016].

BAG3-mediated mitophagy

Bcl-2-associated athanogene 3 (BAG3) is highly expressed in skeletal and cardiac muscles [Homma et al., 2006] and maintains myofibrillar organization and prevents z-disk disruption and muscle degeneration [Hishiya et al., 2010]. BAG3 gene disruption in mice led to myofibrillar degeneration and development of lethal myopathy followed by death 4 weeks post disruption [Homma et al., 2006]. BAG3 also functions as a chaperonic protein and targets misfolded proteins for lysosomal degradation via autophagy pathway [Minoia et al., 2014, Zhang et al., 2014, Gamerdinger et al., 2010] and mutations of BAG3 have led to proteotoxic stress and severe cardiomyopathy [Schänzer et al., 2018]. Alterations in mtDNA, mitochondrial respiration and mitochondrial biogenesis have been reported in patients with myofibrillar myopathies [Vincet et al., 2016]. Furthermore, recent studies have demonstrated that parkin-independent mitophagy occurs in cardiac cells through compensatory mechanisms [Piquereau et al., 2013]. Therefore, recent studies have reported the role of BAG3 in

regulating mitochondrial dynamic and mitochondrial quality control in cardiac cells; however, the exact underlying mechanisms remain elusive [Tahrir et al., 2017, Quintana et al., 2016]. In neonatal cardiomyocytes, BAG3 level significantly increased in mitochondrial fraction under mitochondrial stress and suppression of BAG3 reduced mitophagy and impaired clearance of damaged mitochondria leading to apoptosis induction and significant cardiomyocyte death [Tahrir et al., 2017]. Furthermore, BAG3 mutation resulted in mitochondrial fragmentation and alteration of mitochondrial fission, Drp1, and fusion, Opa1 (cellular optic atrophy-1 protein), proteins in mouse hearts leading to progressive heart failure development [Quintana et al., 2016].

Mitophagy during cardiac development

Mitochondrial dynamic and metabolism change during development [Neary et al., 2014, Gong et al., 2015]. Fetal cardiomyocytes have metabolic tolerance to hypoxia; whereas, after birth oxygen encountered by neonate acts as a driving force for mitochondrial remodeling and biogenesis toward aerobic metabolism to meet the energy demand of adult myocardium [Neary et al., 2014, Papanicolaou et al., 2012, Dorn et al., 2015]. In mouse fetal cardiomyocytes, mitochondria go under mitophagy mediated by Pink1-Mfn2-Parkin to be replaced with mature adult mitochondria within the first 3 weeks of life. Parkin deficiency in adult cardiomyocytes did not provoke any cardiomyopathy; whereas Parkin ablation in fetal mice led to impaired mitochondrial maturation and lethal cardiomyopathy [Gong et al., 2015]. Ablation of mitofusins in embryonic myocardium was lethal [Chen et al., 2011] and perinatal expression of mutated Mfn2 lacking Pink1 phosphorylation site inhibited postnatal mitochondrial maturation and led to metabolic arrest followed by lethal cardiomyopathy by 7 to 8 weeks of age in mice [Gong et al., 2015]. Furthermore, double deficiency of Mfn1/Mfn2 in mid-gestitional cardiac myocytes impaired mitochondrial remodeling, mitochondrial biogenesis and metabolic switch in

postnatal cardiac cells and led to heart failure development by day of 7 followed by survival loss by 16 days of age [Papanicolaou et al., 2012].

Cardiac complications as a result of mitophagy dysregulation

Mitophagy has been reported to play a controversial role under cardiac stress; either protective or detrimental [Zhou et al., 2017, Shirakabe et al., 2016, Zhang et al., 2018]. Mitophagy by eliminating malfunctioning mitochondria avoids release of pro-apoptotic proteins to cytosol and apoptosis activation; and mitophagy impairment causes intracellular accumulation of ROS and increases cells vulnerability to oxidative damage [Zhou et al., 2017, Wild et al., 2010]. ROS are byproducts of OXPHOS and have been reported in cardiovascular complications particularly in cardiac hypertrophy [Dutta et al., 2013, Liu et al., 2012]. Manipulating the metabolic activity of mitochondria by attenuating myocardial oxidative stress ameliorated cardiomyopathy after myocardial infarction [Engberding et al., 2004, Liu et al., 2012]. Autophagy induction in aortic-banded mice attenuated oxidative stress, reduced myocardial infract size and improved cardiac function in hypertrophic myocardium [Ma et al., 2018]. On the other hand, excessive mitophagy is followed by mitochondrial mass loss and myocardial ATP deficiency [Jin et al., 2018]. Therefore, a balance between mitochondrial degradation and mitochondrial biogenesis is of great importance toward myocardial protection under stress. Atrial biopsy of patients undergoing cardiopulmonary bypass during cardiac surgery indicated that both mitophagy and mitochondrial biogenesis were upregulated after heart surgery [Andres et al., 2017].

Mutations of Parkin and Pink1 genes, two key regulators of mitophagy, have been associated with development of degenerative disorders [Barodia et al., 2017]. Parkin-deficient mice had normal hearts [Piquereau et al., 2013, Song et al., 2015]; however, mitochondrial functional abnormalities were observed in those mice [Piquereau et al.,

2013]. Under stress, protective role of Parkin-mediated mitophagy has been reported in several research studies [Song et al., 2015]. Lack of Parkin was accompanied with mitophagy reduction and accumulation of damaged mitochondria after MI [Kubli et al., 2013]. Parkin deficiency exacerbated cardiac and mitochondrial dysfunction under sepsis [Piquereau et al., 2013]. Substantial reduction in the level of PINK1 protein was detected in end-stage heart failure patients [Billia et al., 2011]. PINK1 deficiency in mouse hearts resulted in elevated levels of oxidative stress as well as apoptosis leading to left ventricular dysfunction and cardiac hypertrophy [Billia et al., 2011]. In addition, PINK1 deficiency increased cardiac susceptibility to I/R injury in mice and overexpression of PINK1 protected against I/R injury in cardiac cells [Sidall et al., 2013].

Summary of Specific Aims:

Specific Aim 1: To evaluate the role of HIV-1 Tat in maintaining mitochondrial homeostasis in neonatal cardiomyocytes.

Rationale: HIV infections are associated with the development of cardiomyopathies [Manga et al., 2017]. Antiretroviral therapies decrease the HIV mortality but are associated with peripheral and coronary atrial diseases [Domingo et al., 2008]. HIV-1 Tat functions as a transcriptional transactivator and impacts intracellular gene expression, both nuclear and mitochondrial genes, leading to alterations in mitochondrial function and apoptosis induction [Rodríguez-Mora et al., 2015]. Considering the notion that major energy demand of cardiomyocytes is supplied by mitochondria and energy deficit leads to cardiomyopathy, we hypothesized that Tat may impair cellular homeostasis by impacting mitochondrial oxidative phosphorylation as well as mitochondrial quality control in cardiomyocytes; leading to the accumulation of dysfunctional mitochondria and subsequent activation of apoptosis pathway and cardiomyocyte death.

Specific Aim 1a: This aim evaluates mitochondrial bioenergetics such as ATP level, mitochondrial oxygen consumption rate, calcium signaling and electrophysiological activity in Tat expressing as well as control cardiomyocytes.

Specific Aim 1b: By evaluating changes in mitochondrial mass and translocation of mitophagy proteins, this aim investigates the effect of Tat expression on mitochondrial quality control. In addition, mitochondrial ROS content and morphology are investigated in this aim. Lastly, this aim investigates the signaling pathways through which apoptosis is activated in the presence of Tat.

Specific Aim 2: To evaluate the role of BAG3 in maintaining mitochondrial quality control in neonatal cardiomyocytes.

Rationale: Considering the role of mitochondria in providing the main energy required for cardiac contractility, maintaining mitochondrial homeostasis as a balance between mitochondrial biogenesis and removal is of great importance toward cardiac proper functioning. Although Parkin has been reported as a key regulator of mitophagy in neurons [Narendra et al., 2008], but previous studies concluded that Parkin deletion did not interfere with mitochondrial function or affect cardiac contractility in the heart [Kubli et al., 2013]. Mutations of BAG3 have been reported in patients with cardiovascular disorders [Feldman et al., 2014] and BAG3 deficiency resulted in development of severe myopathy and death at 4 weeks of age in mice [Homma et al., 2006]. Furthermore, it has been reported that HIV-1 Tat protein by enhancing BAG3 levels impacts cellular protein quality control [Bruno et al., 2014]. These observations led us to hypothesize that BAG3 may play an important role in maintaining the homeostasis of mitochondria in cardiomyocytes and suppression of BAG3 under mitochondrial pathological condition may lead to apoptosis activation and cell death.

Specific Aim 2a: This aim evaluates the role of BAG3 in clearance of damaged mitochondria from neonatal cardiomyocytes when mitochondrial damage is induced.

Specific Aim 2b: This aim evaluates how impairment of mitophagy through BAG3 suppression may lead to the upregulation of apoptotic markers and cardiomyocyte death.

Specific Aim 3: To evaluate the impact of BAG3 on turnover and stability of gap junction protein Connexin 43.

Rationale: Heart failure is caused when heart is unable to pump sufficient blood to the organs of body [Billia et al., 2011]. To ensure normal function of heart, mitochondria as cellular power centers must generate enough amounts of ATP molecules and cardiac cells must synchronize their electrical activity during excitation-contraction coupling with the neighboring cells [Gaudesius et al., 2003]. Gap junctions permit the intercellular exchange of ions and small molecules and propagate action potential throughout the myocardium [Goldberg et al., 2004]. Cx43 is highly expressed in gap junction structure and has a short half-life ($t_{1/2}$) of within 1-5 hr in the heart. Impair of Cx43 turnover dysregulates intercellular communications and leads to arrhythmogenesis [Falk et al., 2014]. Considering the importance of BAG3 in protein quality control and protein stability in cardiomyocytes, we hypothesized that BAG3 may play an important role in controlling the quality of Cx43 and evaluated the impact of BAG3 suppression on the turnover of Cx43 under normal and pathological conditions.

Specific Aim 3a: This aim evaluates the impact of BAG3 suppression on Cx43 turnover under normal and pathological conditions.

Specific Aim 3b: This aim evaluates the impact of BAG3 on the stability and half-life of Cx43.

Specific Aim 4: To investigate the impact of BAG3 on electrophysiological activity of neonatal cardiomyocytes. Furthermore, this aim investigates the impact of gap junction inhibition on mitochondrial bioenergetics.

Rationale: Gap junctions propagate action potential initiated by ion channels. Cx43 is highly expressed in gap junction structure in the heart and Cx43 mutations impair action potential conduction leading to arrhythmogenesis [Epifantseva et al., 2017]. Considering the importance of gap junctions in cardiac electrical activity, it is of great importance to evaluate the impact of Cx43 on electrophysiological activity of cardiac cells. Recently we found that BAG3 suppression dysregulated the quality of Cx43 by increasing its degradation. Herein, we hypothesized that BAG3 deficiency impairs electrophysiological activity of primary cardiomyocytes. *In vitro* characterization of cultured cardiomyocytes presents a valid experimental model to better understand intercellular communication of cardiomyocytes in the complex heart tissue. For this purpose, non-invasive MEA system was employed to record extracellular ion currents known as field potentials. MEA generates large data set which requires precise data analysis methods for interpretation. By developing MATLAB codes, important electrophysiological components of the system of spontaneously beating cardiomyocytes such as spike frequency, spike amplitude, and conduction velocity in control and BAG3-suppressed cardiomyocytes were extracted from the complex signal simultaneously recorded by 60 electrodes throughout the culture.

Gap junctions are located on the cell borders and permit metabolic and electrical coupling between the neighboring cardiomyocytes [Zhou et al., 2014]. In addition to the role of Cx43 in intercellular communication, previous studies reported that Cx43 is also localized in the inner mitochondrial membrane of myocardium [Boengler et al., 2005]. Under ischemic preconditioning, Cx43 translocated to mitochondria and played a

cardioprotective role which was independent of Cx43 role in cell-cell communication [Boengler et al., 2005]. However, the precise mechanism through which translocation of Cx43 to mitochondria plays a protective role remains under question. We hypothesized that Cx43 may function as a key player in regulating mitochondrial function and focused on evaluating the impact of Cx43 on mitochondrial bioenergetics under normal and stress conditions.

Specific Aim 4a: This aim evaluates the effect of BAG3 suppression on electrophysiological activity of neonatal cardiomyocytes.

Specific Aim 4b: This aim evaluates the effect of gap junction and Cx43 inhibition on mitochondrial bioenergetics such as calcium uptake and ATP levels.

CHAPTER 2

DYSREGULATION OF MITOCHONDRIAL BIOENERGETICS AND QUALITY CONTROL BY HIV-1 TAT IN CARDIOMYOCYTES

Abstract

Even under treatment with antiretroviral therapy, cardiovascular disease remains a leading cause of morbidity and mortality in HIV positive patients. However, the underlying molecular events responsible for the development of cardiac disease in patients whose viral load is controlled by treatment remains unknown. HIV encoded Tat protein plays a critical role in the activation of HIV gene expression and profoundly impacts infected cell homeostasis as well as the bystander uninfected cells that have taken up Tat released by the infected cells. Since cardiomyocytes function, including excitation-contraction coupling, greatly depends on the energy provided by the mitochondria, in this study we performed a series of experiments to assess the impact of Tat on mitochondrial function and bioenergetics pathways in a primary cell culture model derived from neonatal rat ventricular cardiomyocytes (NRVCs). Our results show that the presence of Tat in cardiomyocytes is accompanied by a decrease in oxidative phosphorylation, a decline in the levels of ATP, and an accumulation of reactive oxygen species (ROS). Moreover, Tat impairs the uptake of mitochondrial Ca^{2+} ($[Ca^{2+}]_m$) and electrophysiological activity of cardiomyocytes. Tat also affects the protein clearance pathway and autophagy in cardiomyocytes under stress due to hypoxia-reoxygenation conditions. A reduction in the level of ubiquitin along with dysregulated degradation of autophagy proteins including SQSTM1/p62 and a reduction of LC3 II were detected in cardiomyocytes harboring Tat. Taken together, our results suggest that, by targeting mitochondria and protein quality control, Tat significantly impacts bioenergetics and autophagy in cardiomyocyte health and homeostasis.

Introduction

HIV positive patients have been reported to be more vulnerable to development of various cardiovascular disorders such as atherosclerosis, myocardial fibrosis and myocardial infarction [Manga et al., 2017, Eugenin et al., 2008]. Although the direct infection of cardiomyocytes by HIV remains controversial but these cells can uptake the HIV proteins released by adjacent infected cells [Fiala et al., 2004]. For example, HIV by infecting myocardial endothelial cells can lead to the chronic inflammatory response and subsequent cardiac dysfunction [Manga et al., 2017]. Moreover, HIV has been reported to infect vascular smooth muscle cells both *in vivo* and *in vitro* leading to the development of vascular disease [Eugenin et al., 2008]. Antiretroviral therapies have played an important role in suppressing HIV progression and reduced HIV mortality but they increase the risk of dyslipidemia and contribute to the development of heart disease [Domingo et al., 2008]. However, the precise molecular mechanism through which HIV causes cardiac problems still remains to be elucidated.

Among the HIV-1 encoded proteins, Tat, a transcriptional activator, has received much attention due to its toxic effect on the infected as well as the uninfected cells which uptake Tat released by infected cells [Nath et al., 2014]. Tat protein led to apoptosis activation and cell death in primary mouse striatal neurons [Singh et al., 2005]. In addition, Tat protein has been reported as one of the key factors in development of neurological complications in HIV-infected patients [Carey et al., 2012]. Tat plays a critical role towards developing cardiomyopathy [Duan et al., 2013, Fang et al., 2009]. Transgenic mice expressing Tat indicated dysregulated cardiac function with reduced heart rate as well as depressed systolic and diastolic function [Fang et al., 2009].

25

However, precise studies are needed to further understand the underlying pathway through which Tat results in cardiac dysfunction.

Mitochondrial abnormalities with impaired metabolic capacity are associated with the development of cardiac dysfunction; as mitochondria are the major energy source for cardiac function [Parihar et al., 2017]. Therefore, it would be of great importance to explore whether Tat alters mitochondrial function leading to the development of HIV cardiomyopathy. In addition, HIV-1 transgenic mouse exposed to stress condition indicated higher risk of cardiac dysfunction. 10 days after open heart surgery, significant reduction in both cardiac contractility and relaxation was observed in HIV-1 transgenic (Tg26) mice; compare to normal littermates [Cheung et al., 2015]. However, the underlying mechanism through which HIV sensitizes cardiac cells to stress condition remains unclear. Autophagy, an intracellular degradation pathway in which dysfunctional proteins and organelles are delivered to lysosome for further degradation, has been reported to be targeted by HIV proteins [Fields et al., 2015]. HIV-1 Tat protein has been shown to interact directly with lysosomal-associated membrane protein 2A (LAMP2A), prevents autophagosome fusion with lysosome and results in decreased autophagy in neuronal cell line [Fields et al., 2015]. Autophagy dysregulation has been reported to be associated with left ventricular dilation as well as depressed contractility and cardiomyopathy [Gustafsson et al., 2008]. Mitophagy, a selective form of autophagy in which damaged mitochondria are targeted for degradation, when impaired led to significant cell death in primary cardiomyocytes [Tahrir et al., 2017].These considerations led us to investigate the effect of HIV-1 Tat on quality control machinery with the main focus on autophagy when cardiomyocytes were subjected to various stress conditions.

In this study we demonstrate that HIV-1 Tat leads to the significant loss of mitochondrial metabolic function and increase in the accumulation of toxic ROS. In addition, Tat dysregulated the mitochondria calcium uniporter (MCU)-mediated mitochondrial Ca^{2+} uptake and electrophysiological activity of cardiomyocytes. Moreover, we found that Tat interfered with autophagy initiation and proper clearance of autophagic proteins when cardiomyocytes were exposed to hypoxia/reoxygenation

Experimental

Cardiomyocyte Isolation and Culture Conditions. All animal experiments were performed in accordance with the guidelines of Temple University Institutional Animal Care and Use Committee. NRVCs were isolated from 1-2 day old Harlan Sprague-Dawley rats following the protocol previously described [Gupta et al., 2016]. Isolated NRVCs were then maintained in Dulbecco's Modified Eagle Medium (DMEM, Life Technologies) supplemented with 2% fetal bovine serum (FBS, Denville Scientific Inc.) and 25 µg/mL gentamicin (Life Technologies) and maintained in a humidified incubator at 37°C and 5% CO_2.

Adenoviral Transduction. NRVCs were transduced with Ad-Tat with multiplicity of infection (MOI) of 1 in reduced volume of FBS-free DMEM at 37°C for 2 hours after which medium was replaced with DMEM supplemented with 2% FBS and 25 µg/mL gentamicin (Life Technologies). Experiments were performed 72 h post-infection. Ad-null (Vector Biolabs) transduction was used as an internal control.

NRVCs were transduced with autophagy reporter construct mRFP-EGFP-LC3 (Ad-ptfLC3) in the presence or absence of Tat transduction and analyzed 24 hr post transduction.

Western Blotting. NRVCs were washed with PBS and then scraped in RIPA lysis buffer (25 mM Tris-HCl pH 7.6, 150 mM NaCl, 1% NP-40, 1% sodium deoxycholate, 0.1% SDS) supplemented with fresh protease inhibitor cocktail (Sigma-Aldrich). Equal aliquots of cell lysates were loaded onto 10% or 12% SDS-polyacrylamide gels for electrophoresis using Bio-Rad's western blotting system. The gels were transferred on to wet 0.1 µm nitrocellulose membranes (LI-COR, Inc., Lincoln, NE). Membranes were probed with primary antibodies (3 hr at RT) and washed with PBST (1 x, 5 min)

containing 0.5% Tween 20 and PBS (3 x, 5 min ea.). Blots were then probed with appropriate secondary antibodies (1 hr at RT) followed by washing with PBST and PBS. Blots were scanned with ODYSSEY® CLx Imaging system (LI-COR, Inc., Lincoln, NE). Protein band intensities were quantified using Image Studio Software. The following antibodies were used for western blotting: BAG3 (Proteintech, 10599-1-AP), SQSTM1/p62 (Cell Signaling Technology, 5114), LC3 (Sigma, L8918), GAPDH (Santa Cruz, sc-32233), Cox-2 (Santa Cruz, sc-1745), Cytochrome c (Cell Signaling Technology, 4272), BAX (Santa Cruz, sc-493), Ubiquitin (Santa Cruz, sc-8017), NDUFA4L2 (Abcam, ab74138), Phospho-AKT (Cell Signaling Technology, 9271), ATG7 (Cell Signaling Technology, 2631) and Tat (Thermo Fisher NIH AIDS Reagent Program, R705).

RNA Isolation and Quantitative Real-Time RT-PCR (qRT-PCR). RNA was extracted using RNAeasy kit (Ambion) followed by on-column DNase digestion (QIAGEN). The synthesis of cDNA was performed by utilizing 1 µg of the extracted RNA via reverse transcription process. The synthesized cDNA was used for qRT-PCR by using LightCycler® 480 SYBR Green I Master (Roche) in total reaction volume of 20 µL. β-actin primer was used as a housekeeping gene to normalize data. The following primers were used: SQSTM1/p62 FW: GAGTCATGCTGCACTCCACT; RV: TATCAGGCAGGAATGATGGA.

Immunocytochemistry. Immunocytochemistry analysis was described previously [Tahrir et al., 2017]. Briefly, fixed cells were permeabilized with 0.5% Triton-X 100 followed by incubation with glycine and blocking solutions. Afterwards, cells were incubated with primary and Alexa Fluor® secondary antibodies (Thermo Fisher Scientific). Cells were then mounted using VECTASHIELD Hard set medium (Vector Laboratories) and imaged using Leica fluorescent microscope.

Cell Cycle Assay. Transduced NRVCs were trypsinized, washed and suspended in 1 mL PBS. The suspended cells were fixed immediately in 70% chilled ethanol followed by centrifugation (4000 rpm, 10 min) and PBS wash to eliminate ethanol. Cell pellets were resuspended in 300 µL of PBS supplemented with 0.5 mg/mL propidium iodide and10 mg/mL RNA A. After incubation at 37°C for 30 min, cells were chilled at 4°C for 1 hr and analyzed with Flow Cytometry (FACS).

Cell Viability Assay. NRVCS were seeded in 96-well plates (10,000 cells/well) and incubated with CellTiter-Blue® viability assay reagent (Promega) at 37°C for 2 hr followed by measuring the fluorescence using a plate reader with excitation and emission maximum at 575 and 590 nm respectively.

Annexin Apoptosis Assay. Transduced NRVCS were trypsinized, washed and suspended in 500 µL DMEM 2% FBS. 100 µL of Guava Nexin® reagent was added to 100 µL of the cell suspension followed by incubation in the dark at RT for 20 minutes. Percentage of cells undergoing apoptosis or necrosis was determined with FACS analysis. Staurosporine-treated cells were used as a positive control.

ATP Assay. NRVCs were lysed and the ATP level was measured using an ATP determination kit (Molecular Probes) as per manufacturer's instructions. 10 µL of the cell lysate was added to the 90 µL of the standard reaction solution (8.9 mL dH2O, 0.5 mL 20X reaction buffer, 0.1 mL 0.1M DTT, 0.5 mL of 10 mM D-luciferin and 2.5 µL firefly luciferase (5 mg/ml)) and luminescence was measured using a luminometer (Femtomaster FB 12 luminometer, Zylux). CCCP-treated cells were used as a positive control for ATP depletion.

Oxygen Consumption Rate (OCR) and Extracellular Acidification Rate (ECAR) Measurement. NRVCs were plated in XF96 cell culture microplates (Seahorse

Bioscience) at a density of 45,000 cells/well. OCR was measured using a seahorse XF96 Analyzer (Seahorse Bioscience) according to the manufacturer's protocol. The XF^e96 extracellular flux assay kit (Seahorse Bioscience) was first calibrated using XF calibrant solution (Seahorse Bioscience) by overnight incubation in a non-CO_2 incubator at 37°C. The XF^e96 extracellular flux assay kit was loaded with various inhibitors of mitochondrial ETC complexes including oligomycin, FCCP, Rotenone and Antimycin A using a XF cell mito stress test kit (Seahorse Bioscience). Cells were incubated with XF Assay medium (Seahorse Bioscience) in a non-CO_2 incubator at 37°C for 1 hr before recording. Mitochondrial complexes were inhibited by sequential adding of inhibitors and changes in OCR and ECAR were measured. OCR and ECAR were normalized to the number of cells.

ROS Determination Assay. NRVCs cultured on microscope cover glasses (Fisherbrand) were incubated with 1 mM MitoSOX red (Life Technologies) for 30 min. Cells were monitored using confocal microscopy and MitoSOX red signal was quantified with Image J.

Simultaneous Measurement of Mitochondrial Ca^{2+} Uptake and Mitochondrial Membrane Potential ($\Delta\Psi_m$). The measurement of Ca^{2+} uptake and $\Delta\Psi_m$ was performed based on the protocol previously described [Tomar et al., 2016]. Briefly, transduced cells were trypsinized, washed with DMEM, and bathed in an intracellular medium (120 mM KCl, 10 mM NaCl, 1 mM KH_2PO_4, 20 mM Hepes-Tris, pH 7.2 and 2 µM thapsigargin). The cells were permeabilized with digitonin (40 µg/ml), loaded with bath Ca^{2+} indicator Fura2FF (1 µM) and $\Delta\Psi_m$ indicator JC-1 (800 nM). Simultaneous measurement of extramitochondrial Ca^{2+} ($[Ca^{2+}]_{out}$) clearance and $\Delta\Psi$ was measured using a multiwavelength excitation dual-wavelength emission fluorimeter (Delta RAM, PTI). After reaching steady state, series of extramitochondrial Ca^{2+} pulses (10 µM) were added and

the rate of mitochondrial Ca^{2+} uptake was measured as a function of decrease in bath Ca^{2+} fluorescence.

Multi-electrode Array (MEA) Recording. NRVCs were plated on MEA plates (Multichannel Systems, Germany) pre-coated with EmbryoMax® 0.1% Gelatin Solution (Millipore) at a density of 1000 cells/mm^2. Each MEA plate contains 60 titanium nitrate (TiN) electrodes with diameter of 30 µM positioned in a rectangular grid. Extracellular action potential was recorded at initial state before any transduction using MEA-1060 system (Multichannel Systems, Germany). Cells were then transduced with either Ad-Tat or Ad-null and extracellular action potential was recorded post transduction. The sampling frequency was set to 2000 kHz and an online built-in bandpass filter was utilized throughout the recording. Data were recorded using the MC_Rack software and further analyzed with MATLAB®.

Mitochondrial Mass. Transduced cardiomyocytes were incubated with 50 nM MitoTracker Red (Thermo Fisher Scientific) for 30 min at 37°C followed by fluorescence analysis using flow cytometry.

Statistical Analysis. Student's *t*-test was used to assess statistical differences between two pairs of data. *P*<0.05 was considered significant.

Results

HIV-1 Tat Dysregulates Mitochondrial Bioenergetics in Cardiomyocytes

As a first step to investigate the impact of Tat on cardiomyocyte bioenergetics pathway, we measured cellular ATP levels in control and Tat expressing NRVCs using a luciferase-based ATP assay. Data showed that the expression of Tat in NRVCs significantly reduced cellular ATP levels (Figure 2.1A). Next we asked whether the decrease in cellular ATP is due to impaired OXPHOS. We measured the oxygen consumption rate (OCR) in control and Tat expressing NRVCs and found significant decrease in basal and maximal OCR as well as ECAR in cells expressing Tat compared to control (Figure 2.1B-E). Additionally, we noticed that the impaired OXPHOS activity was accompanied by decrease in the levels of NDUFA4L2 (NADH dehydrogenase, complex I) and cytochrome *c* (complex III) and increase in the level of Cox-2 (Cytochrome c oxidase, complex IV) (Figure 2.1F-K). Because complex I and complex III are the major source of mitochondrial ROS (mROS) production, one may expect uncontrolled leakage of electrons from complex I and III, and increased level of mROS production. Consistent with this notion that we observed decrease in NDUFA4L2 and Cytochrome *c* abundance, mROS levels significantly increased in NRVCs expressing Tat (Figure 2.1L-M). Together these data suggest that Tat transduced cardiomyocytes show reduced mitochondrial respiratory capacity leading to lower ATP level and accumulation of mROS.
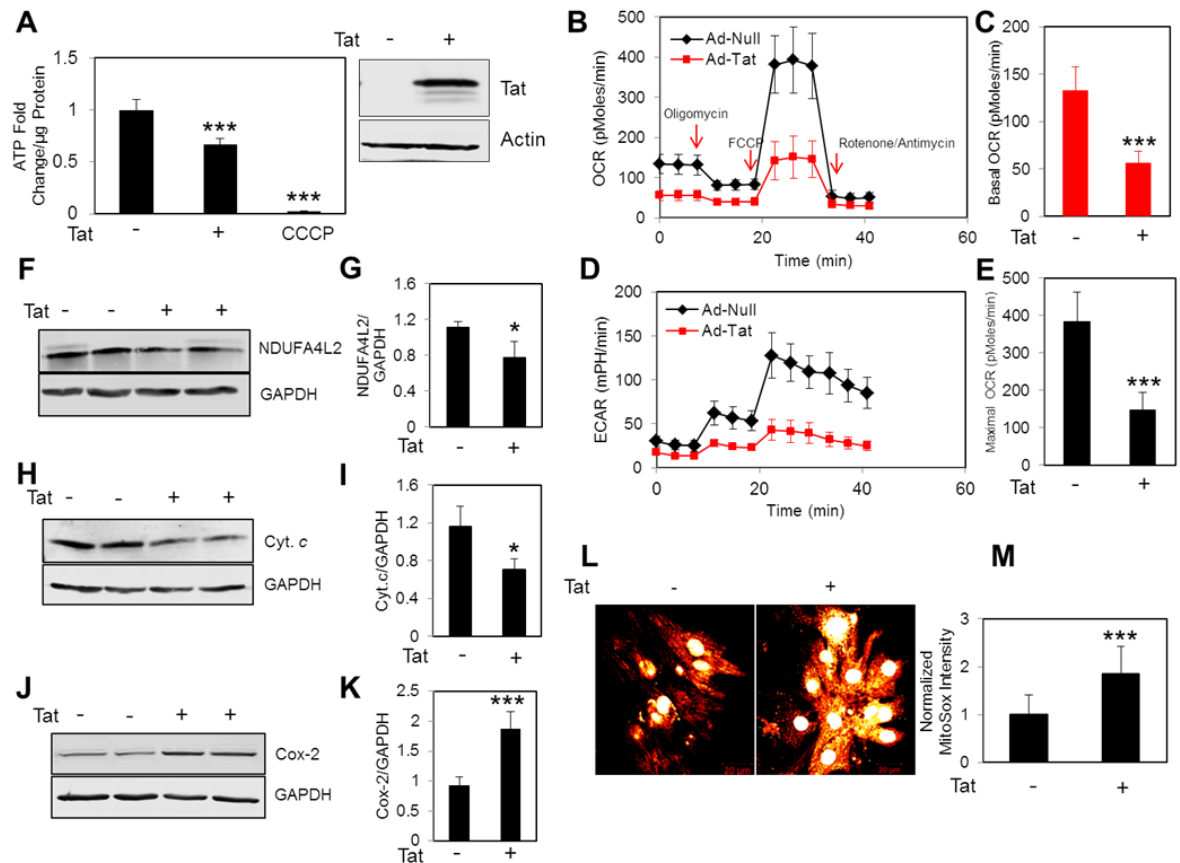
Figure 2.1. Tat dysregulates mitochondrial bioenergetics. NRVCs were transduced with either Ad-Tat or Ad-null for 3 days and then mitochondrial bioenergetics was assessed by various assays. **(A)** ATP levels were measured using luciferase-based assay in whole cell lysates. NRVCs were treated with CCCP (50 μM, 4 hr) as a positive control of ATP depletion. Data were normalized to ATP level in cells transduced with Ad-null. **(B-E)** NRVCs were subjected to subsequent injections of mitochondrial inhibitors including Oligomycin, FCCP and Rotenone/Antimycin A and OCR and ECAR were measured using XF96 Seahorse. Data were normalized to the number of cells. Western blotting analysis showed that **(F-G)** NDUFA4L2 and **(H-I)** Cyt. *c* levels decreased and **(J-K)** Cox-2 level increased in the presence of Tat. (L-M) NRVCs were stained with MitoSOXred and imaged with a confocal fluorescent microscope. The mitochondrial red signal was quantified with Image J analysis software. $^{*}P<0.05$; $^{***}P<0.001$.

HIV-1 Tat Dysregulates Ca^{2+} Uptake and Electrophysiological Activity of Cardiomyocytes

Because we observed increased mROS levels, next we assessed the $\Delta\Psi$ and mitochondrial Ca^{2+} uptake. Intracellular calcium flux is one of the key regulators of cardiac contractility. Mitochondria calcium uniporter functions as an exchange system which facilitates Ca^{2+} uptake by mitochondria in a $\Delta\Psi$ dependent manner [Luongo et al., 2015]. As seen in Figure 2.2A-D, expression of Tat in NRVCs significantly reduced the MCU-mediated mitochondrial Ca^{2+} uptake as a consequence of collapse in $\Delta\Psi$ after a 10 μM Ca^{2+} bolus.

In another experiment we examined whether Tat impacts cardiac contractility. To this end, we used MEA system to record electrical signal from beating NRVCs known as extracellular action potential over time. Data showed that Tat expression attenuated the amplitude and lowered the frequency of firing (number of spikes generated by cardiomyocytes per minute). 96 hr post transduction spikes completely suppressed in Tat expressing cells whereas these reductions were not observed in control cells (Figure 2.2 E and F).
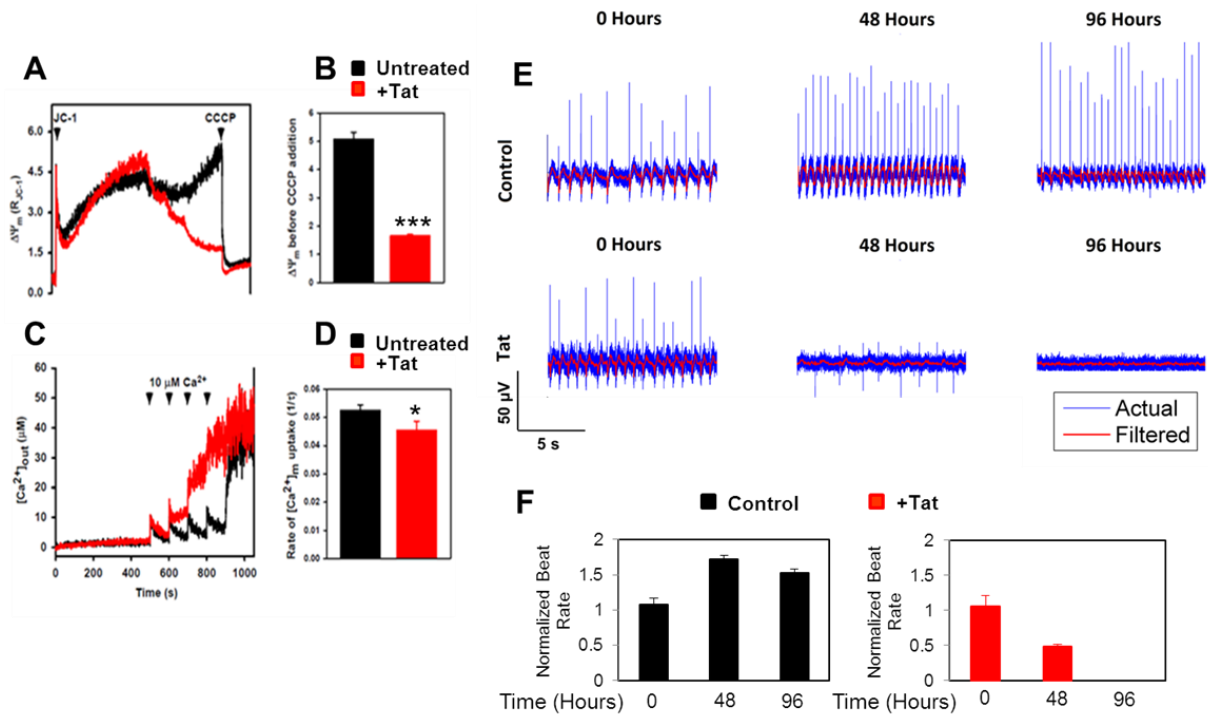
Figure 2.2. Tat dysregulates $[Ca^{2+}]_m$ uptake and electrophysiological activity. Trypsin-detached NRVCs were resuspended in an intracellular-like media, permeabilized with digitonin (40 μg/ml), loaded with Ca^{2+} and $\Delta\Psi_m$ indicator Fura-2FF, and JC-1. After reaching steady state, 10 μM Ca^{2+} pulses were added and extramitochondrial Ca^{2+} ($[Ca^{2+}]_{out}$) clearance and changes in $\Delta\Psi_m$ were recorded before adding CCCP (2 μM) to collapse $\Delta\Psi_m$ and $[Ca^{2+}]_m$ uptake. **(A)** $\Delta\Psi_m$ decreased in the presence of Tat after addition of Ca^{2+} pulses. **(B)** $\Delta\Psi_m$ was quantified based on the data shown in (A). **(C)** $[Ca^{2+}]_{out}$ at each time point was recorded. **(D)** $[Ca^{2+}]_m$ uptake rate was calculated as a function of bath Ca^{2+} clearance.**(E)** Electrophysiological activity of NRVCs was recorded based on the extracellular action potential measured by a multi-electrode array system in the presence or absence of Tat.**(F)** Number of spikes/min was calculated based on the data shown in (E). $^{*}P<0.05$; $^{***}P<0.001$.

HIV-1 Tat Triggers Apoptosis in cardiomyocytes

As mitochondrial permeabilitfy transition pore (MPTP) can be sensitized by both mROS and mitochondrial Ca^{2+} overload, we anticipated increased mROS production in Tat expressing NRVCs sensitized the opening of MPTP leading to cell death as evidenced from the collapse in $\Delta\Psi$ (Figure 2.2A). To further verify whether the Tat expressing NRVCs are prone to apoptotic cell death, we performed Annexin-V staining and flow cytometric analysis. Treatment with staurospoine (10 µM, 4 hr) was performed as a control. Results showed that 72 hr post transduction Tat caused significant induction of apoptosis but not necrosis in cardiomyocytes. As expected cellular viability in Tat expressing NRVCs was significantly reduced by 20% (Figure 2.3A-C). Excessive ROS production results in the activation of cell death signaling pathways in which mitochondrial membrane permeability increases leading to the release of pro-apoptotic factors and activation of caspases. Caspase activation by promoting the cleavage of cellular DNA and proteins commits cells to death [Fulda et al., 2012]. Cell cycle analysis showed that Tat led to the significant fragmentation of cellular DNA (Figure 2.3D and E).

We then examined changes in the level of some important signaling proteins involved in apoptosis. AKT is one of the key anti-apoptotic proteins which inhibits caspase activation and promotes cell survival [Fulda et al., 2012]. The level of phospho-AKT increased in the presence of Tat (Figure 2.3F and G); suggesting that protective pathways are activated to minimize cell death. On the other hand, the level of pro-apoptotic protein, BAX, significantly increased in the presence of Tat (Figure 2.3H and I).
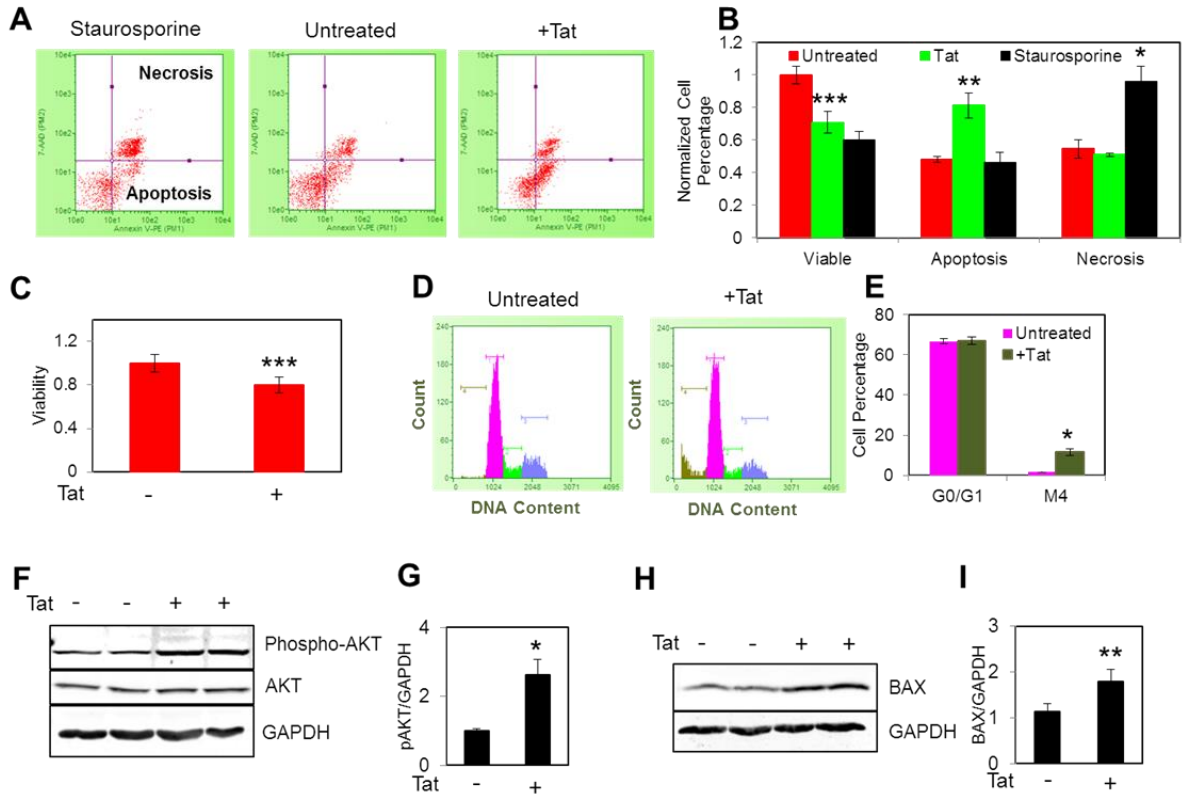
Figure 2.3. Tat induces apoptosis in neonatal cardiomyocytes. (A-B) Transduced NRVCs were stained with Annexin-V and the percentage of apoptotic and necrotic cells was measured with FACS analysis. **(C)** NRVCs were plated in 96 well plates and 3 days post transduction were treated with CellTiter-Blue® viability assay reagent (ex/em of 575 nm/590 nm) and emission fluorescent was measured. **(D-E)** PI-based cell cycle assay showed that DNA fragmentation significantly increased by Tat expression. **(F-G)** Western blotting analysis showed that the level of anti-apoptotic protein phosphor-AKT significantly increased in the presence of Tat. **(H-I)** Western blotting analysis showed that the level of pro-apoptotic protein BAX significantly increased in the presence of Tat. $^{*}P<0.05$; $^{**}P<0.001$; $^{***}P<0.001$.

HIV-1 Tat Interferes with Autophagy Initiation

Autophagy is one of the key intracellular events which upregulates during ATP reduction and through degradation of nonessential components and macromolecules plays a crucial role in maintaining cellular homeostasis and survival [Russel et al., 2014]. Autophagy dysregulation has been reported to be associated with cardiomyocyte death [Tahrir et al., 2016; Su et al., 2016]. Considering ATP reduction in Tat expressing cells we next wanted to investigate how and through which mechanism autophagy pathway is affected by Tat. Inhibition of proteasome has been reported as an activator of autophagy-lysosome pathway [Gamerdinger et al., 2011]. NRVCs were treated with proteasome inhibitor, MG132, and expression of autophagy proteins such as LC3 and p62 were investigated. Western blotting data showed that The level of autophagy protein p62 increased in control cells but not in Tat-transduced cells after treating the cells with MG132 (5 μM, 12hr). In addition, LC3 II levels did not increase in Tat-transduced cells after MG132 treatment and the level of ATG7 reduced in Tat-transduced cells after MG132 treatment; indicating that Tat-transduced cells were defective in activating the autophagy-lysosome pathway (Figure 2.4A-D).

Fluorescent microscopy showed that Tat localized in both nucleus and cytosol of cardiomyocytes (Figure 2.4E). Western blotting data also showed that Tat protein was present in both nuclear and cytosolic fractions when a nuclear extraction kit was used. Lamin A/C and GAPDH proteins were used as nuclear and cytosolic markers respectively (Figure 2.4F). Since levels of Tat were significant in cell nuclei, we evaluated the effect of Tat on the expression of the autophagy protein p62. RT-qPCR results showed that p62 mRNA level was significantly reduced in Tat-transduced cells compared to the control cells after treating the cells with MG132 (Figure 2.4G).

In another experiment we evaluated the effect of Tat on the level of p62 protein when NRVCs were treated with well-known autophagy activator Rapamycin in the presence or absence of Baf A1 as an inhibitor of autophagolysosome formation. Data showed that the level of p62 increased in NRVCs after Rapamycin treatment when autophagy flux was inhibited by Baf A1; while it did not change in Tat expressing cells (Figure 2.4H). Taken together, these results state that Tat interferes with autophagy and upregulation of autophagy proteins; and p62 is one of the major targets for Tat.
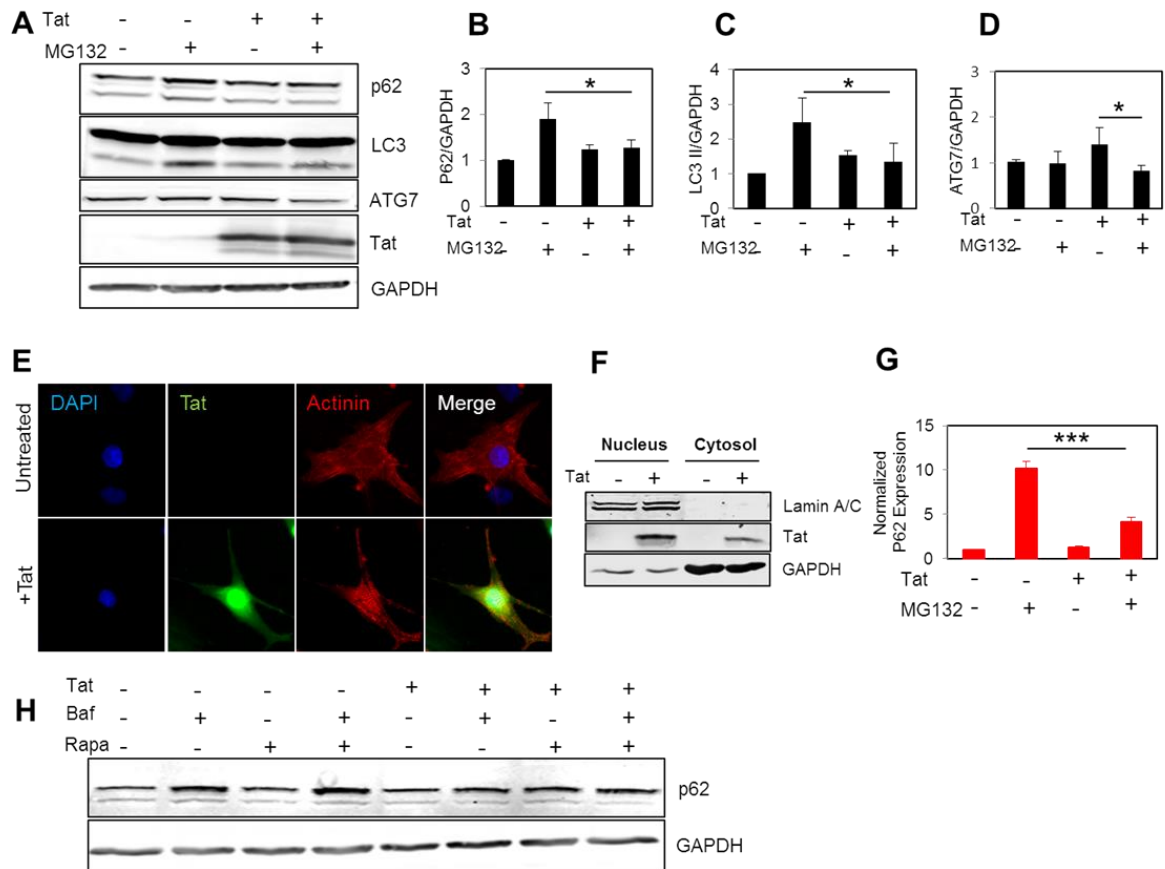
Figure 2.4. Tat interferes with autophagy initiation in neonatal cardiomyocytes. (A-D) NRVCs were transduced with either Ad-Tat or Ad-null for 72 hr in the presence or absence of MG132 (5 µM, 12 hr) and the level of autophagy proteins p62 and LC3 were quantified using western blotting analysis. **(E)** ICC data showed that Tat is highly expressed in cellular nucleus and cytosol. **(F)** Nuclear fractionation data showed that Tat is highly expressed in cellular nucleus. **(G)** RT-qPCR data showed that Tat impaired upregulation of p62 mRNA in the presence of MG132 (5 µM, 12 hr).**(H)** Cells were treated with autophagy activator Rapamycin (50 nM, 24 hr) and the level of p62 protein was analyzed in the presence or absence of Baf A1. $^{*}P<0.05$; $^{***}P<0.001$.

HIV-1 Tat Dysregulates Mitochondrial Quality Control in Cardiomyocytes

In order to measure mitochondrial mass, transduced NRVCs were stained with MitoTracker Red followed by the analysis of fluorescent intensity using FACS analysis. Data showed that Tat transduction led to increase in mitochondrial mass (Figure 2.5A and B). Tat-induced mitochondrial hyperpolarization in neurons has been reported in previous research studies [Norman et al., 2007; Perry et al., 2005]. Fluorescent microscopy showed that mitochondrial morphology changed from filamentous network in control cells into accumulated interconnected network in Tat expressing cells (Figure 2.5C). In order to investigate whether increase in mitochondrial mass happens due to the impairment of mitophagy, selective form of autophagy in which mitochondria is targeted for further degradation and removal, in the presence of Tat, mitochondrial and cytosolic fractions were isolated and analyzed for autophagy proteins. Data showed that LC3 II recruitment to mitochondria significantly reduced in Tat expressing cells compared to control cells (Figure 2.5D and E).
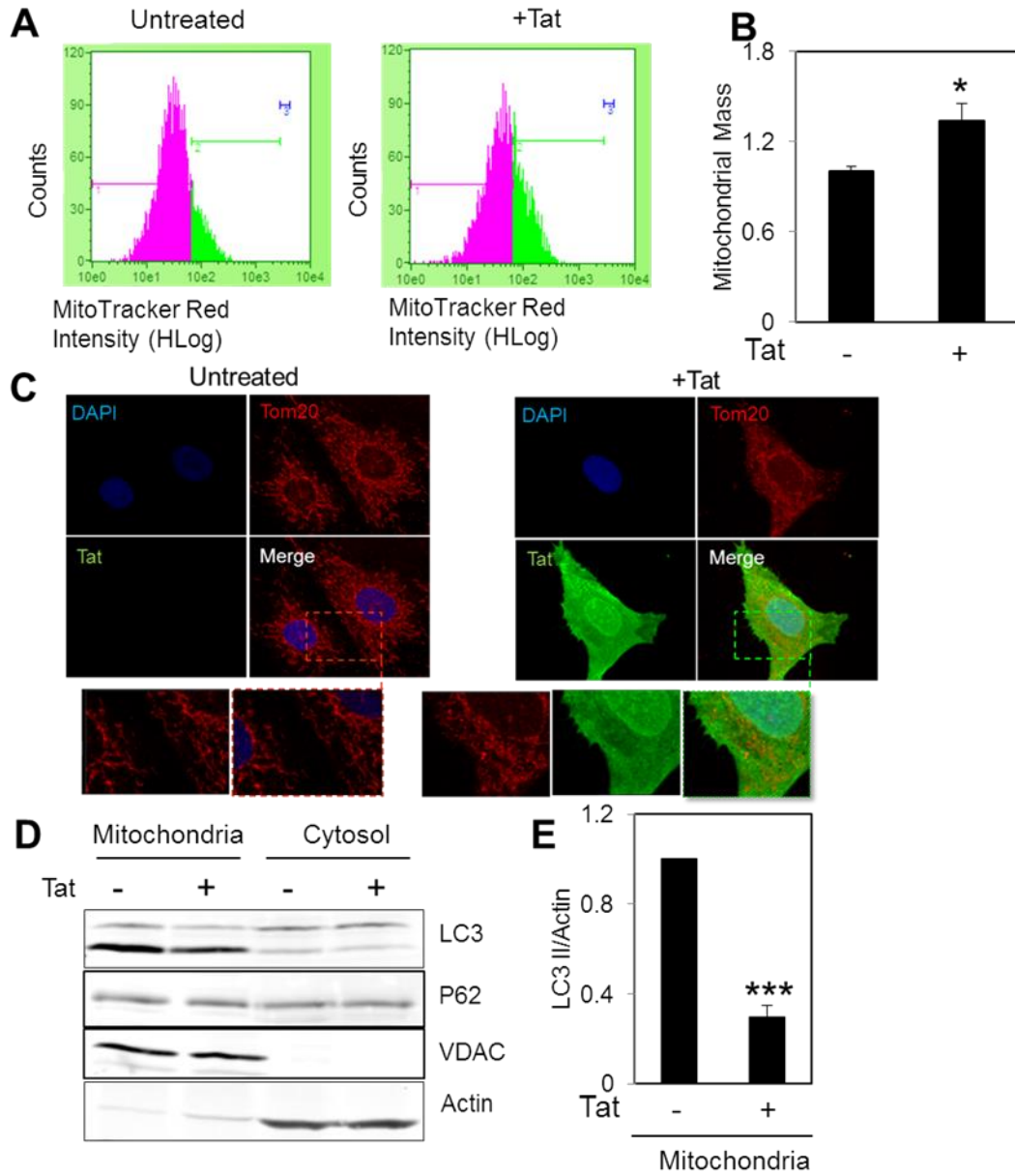
Figure 2.5. Tat expression increases mitochondrial mass and impairs mitophagy. (A-B) Transduced NRVCs were incubated with 50 nM MitoTracker Red for 30 min at 37°C and fluorescent intensity was analyzed using FACS analysis. **(C)** ICC by using antibody against Tom20 showed that Tat altered mitochondrial morphology. **(D-E)** Mitochondrial isolation indicated that LC3 II recruitment to mitochondria significantly reduced in the presence of Tat. $^{*}P<0.05$, $^{***}P<0.001$.

HIV-1 Tat Dysregulates Autophagy after Hypoxia/Reoxygenation

Hypoxia was reported to be associated with fragmentation of mitochondrial network and activation of autophagy machinery for clearance of damaged mitochondria [Liu et al., 2012]. In autophagy process dysfunctional organelles and damaged proteins are tagged by ubiquitin in a process called ubiquitination and targeted to lysosome for further degradation. p62 functions as an autophagy receptor and binds to ubiquitin tags as well as LC3 on phagophore membrane and sequesters substrate into autophagosomes [Fimia et al., 2013]. To investigate how the autophagy pathway was affected by Tat in cells under pathological stress, we incubated NRVCs under hypoxia/reoxygenation conditions, in the presence or absence of Baf A1. Data showed that Tat transduction resulted in decreased levels of ubiquitination in NRVCs. When autophagy flux was inhibited by Baf A1 the levels of both LC3 and p62 proteins increased in control cells as degradation of these proteins occurs by lysosome in autophagy-lysosome pathway. Lysosomal degradation of p62 reduced in Tat expressing cells under normal condition and no significant increase in p62 level was found in Tat expressing cells under hypoxia/reoxygenation when the autophagy flux was inhibited. In addition, autophagy markers LC3 I and LC3 II significantly reduced under hypoxia/reoxygenation when Tat was present (Figure 2.6A-C). Microscopic imaging after AdptfLC3 transduction also showed that LC3 puncta reduced in Tat expressing cardiomyocytes compared to control cells when cells were exposed to H/R stress condition. These results indicate that Tat transduction significantly reduced autophagy and impaired lysosomal degradation of p62 (Figure 2.6D and E).
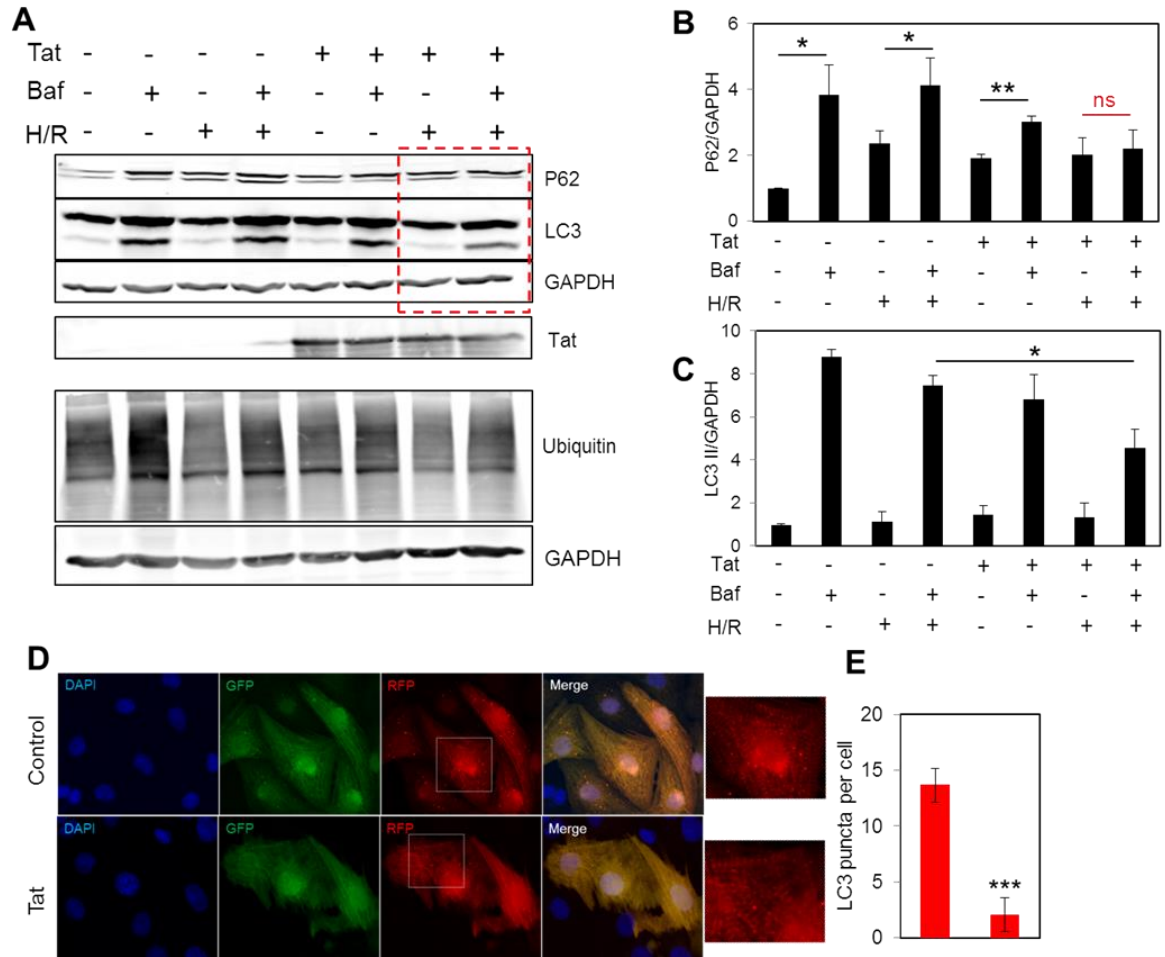
Figure 2.6. Tat expression dysregulates autophagy under hypoxia/reoxygenation. (A-C) NRVCs were subjected to hypoxic condition for 14 hr followed by reoxygenation for 4 hr in the presence or absence of Baf A1. The levels of autophagy proteins p62, LC3 and Ub were analyzed with western blotting. **(D-E)** NRVCs were transduced with Ad-ptfLC3 for 24 hr in the presence or absence of Tat transduction and subjected to H/R and monitored for LC3 puncta. *$P<0.05$; **$P<0.01$; ***$P<0.001$.

Discussion

HIV-1 infection has been reported to be associated with the development of cardiomyopathy. In one study on patients with HIV cardiomyopathy, hearts were reported to be hypertrophic with increased average heart weight from 337 g (healthy) to 580 g (HIV positive) [Fiala et al., 2004]. Valvular heart disease and vasculopathy have been reported in HIV infected patients [Manga et al., 2017]. Current antiretroviral therapies utilized in the treatment of HIV-infected patients may aggravate the development of peripheral and coronary arterial diseases [Barbaro 2002]. Therefore, understanding the precise mechanism by which HIV-1 infection causes cardiac dysfunction plays an important role toward the design and development of novel and less toxic therapies. Herein, we targeted HIV-1 Tat for further studies as Tat by functioning as a transactivator controls viral replication [Jeang et al., 1999]. Moreover, Tat alters intracellular gene expression; leading to changes in organelle function and cell death [Rodríguez-Mora et al., 2015].

Our results unequivocally demonstrate that Tat significantly diminished cellular ATP level, reduced OCR and increased ROS accumulation in mitochondria. Lower levels of Cytochrome *c* and NDUFA4L2 in Tat-transduced NRVCs partly accounted for reduced electron transport chain activity and oxidative phosphorylation. ROS has been reported to play an important role in dysregulating cellular homeostasis contributing to the development of cardiac disease [Sugamura et al., 2011]. ROS accumulation causes mutations of mitochondrial DNA (mtDNA) and damages the respiratory chain system [Rodríguez-Mora et al., 2015]. In addition, our results showed that the level of Cox-2 significantly increased with Tat expression. Cox-2 is a component of complex IV and encoded by mtDNA [Rodríguez-Mora et al., 2015]. Expression of genes encoded by mtDNA is regulated by nuclear-encoded respiratory factor 1 (*NRF-1*) and mitochondrial

46

transcription factor A (*TFAM*) [Rodríguez-Mora et al., 2015]. It is conceivable that HIV-1 Tat, by altering the expression of nuclear and mitochondrial genes, further exacerbated damages in mitochondrial electron transport chain with resultant reduction in oxidative phosphorylation. We previously reported that ATP depletion in NRVCs by proton uncoupler CCCP enhanced the level of Cox-2 [Tahrir et al., 2016]. Cox-2 increase is indicative of higher cellular ATP demand which leads to the increase in the expression of ETC proteins for enhanced electron transfer within mitochondria. Our data showed that mitochondrial reserve capacity was significantly suppressed in the presence of Tat; indicating that the capability of mitochondria to meet excess energy demand under stress was compromised; and thus rendering cells to be less able to cope with stress conditions [Hill et al., 2009].

Ca^{2+} uptake by mitochondria is critically important to cellular signaling as well as matching energy demand with energy production by virtue of mitochondrial Ca^{2+}-dependent dehydrogenases [Griffiths and Rutter 2009; Denton & McCormack, 1980]. In the presence of Tat both Ca^{2+} uptake and $\Delta\Psi_m$ were significantly reduced when 10 µM Ca^{2+} pulses were added. Extracellular action potential measurement over time indicated that Tat expression suppressed cardiac contractility 96 hr post transduction.

Apoptosis induction in HIV-infected patients leads to AIDS development [Maldarell et al., 1995] and cardiomyocyte apoptosis in those patients has been reported as a key event leading to HIV cardiomyopathy [Twu et al., 2002]. Our results showed that Tat significantly induced apoptosis but not necrosis in NRVCs. The level of pro-apoptotic protein BAX significantly increased in the presence of Tat. AKT is one of the critical proteins in regulation of mitochondria-related apoptosis [Fulda 2012]. Upon activation by phosphorylation, pAKT phosphorylates key apoptotic proteins such as BAX suppresses mitochondrial permeabilization and subsequent apoptosis and caspase activation

signaling [Fulda 2012]. Our results showed that the level of pAKT protein increased in Tat-transduced cells; which explains how activation of protective signaling proteins may minimize cell death.

Autophagy by recycling the essential macromolecules through degradation of organelles and long-lived proteins promotes cell survival [Gustafsson et al., 2008]. It was reported that autophagy receptor p62 interacts with Tat and target if for degradation and p62 knockdown led to the increase in Tat protein level in Flag-Tat transfected HEK cells. In this system, treatment of cells with autophagy inducer torin 1 caused significant degradation of Tat; while this degradation was inhibited when autophagy gene Atg7 was knocked down [Sagnier et al., 2014]. Colocalization of autophagy proteins LC3 and Beclin1 were observed with HIV proteins Gag and Nef, respectively [Kyei et al., 2009]. It was previously reported that MG132 treatment in cardiomyocytes increased the expression of autophagy proteins toward the activation of autophagy-lysosome pathway [Tahrir et al., 2016]. We found that Tat expression led to the suppression of autophagy-lysosome pathway since the level of autophagy proteins p62 and LC3 II were significantly reduced when proteasome pathway was blocked using MG132 compared to the control cells. RT-qPCR data indicated that Tat significantly suppressed mRNA expression of p62. It was reported that HIV-1 Tat interfered with the initiation of autophagy by decreasing the level of autophagy marker LC3 II and increasing the level of autophagy inhibitor Akt in monocyte-derived macrophages after treating the cells with autophagy inducer, Rapamycin [Van Grol et al., 2010].

Autophagy plays a dual role either as a protective signaling or excessive autophagy can cause cellular death through degradation of cellular essential components [Gustafsson et al., 2008]. For example, it was found that HIV-1 envelope glycoprotein (Env) caused Beclin1 accumulation. Knock down of Beclin1 and Atg7 proteins in this condition

inhibited cell death [Espert et al., 2006]. On the protective side, Su et al., reported that autophagy induction in cultured cardiomyocytes as well as *in vivo* mice model was associated with survival enhancement and infarct size reduction after ischemia/reperfusion [Su et al., 2016]. When transduced cells were subjected to H/R in the presence or absence of Baf A1, we found that ubiquitination was reduced in the presence of Tat. Autophagy receptor p62 binds to the ubiquitin-tagged substrates and targets them for further degradation [Sagnier et al., 2014]. Under H/R stress condition, Tat expression significantly blocked lysosomal degradation of p62 and reduced LC3 II level. In addition to the apoptotic cell death which is followed by caspase 3 activation, autophagy cell death as a result of the accumulation of autophagic cargos can lead to cell death in the absence of caspase 3 activation [Espert et al., 2006].

Mitophagy is selective degradation of defective mitochondria by autophagy machinery. Mitochondrial mass significantly increased in Tat expressing cells. In addition, mitochondrial isolation indicated that LC3 II level in mitochondrial fraction of Tat transduced cells reduced compared to control cells. Although microscopic imaging showed that Tat expression led to the alteration in the morphology of mitochondrial network, but mitochondrial fragmentation as essential component for mitophgay induction was not observed in the presence of Tat. Together these data suggest that mitochondrial quality control was adversely affected by Tat (Figure 2.7A-B).
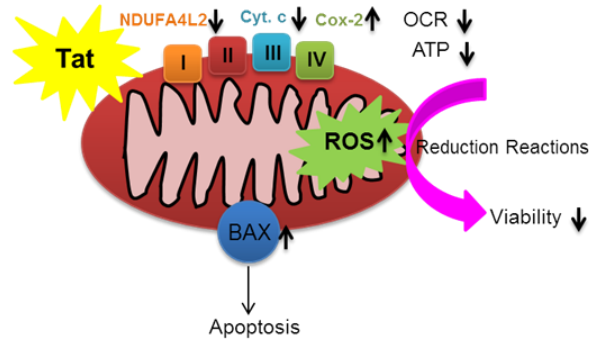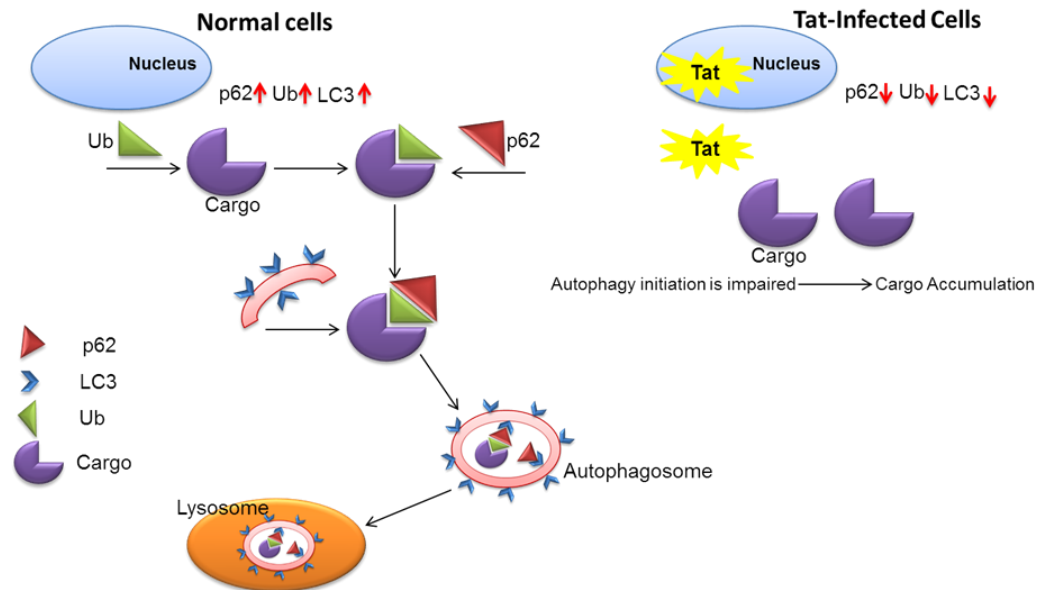
Figure 2.7. Schematic diagram of HIV-1 Tat impact on mitochondrial bioenergetics and autophagy in cardiomyocytes. (A) Tat expressing cells indicated reduced viability and increased level of apoptosis. Tat expression led to the dysregulation of oxidative phosphorylation, reduced ATP level and enhanced ROS production. **(B)** HIV-1 Tat reduced the level of autophagy proteins as well as impaired proper degradation of autophagic protein, p62, under hypoxia/reoxygenation stress condition.

CHAPTER 3

ROLE OF BAG3 IN MITOCHONDRIAL QUALITY CONTROL IN NEONATAL CARDIOMYOCYTES

Abstract

Mitochondrial abnormalities impact the development of myofibrillar myopathies. Therefore, understanding the mechanisms underlying the removal of dysfunctional mitochondria from cells is of great importance toward understanding the molecular events involved in the genesis of cardiomyopathy. Earlier studies have ascribed a role for BAG3 in the development of cardiomyopathy in experimental animals leading to the identification of BAG3 mutations in patients with heart failure which may play a part in the onset of disease development and progression. BAG3 is co-chaperone of heat shock protein 70 (HSP70), which has been shown to modulate apoptosis and autophagy, in several cell models. In this study, we explore the potential role of BAG3 in mitochondrial quality control. We demonstrate that siRNA mediated suppression of BAG3 production in neonatal rat ventricular cardiomyocytes (NRVCs) significantly elevates the level of Parkin, a key component of mitophagy. We found that both BAG3 and Parkin are recruited to depolarized mitochondria and promote mitophagy. Suppression of BAG3 in NRVCs significantly reduces autophagy flux and eliminates expression of Tom20, an essential import receptor for mitochondria proteins, after induction of mitophagy. These observations suggest that BAG3 is critical for the maintenance of mitochondrial homeostasis under stress conditions, and disruptions in BAG3 expression impact cardiomyocyte function.

Keywords: BAG3, Parkin, Tom20, mitophagy, proteasome

Introduction

BAG3 is a member of the BAG family of proteins which functions as a regulator of the Hsp70/Hsc70 chaperone system (Rosati et al., 2011). In cardiac muscle, BAG3, through association with the sarcomeric Z-disk, maintains the integrity and contractility of heart muscle. Mutations in the BAG3 gene have been reported to cause the cardiac muscle disorder known as familial dilated cardiomyopathy (DCM) (Arimura et al., 2011). BAG3 is critical for survival; its deficiency in mice caused skeletal and cardiac tissue abnormalities and strong myofibrillar degeneration which led to massive induction of apoptosis followed by death after 4 weeks (Homma et al., 2006). Furthermore, reduction of BAG3 in adult mouse ventricular myocytes interfered with contraction and calcium signaling (Feldman et al., 2016). Recent studies have demonstrated enhanced expression of BAG3 and increased levels of its chaperonic activity along with heat shock proteins during cellular stress and aging, suggesting a crucial role for BAG3 in determining the cellular stress response (Behl et al., 2011). BAG3 is known to play an important role in intracellular protein homeostasis by participating either in protein folding and/or clearance of damaged proteins (Rodriguez et al., 2016). To this end, BAG3 functions along with other proteins such as SQSTM1/p62 (referred to as p62 from here on), HSP70, and LC3 in a process called macroautophagy in which misfolded or damaged proteins and organelles are sequestered within autophagosomes and targeted to lysosomes for degradation (Behl et al., 2011). In this process, BAG3 targets misfolded proteins to the aggresome for further degradation through interaction with the dynein motor (Gamerdinger et al., 2011). Moreover, BAG3 functions as an anti-apoptotic protein and inhibits apoptotic cell death through its interactions with Bcl-2 family proteins (Arimura et al., 2011; Liao et al., 2001).

Mitochondrial homeostasis is maintained by proper balance between the mitochondrial biogenesis and degradation (Palikaras et al., 2014). Dysregulation of mitochondrial homeostasis plays an important role in the development of various types of disease in which mitochondrial abnormalities have been described, including cancer, neurodegeneration, and cardiomyopathies (Vincow et al., 2013; Chan et al., 2011; Maron et al., 2006). For example, damage to the mitochondrial respiratory chain, a metabolic pathway in which electrons move along with the mitochondrial inner membrane to reduce oxygen and generate ATP, leads to the uncontrolled generation of reactive oxygen species (ROS) which, by oxidizing cellular components, act as a stress signal and lead to caspase activation, thus triggering apoptotic signaling pathways (Selivanov et al., 2011). In support of this finding, abnormalities in mitochondrial distribution, morphology, and respiratory chain function have been reported in patients with myofibrillar myopathies. In addition, alteration of NADH, SDH or COX distribution is a hallmark feature of many myofibrillar disorders (Jackson et al., 2015). Parkin, encoded by the *PARK2* gene, has been reported as an important regulator of mitochondrial quality control and mutations associated with Parkin are associated with the development of neurodegenerative diseases such as the autosomal recessive form of Parkinson's disease (Yoshii et al., 2011). Mitochondrial quality control machinery maintains mitochondrial homeostasis by targeting the dysfunctional mitochondria for degradation and clearance. Parkin as a component of mitochondrial quality control machinery translocates from the cytosol to the mitochondria in response to mitochondrial membrane potential loss, depolarization, and targets damaged and dysfunctional mitochondria for degradation and clearance via ubiquitination (Narendra et al., 2008). In this regard, recent studies have focused on utilizing Parkin overexpression to enhance the elimination of damaged mitochondria as well as understanding potential mechanisms

of mitochondrial quality control and maintenance within cells (Yoshii et al., 2011; Narendra et al., 2008; Kim et al., 2013)**.**

Previous studies concluded that Parkin deletion did not interfere with cardiomyocyte contractility or affect mitochondrial characteristics, while disruption of the mitochondrial fission protein, Drp1 (dynamin-related protein 1), led to both alterations of the cardiac phenotype and myocardial dysfunction (Cao et al., 2015). These observations, along with the role of mitochondrial abnormalities in the development of myofibrillar myopathies, led us to hypothesize that BAG3 may play an important role in the clearance of dysfunctional mitochondria. Thus, we investigated the role of BAG3 in the clearance of damaged mitochondria in response to treatment with the electron uncoupler, carbonyl cyanide m-chlorophenylhydrazone (CCCP). We observed an increase in Parkin expression in response to knockdown of BAG3 and identified the translocation of both Parkin and BAG3 to the depolarized mitochondria thus promoting its degradation. Although no direct interaction between BAG3 and Parkin was detected, BAG3 suppression significantly reduced the clearance of Tom20 after CCCP treatment, indicating that mitophagy is impaired in the absence of BAG3. To our knowledge, this is the first study reporting BAG3 as a key regulator of mitophagy induced by CCCP electron transport chain uncoupler.

Experimental

Cell Isolation and Culture Conditions. All experiments were performed under protocols approved by the Temple University Institutional Animal Care and Use Committee. Cardiomyocytes were isolated from 1-2 day old Sprague-Dawley rats (Charles River) as previously described (Gupta et al., 2016). Isolated cells were cultured in Dulbecco's modified Eagle medium (DMEM, Life Technologies) supplemented with 2% fetal bovine serum (FBS, Denville Scientific inc.) and 25 µg/mL Gentamicin (Life Technologies).

Adenoviral Transduction. Cardiomyocytes were transduced in a minimal volume of DMEM containing either Adeno-null (Vector Biolabs), as an internal control, or Adeno-siBAG3 (Vector Biolabs) with a multiplicity of infection of 2 at 37°C for 2 hr, then refed with medium containing 2% FBS and 25 µg/mL Gentamicin. 72 hr post-transduction, cells were subjected to other treatments.

Plasmids and Transfections. HEK cells were transfected using Lipofectamine 3000 transfection reagent (Life Technologies) according to the manufacturer's instructions. Cells were incubated with Opti-MEM reduced-serum medium (Life Technologies) with YFP-Parkin (Addgene) with or without BAG3 siRNA (Dharmacon) for 2 hr, then fed with culture medium (DMEM, 10% FBS, 25 µg/mL Gentamicin) followed by overnight incubation. Medium then was replaced with culture medium and 48 hr post-transfection, cells were subjected to other treatments.

Mitochondrial Isolation. Mitochondrial enriched fractions were prepared using the sucrose gradient method. Cells were scraped in mitochondrial isolation buffer containing 250 mM sucrose, 10 mM Tris-HCl (pH 7.4), and 0.1 mM EGTA and homogenized using glass teflon homogenizers. Cells then were centrifuged at 4,000 rpm for 10 min to pellet

nuclei and cell debris. Supernatant was transferred to a new tube and centrifuged at 14,000 rpm for 30 min to pellet mitochondria. Mitochondrial pellets were washed two times with mitochondrial isolation buffer and then lysed in RIPA lysis buffer (25 mM Tris-HCl, 150 mM NaCl, 1% NP-40, 1% sodium deoxycholate, 0.1% SDS) for further analysis.

Western Blotting. Cells were washed with PBS and then lysed in RIPA lysis buffer supplemented with 10% protease inhibitor cocktail (Sigma-Aldrich) and rotated at 4°C for 30 min. Insoluble material was separated by centrifugation at 14,000 rpm for 10 min and supernatants containing soluble proteins were used for further analysis. Protein concentration was determined using Bio-Rad protein assay reagent (Bio-Rad). Equal amounts of proteins were resolved by 10% or 12% SDS-polyacrylamide gels and transferred onto nitrocellulose membranes (LI-COR, Inc., Lincoln, NE). Membranes were blocked in Odyssey blocking buffer (LI-COR) for 1 hr at room temperature (RT) and then incubated with primary (3 hr at RT) and secondary (1 hr at RT) antibodies followed by washing with PBST containing 0.5% Tween 20 (Amresco, 1 x, 5 min) and PBS (3 x, 5 min ea.). After staining with secondary antibodies, membranes were scanned with an Odyssey® CLx Imaging System (LI-COR, Inc., Lincoln, NE) The following primary antibodies were used for Western blotting: BAG3 (Proteintech, 10599-1-AP), SQSTM1/p62 (Cell Signaling Technology, 5114), Parkin (Abcam, ab77924), HSP70 (Santa Cruz Biotech, sc-1060), LC3 (Sigma, L8918), PINK1 (Abcam, ab23707), Tom20 (Abcam, ab199641), GAPDH (Santa Cruz, sc-32233), β-Actin (Santa Cruz, sc-47778), VCP (Santa Cruz, sc-20799), Beclin-1 (Cell Signaling Technology, 3738), Cox-2 (Santa Cruz, sc-1745), Cytochrome c (Cell Signaling Technology, 4272), BAX (Santa Cruz, sc-493) and BAD (Cell Signaling Technology, 9292).

RNA Isolation and Quantitative Reverse Transcription-PCR (qRT-PCR). RNA was extracted from NRVCs using the RNeasy Mini Kit (Ambion) according to the manufacturer's protocol. On column DNA digestion was performed using DNase I (QIAGEN) to decrease DNA contamination in the eluted RNA solution. 1 μg of the isolated RNA was used for reverse transcription and cDNA synthesis with M-MLV Reverse Transcriptase (Invitrogen). qRT-PCR was performed in 20 μL reaction volume with 10 μL SybrGreen master mix (Roche) and Primers. β-actin was used as a reference gene to normalize data. The following primers were used: Park2 FW: 5'-ACCCAACCTCAGACAAGGAC-3'; Park2 RV: 5'-AGACAGGGTTCCTGACATCC-3'; BAG3 FW: 5'-GGCCCTAAGGAAACTGCAT-3'; BAG3 RV: 5'-GGGAATGGGAATGTAACCTG-3'; HSP70 FW: 5'-GCTTCAGACCTCCCTTTGAG-3'; HSP70 RV: 5'-TCCAAGATGCTACGAAGTGG-3'; SQSTM1/p62 FW: 5'-GAGTCATGCTGCACTCCACT-3'; SQSTM1/p62 RV: 5'-TATCAGGCAGGAATGATGGA-3'.

Fluorescence Microscopy. Cells were washed with PBS, fixed with 4% paraformaldehyde (10 min at RT), and permeabilized using 0.5% Triton-X (10 min at RT). Cells then were masked with 0.1 M glycine (pH 3.5, 30 min at RT) followed by blocking (1% BSA, 0.1% Tween 20 in 1x PBS, 30 min at RT). Cells were probed with primary antibody (overnight at 4°C), rinsed in PBS and stained with Alexa Fluor® secondary antibody (Thermo Fisher Scientific) for 1 hr at RT. After mounting in VECTASHIELD hard set mounting medium with DAPI (Vector Laboratories), images were acquired using Leica fluorescent microscope. Tom20 (Abcam, ab56783), BAG3 (Proteintech, 10599-1-AP) and Parkin (Abcam, ab15954) were used as primary antibodies.

ATP Assay. Intracellular ATP was measured using the ATP determination kit (Molecular Probes) according to the manufacturer's protocol. Mitochondria were isolated as described above and lysed in RIPA buffer. Standard reaction solutions containing 8.9 mL dH2O, 0.5 mL 20X reaction buffer, 0.1 mL 0.1M DTT, 0.5 mL of 10 mM D-luciferin and 2.5 uL firefly luciferase (5 mg/mL) were prepared. 10 μL of the lysed mitochondria was added to 90 μL of the standard reaction solution and the luminescence was immediately read using a luminometer (Femtomaster FB 12 luminometer, Zylux).

Cell Death Assays. NRVCs were plated in 96-well plates at a density of 10,000 cells/well. Cells were transduced with either Ad-null or Ad-siBAG3 for 72 hr followed by treatment with different concentrations of CCCP. Cell death was measured using the SYTOX Green cell death assay (Invitrogen. Cells were incubated with SYTOX Green solution for 15 minutes at 37°C followed by measurement of fluorescent emission at excitation/emission maxima of 504/523 nm to detect cells with damaged plasma membranes (SYTOX Green DNA intercalation) vs. live cells (impermeable to SYTOX Green) using a spectrophotometer.

Statistical Analysis. Student's t-test was used to determine the statistical significance of differences between two pairs of data. $P < 0.05$ was considered as statistically significant.

Results

BAG3 knockdown decreases autophagy flux and BAG3 translocates to the mitochondria upon depolarization

In order to assess the role of BAG3 in the regulation of autophagy, cells were treated with either CCCP (20 µM, 6 hr) or bafilomycin A1 (Baf A1, 50 nM, 6 hr) and autophagic activity was evaluated by measuring LC3 I cleavage, an indicator of autophagy, using an anti-LC3 antibody to detect LC3 II on the autophagosomal outer membrane (Pankiv et al., 2007). CCCP was utilized to uncouple the proton gradient and interfere with the electron transport chain across mitochondrial membrane, leading to loss of the mitochondrial membrane potential. CCCP treatment activated mitophagy and increased LC3 II levels, but autophagy flux was reduced in NRVCs with lower levels of BAG3 compared to control cells. Unexpectedly, co-treatment with CCCP and bafilomycin A1 led to a decrease in both LC3 I and LC3 II levels; suggesting that the mitophagy pathway may be inhibited when mitochondrial damage is induced and the lysosome is blocked. Moreover, reductions in LC3 I and LC3 II under these conditions were significantly higher in cells with reduced BAG3 levels compared to control cells. In order to ensure the inhibition of autophagy, the autophagy receptor, p62, was examined and results revealed a significant reduction in p62 levels after bafilomycin A1 and CCCP treatment in BAG3 knock-down cells; indicating an important role for BAG3 in regulating mitophagy (Figure 3.1A).

Since longer stress conditions may result in the complete degradation of autophagy proteins, we examined cells treated with CCCP for a shorter time period (4 hr) and mitochondrial enriched fractions were then isolated by sucrose gradient separation. Results revealed that BAG3 levels did not change in the whole cell lysates (Figure 3.1B). By isolating mitochondria, we found that BAG3 translocated to the mitochondrial fraction

in response to the membrane potential loss (Figure 3.1C). Interestingly, BAG3's binding partner, HSP70, did not translocate to mitochondria. Parkin translocation from the cytosol to the depolarized mitochondria was observed, as has been reported by others (Narendra et al., 2008) and BAG3 knock-down significantly increased Parkin recruitment. p62, Beclin1 and valosin-containing protein (VCP) also translocated to the mitochondria after depolarization, while their degradation was not observed in the whole cell extracts (Figure 3.1B and 3.1C).
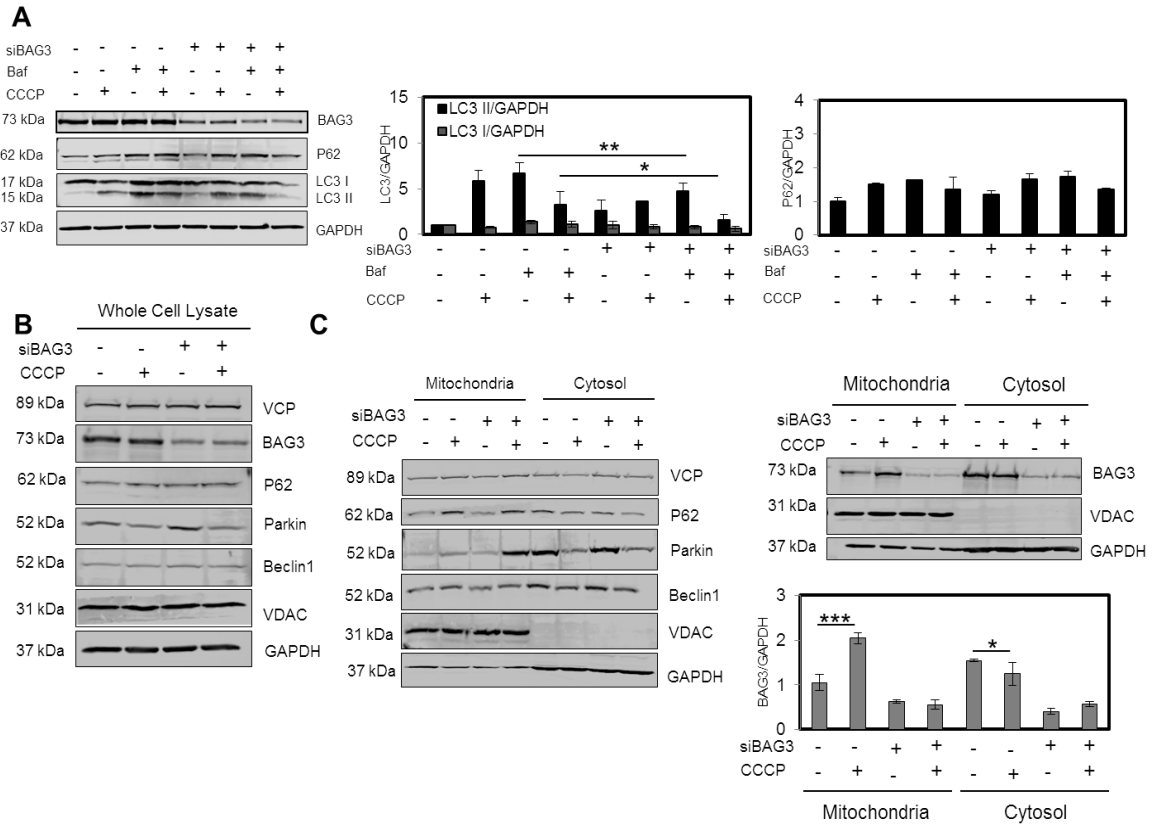
Figure 3.1. BAG3 regulates autophagy and is recruited to mitochondria upon depolarization. (A) NRVCs were treated with CCCP (20 μM, 6 hr) in the absence or presence of Bafilomycin A1 (Baf, 50 nM, 6 hr) and autophagy markers LC3 and p62 were evaluated using Western blot analysis. CCCP treatment increased autophagy marker, LC3 II, and BAG3 knock-down cells had lower autophagy flux compared to control cells. **(B)** The protein expression analysis of the whole cell extract after treatment with CCCP (20 μM, 4 hr). **(C)** NRVCs were treated with CCCP (20 μM, 4 hr) and then mitochondrial fraction was isolated. Mitochondrial and cytosolic fractions were analyzed using Western blot analysis. BAG3 and Parkin translocated to mitochondria upon depolarization and BAG3 knock-down increased the level of Parkin translocated to depolarized mitochondria. VDAC and GAPDH were used as markers of mitochondria and cytosol, respectively (data were normalized with respect to GAPDH).

BAG3 promotes mitochondrial degradation through the autophagy-lysosome pathway when the proteasome is inhibited

Upregulation of BAG3 expression upon proteasome inhibition has been previously reported and BAG3 is believed to mediate the initiation of the autophagy-lysosomal degradation pathway (Liu et al., 2013). We further investigated the mechanism through which BAG3 promotes mitochondrial clearance by inhibiting proteasome activity using MG132 (5 µM for 12 hr). LC3 II levels increased upon blocking of proteasome activity suggesting the activation of autophagy in the absence of the proteasome degradation pathway. Furthermore, proteasome inhibition led to an increase in BAG3, HSP70, and p62 protein levels (Figure 3.2A). When cells were treated with both MG132 and CCCP for 12 hr, BAG3, HSP70, and p62 proteins returned to their basal levels. The ratio of a given protein level to actin level as an internal control is presented in Fig. S1. Moreover, qRT-PCR data showed that mRNA level of these proteins increased when cells were treated with either CCCP or MG132 (Figure 3.2B). Collectively, these data suggest that BAG3, HSP70, and p62 proteins mediate the disposal of damaged mitochondria and their levels are maintained within the normal range under stress conditions.

Fluorescence microscopy showed the localization of BAG3 to perinuclear aggresomes when proteasomal activity was inhibited. Interestingly, these aggresomes were surrounded by a Tom20 network (Figure 3.2C). BAG3 levels in both mitochondria and cytosol fractions increased after proteasome inhibition (Figure 3.2D).
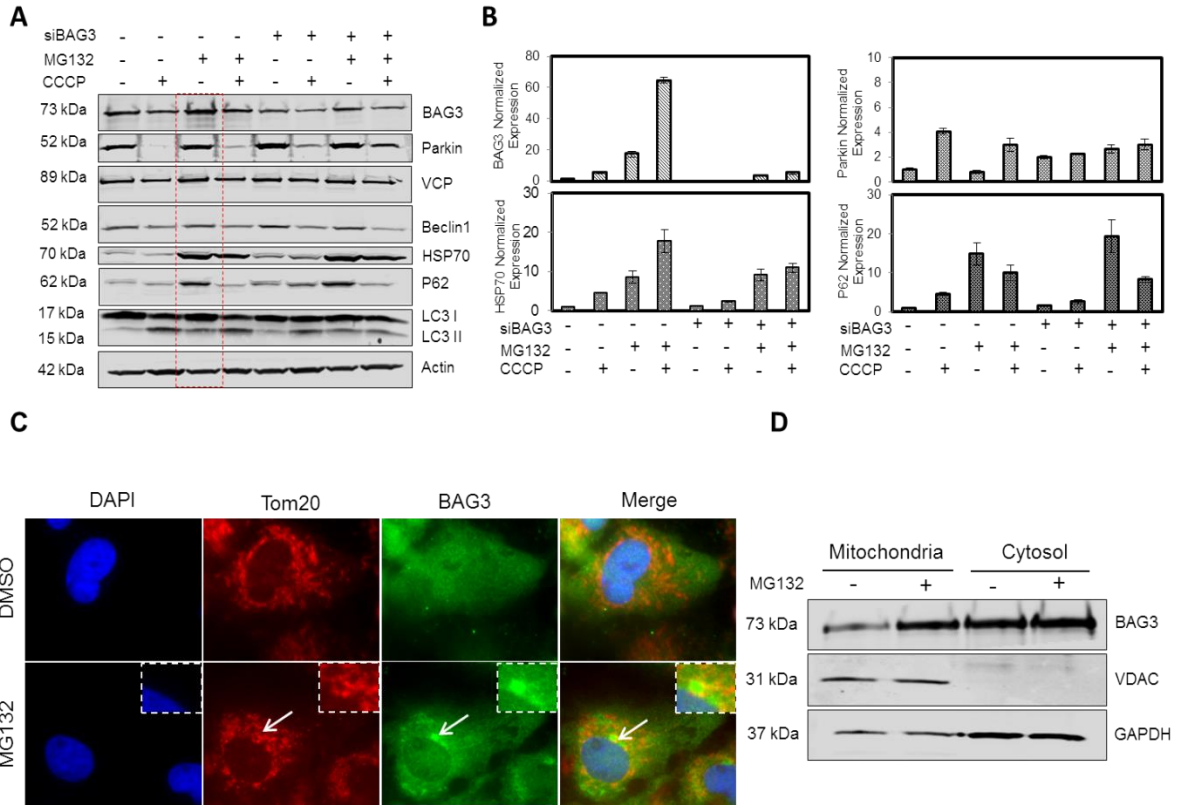
Figure 3.2. BAG3 mediates clearance of defected mitochondria through autophagy-lysosome when proteasome is inhibited. NRVCs were treated with CCCP (20 μM) in the presence or absence of MG132 (5 μM). 12 hr post-treatment, cells were analyzed with **(A)** Western blot for protein analysis or **(B)** qRT-PCR for mRNA expression analysis. **(C)** NRVCs were treated with MG132 (20 μM, 5 hr) and BAG3 and Tom20 localizations were visualized with a fluorescence microscope. **(D)** Mitochondrial and cytosolic fractions were analyzed for BAG3 translocations after proteasome inhibition (20 μM, 5 hr). By inhibiting proteasome, LC3 II level increased, suggesting activation of autophagy-lysosome degradation pathway in the absence of proteasome-ubiquitin pathway. Both mRNA and protein expressions of BAG3, HSP70 and P62 increased by inhibiting proteasome; while Parkin level remained unchanged.

BAG3 knockdown increases Parkin levels and impairs clearance of depolarized mitochondria

Fluorescence microscopy showed that 2 hr CCCP (20 μM) treatment caused fragmentation of the mitochondrial network in that Parkin translocated from the cytosol to the fragmented Tom20 network (Figure 3.3A). Parkin degradation was also observed along with degradation of damaged mitochondria as seen by Western blotting of lysates from NRVCs treated with 20 μM CCCP for 6 hr. Interestingly, reduction of BAG3 levels in NRVCs led to a significant increase in endogenous Parkin levels (Figure 3.3B). Numerous studies have utilized cellular systems that overexpress Parkin for studying the mitochondrial degradation pathway. In light of these observations, we investigated the effect of BAG3 on the expression of exogenous Parkin in the rat cardiac moyoblast cell line, H9c2. Flow cytometry analysis showed that BAG3 knock-down significantly enhanced exogenous Parkin expressed as a YFP-tagged fusion protein (Figure 3.3C and S2). These observations indicate that BAG3 regulates both endogenous and exogenous expression of Parkin, suggesting that BAG3 may function upstream of Parkin in the mitochondrial clearance pathway.

In another experiment, we investigated the effect of BAG3 on the mitochondrial outer membrane protein, Tom20. Our results showed that BAG3 knock-down significantly decreased the clearance of damaged Tom20 in NRVCs treated with 20 μM of CCCP for 12 hr (Figure 3.3D).
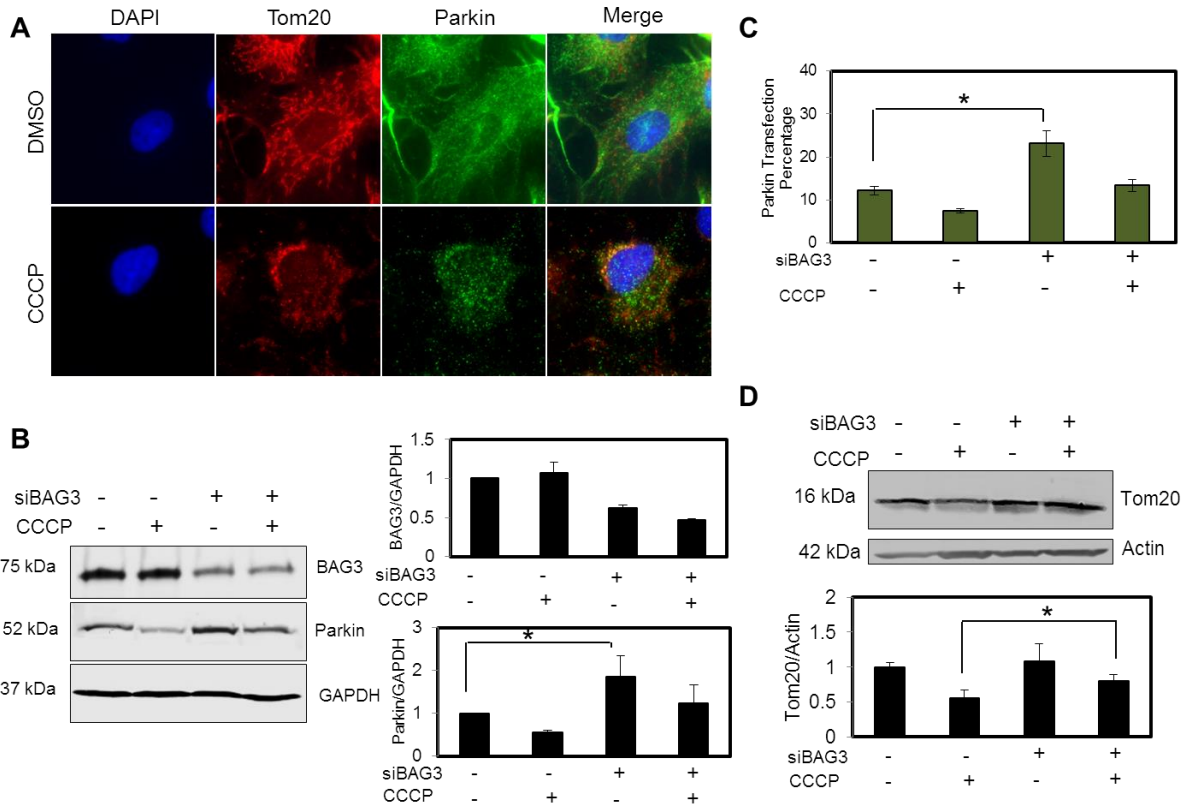
Figure 3.3. BAG3 regulates Parkin expression and BAG3 knock down impairs mitophagy in cardiomyocytes. (A) CCCP (20 µM, 2 hr) treatment caused the fragmentation of Tom20 network and Parkin was recruited to the depolarized mitochondria. **(B)** Parkin degraded along with the mitochondrial degradation after CCCP treatment (20 µM, 6 hr). Parkin endogenous level increased as a result of BAG3 knock down. **(C)** H9c2 cells were transfected with YFP-Parkin with or without BAG3 siRNA. 48 hr after transfection, cells were treated with DMSO or CCCP (20 µM, 4 hr) and fluorescent signal was detected using flow cytometry analysis. Cells with BAG3 suppression showed higher levels of Parkin expressions. **(D)** Knock down of BAG3 significantly inhibited the clearance of Tom20 after CCCP treatment (20 µM, 12 hr).

BAG3 knock-down increases sensitivity to apoptosis

Three days after transduction, NRVCs were treated with 20 µM CCCP for 4 hr and then mitochondrial fractions were isolated to analyze ATP level. Intracellular ATP levels were decreased upon treatment of cells with CCCP. Although knock-down of BAG3 only changed ATP levels after CCCP treatment, NRVCs knocked-down for BAG3 had higher ATP levels compared to control cells. Here, BAG3 expression was measured in cytosolic protein extracts (Figure 3.4A). Western blot data also showed that levels of the mitochondrial-encoded Cox-2 protein in the whole cell protein lysates increased after CCCP treatment (Figure 3.4B).

In order to investigate the role of BAG3 in mitochondria-associated apoptosis, NRVCs were treated with 20 µM CCCP for 6 hr and the expressions of pro-apoptotic proteins such as Bcl-2-associated death protein (BAD) and Bcl-2-associated X protein (BAX) were analyzed by Western blot. BAD and BAX are involved in the initiation of apoptosis and their upregulation is associated with increased cell death (Brunelle et al., 2009). Cytochrome c levels were elevated after CCCP treatment. BAX and BAD levels were upregulated after CCCP treatment in whole cell extracts from NRVCs knocked-down for BAG3, indicating that BAG3 knock-down sensitizes the cells to mitochondrial stress conditions (Figure 3.4C).

In another experiment, cell death was measured after 6 hr treatment of NRVCs with increasing concentrations of CCCP. Results showed that BAG3 knock-down significantly increased cell death as measured by SYTOX Green when mitochondrial stress was applied (Figure 3.4D).
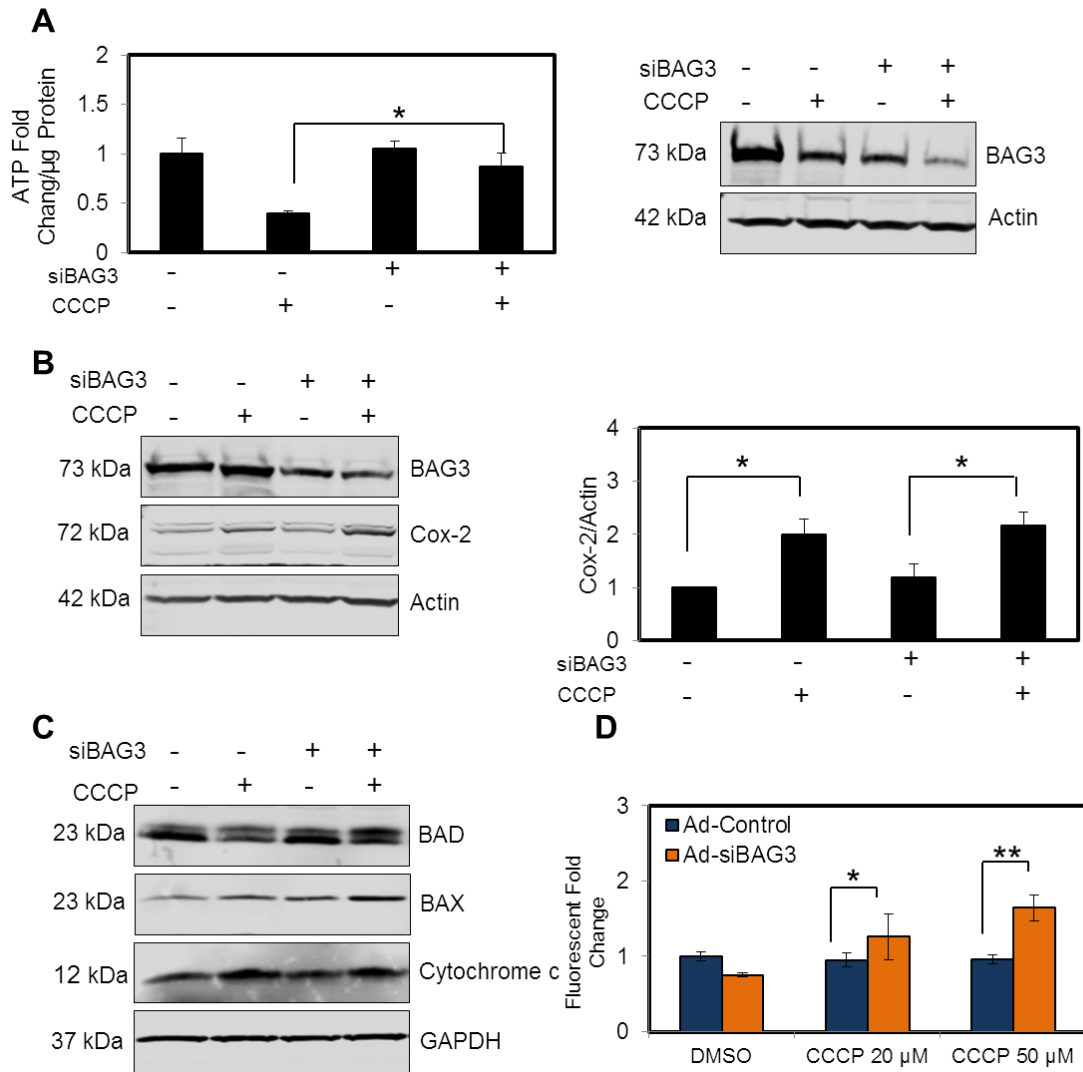
Figure 3.4. Cellular death and bioenergetics assays after CCCP treatment. (A) Mitochondrial fractions were isolated and intracellular ATP level was measured. CCCP treatment led to the decrease in ATP level. BAG3 knock-down cells showed a higher ATP level compared to the control cells treated with CCCP, suggesting the impairment of mitochondrial clearance in the absence of BAG3. **(B)** Cox-2 protein level increased after CCCP treatment. **(C)** The expression of pro-apoptotic proteins after CCCP treatment was analyzed using Western blot analysis. **(D)** NRVCs were treated with CCCP (20 µM or 50 µM) and cell death was analyzed using SYTOX Green cell death assay. BAG3 knock-down cells showed more sensitivity to mitochondrial stress condition. *$P<0.05$; **$P<0.01$.

Discussion

The results presented herein show that BAG3 and Parkin both translocate to mitochondria upon depolarization. BAG3 knockdown impaired the clearance of damaged Tom20 and increased the level of Parkin translocated to the mitochondria after CCCP treatment. It was previously reported that BAG3 knock-down increased the amount of mitochondria in HeLa cells (Rodriguez et al., 2016). The accumulation of dysfunctional mitochondria within cells has been implicated in the development of neurodegenerative disorders such as Parkinson's disease. In this regard, mitophagy functions as a protective response and selectively targets damaged mitochondria for degradation (Matsuda et al., 2015). Upon mitochondrial depolarization, Parkin as an E3 ubiquitin ligase ubiquitinates the damaged mitochondria in a PINK1-dependent manner (Vincow et al., 2013). The ubiquitin tag is then recognized by the mitophagy machinery and the selected mitochondria are targeted for lysosomal degradation. This model was further refined by Lazarou et al., (2015) reporting that PINK1 phosphorylates ubiquitin thus activating Parkin recruitment, and Parkin triggers recruitment of autophagy receptors by adding ubiquitin chains to the mitochondrial outer membrane proteins. Moreover, the recruitment of the autophagy receptors, NDP52 and Optineurin (OPTN), by PINK1 were found to be independent of Parkin, as this was observed in HeLa cells lacking Parkin (Lazarou et al., 2015). Moreover, *in vivo* studies showed that even though mitochondrial fragmentation was observed in respiratory chain-deficient dopaminergic neurons, Parkin did not translocate to the defective mitochondria and the absence of Parkin did not alter the clearance of dysfunctional mitochondria (Sterky et al., 2011). These observations are highly consistent with our findings indicating that BAG3 may function upstream of Parkin in mitochondrial clearance.

The two main pathways through which intracellular degradation is carried out to maintain protein quality control are the ubiquitin-proteasome and the autophagy-lysosome pathways (Pankiv et al., 2007). Parkin has been reported to mediate the proteasomal degradation of mitochondrial outer membrane proteins (Chan et al., 2011; Yoshii et al., 2011). In mouse embryonic fibroblasts overexpressing Parkin, the degradation of mitochondrial outer membrane proteins happened through Parkin-mediated proteasomal pathway while the degradation of inner membrane and matrix proteins relied mainly on mitophagy (Yoshii et al., 2011). We found that Parkin levels did not increase by blocking proteasome activity, suggesting the possibility of a dual role for Parkin in both ubiquitin-proteasome and autophagy-lysosome pathways.

BAG3 has been reported to play an important role in regulating autophagy through aggresome targeting. In this pathway, BAG3 transports HSP70-bound substrates to aggresomes residing in the perinuclear area by interacting with microtubules. The cargo is then directed to lysosomes through the autophagy process for degradation (Gamerdinger et al., 2011). It has been reported that the HSP70 chaperon protein functions in protein quality control through recognition of misfolded proteins (Behl et al., 2011). BAG3 binds to the ATPase domain of HSP70 through its BAG domain and modulates its chaperonic activity (Liu et al., 2013; Arimura et al., 2011; Behl et al., 2011). Although BAG3 translocates to depolarized mitochondria, no such translocation was observed for HSP70. These results suggest that BAG3 may function upstream of HSP70 in the recognition of cargo in the mitophagy process.

Our results indicate that the autophagy receptor, p62, translocated to the mitochondria upon membrane potential loss. SQSTM1 has been reported to play a protective role under conditions of proteasome inhibition (Milan et al., 2015). p62 functions as a cargo receptor and binds to both ubiquitinated and non-ubiquitinated substrates and triggers

their autophagic clearance (Pankiv et al., 2007; Watanabe et al., 2011; Behl et al., 2011).

Beclin 1 is the mammalian homolog of yeast Vp30/Atg6 and is essential for autophagosome formation. Upon blockage of the ubiquitin-proteasome pathway in HepG2 cells, BAG3 promoted autophagy initiation; which was not suppressed by silencing of Beclin 1, indicating a non-canonical autophagy initiation (Liu et al., 2013). VCP functions as a segregase in Parkin-mediated mitophagy and extracts autophagy components from the ubiquitinated proteins. VCP mutations in mouse embryonic fibroblasts overexpressing Parkin impaired mitophagy (Kim et al., 2013). Our results showed that both Beclin 1 and VCP translocated to the depolarized mitochondria and their degradation in whole cell lysate was observed upon treatment of the cells with CCCP.

Our data indicate that CCCP treatment causes ATP depletion in cardiomyocytes. CCCP interferes with mitochondrial ATP synthesis by damaging the electron transport chain and causes uncontrolled oxygen consumption. The mitochondrial encoded protein, Cox-2, which plays a role in electron transport, increases to maintain ATP homeostasis. Cells with reduced BAG3 expression indicated higher ATP levels compared to those maintaining basal BAG3 levels when they were treated with CCCP, suggesting less clearance of mitochondrial proteins. HeLa cells overexpressing Parkin showed faster clearance of depolarized mitochondria and less cell viability when they were cultured in galactose media compared to cells with endogenous Parkin level; indicating that more mitochondrial clearance caused a lower ATP concentration and led to cell death when glycolysis was inhibited (Narendra et al., 2008).

Accelerated cell death in cardiomyocytes is accompanied with the development of degenerative cardiovascular diseases (Brunelle et al., 2009). BAG3 functions as an anti-apoptotic protein through interaction with Bcl2 (Knezevic et al., 2015). Apoptotic cell death significantly increased in neonatal rat cardiomyocytes with BAG3 mutations (Arimura et al., 2011). High levels of BAG3 were found in pancreatic tumor cells compared to normal pancreas tissue which promoted malignancy by functioning as an anti-apoptotic protein (Liao et al., 2001). BAX and BAD belong to the Bcl2 protein family and function as pro-apoptotic proteins. Higher levels of BAX in pancreatic cancer cells were associated with longer survivability of pancreatic cancer patients (Liao et al., 2001). Cytochrome c levels significantly increased in response to CCCP treatment. BAX and BAD showed higher levels in BAG3 knock-down cells compared to the control cells after CCCP treatment. Increased levels of these pro-apoptotic proteins in the cells with reduced BAG3 levels makes cells more susceptible to death when mitochondrial stress is induced. Moreover, when the autophagic machinery is not working properly to clear damaged mitochondria, cells are exposed to the toxic effects of free radicals and oxidative stress which trigger death signaling. Collectively, these results indicate that BAG3 plays a vital role in mitochondrial quality control within cardiomyocytes and its reduction impairs the clearance of damaged mitochondria (Figure 3.5).
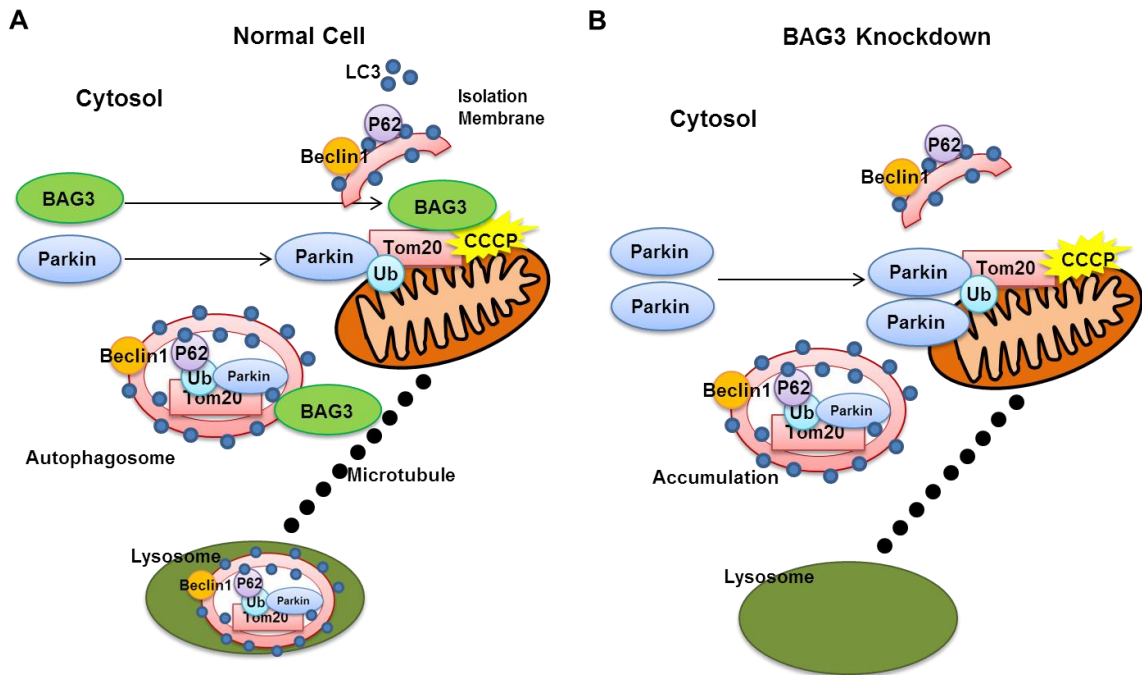
Figure 3.5. Schematic diagram of Tom20 degradation in cardiomyocytes. (A) BAG3 and Parkin translocate from cytosol to mitochondria upon depolarization. Parkin functions as an E3 ubiquitin ligase and ubiquitinates Tom20. Tom20 is then sequestered within autophagosome and BAG3 through interactions with microtubule, targets the cargo for lysosomal degradation. **(B)** BAG3 knockdown increases Parkin expression and more Parkin translocates from cytosol to depolarized mitochondria. Autophagy flux decreases and Tom20 clearance is impaired when BAG3 is not present, suggesting that BAG3 is one of the key regulators of mitophagy in cardiomyocytes.

5. Supplementary Figures
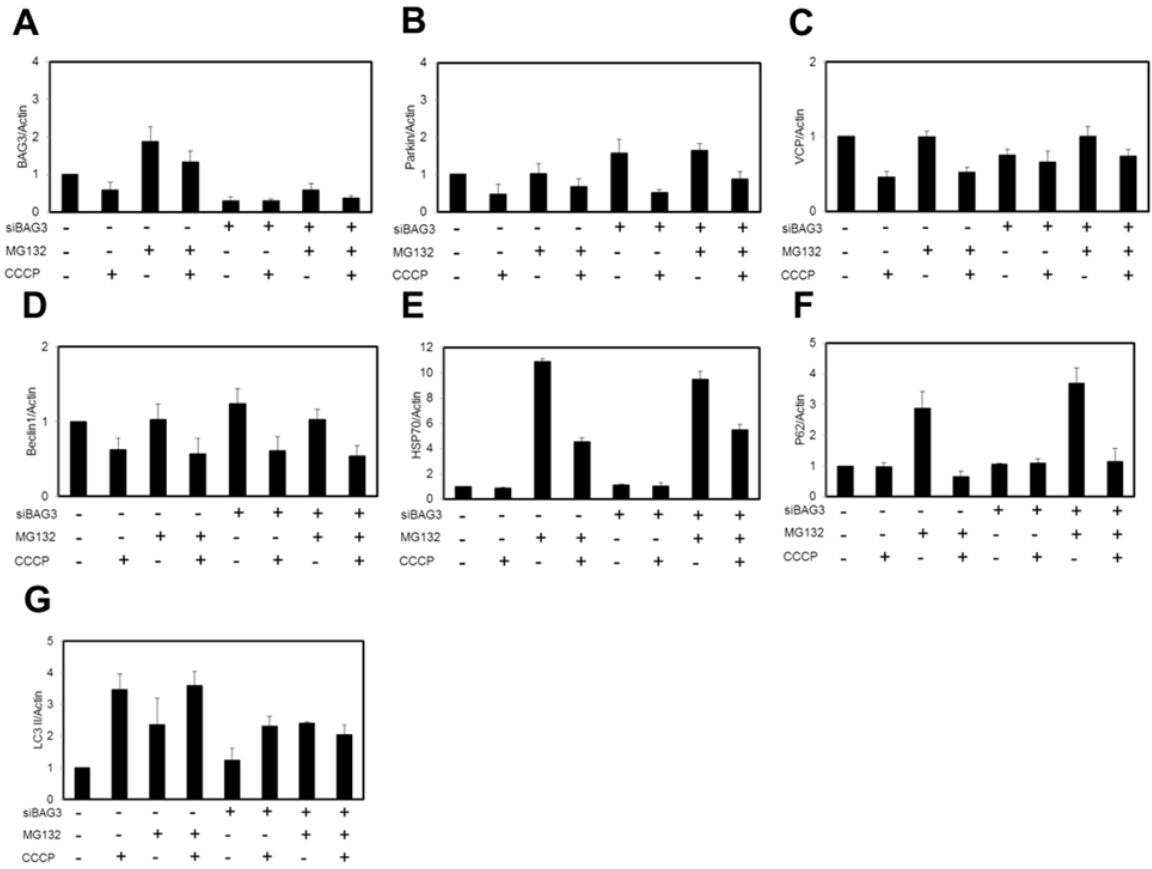
Figure S 1. Protein level normalized to Actin level after proteasome inhibition. NRVCs were treated with MG132 (5 µM, 12hr) in the presence or absence of CCCP (20 µM, 12 hr). Protein levels of **(A)** BAG3, **(B)** Parkin, **(C)** VCP, **(D)** Beclin 1, **(E)** HSP70, **(F)** P62 and **(G)** LC3 II are normalized to Actin levels.
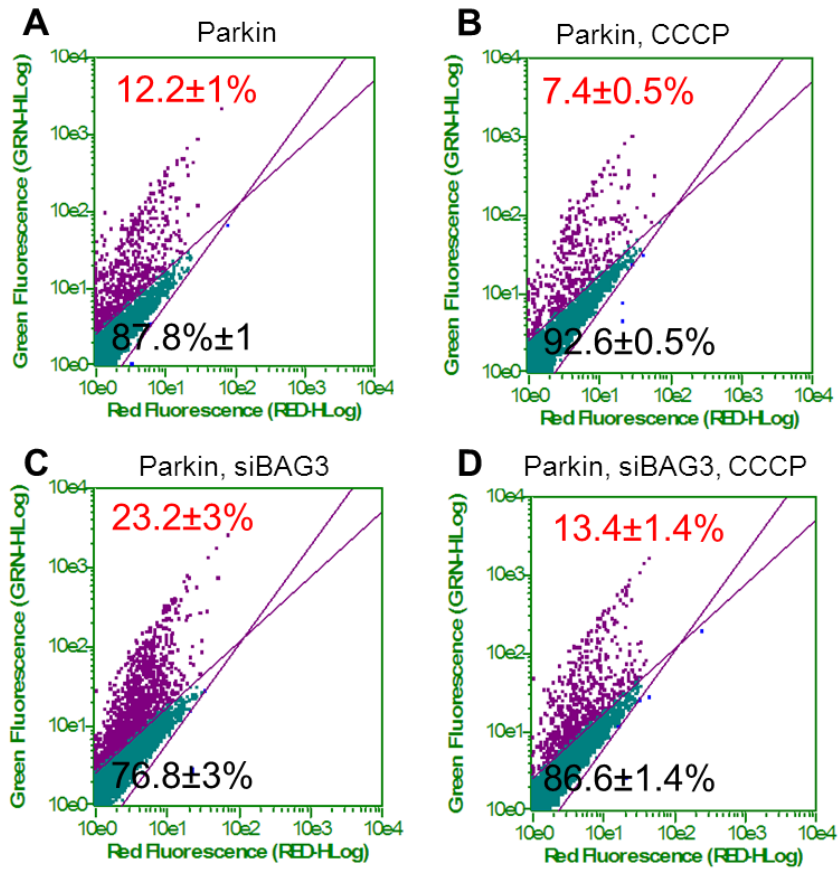
Figure S 2. BAG3 increases exogenous Parkin expression. H9c2 cells were transfected with fluorescent Parkin plasmid with or without BAG3 siRNA and fluorescent signals were detected using flow cytometry in **(A)** Parkin overexpression **(B)** Parkin overexpression and CCCP treatment, **(C)** Parkin overexpression and BAG3 knockdown, and **(D)** Parkin overexpression, BAG3 knockdown and CCCP treatment conditions.

CHAPTER 4

ROLE OF BAG3 IN QUALITY OF GAP JUNCTION PROTEIN, CONNEXIN 43, IN CARDIOMYOCYTES

Abstract

BAG3 is a stress-induced pleiotropic protein involved in both autophagy and apoptosis. Ablation of the BAG3 gene causes a broad range of pathology in the heart. In cardiomyocytes, changes in BAG3 perturb expression and activity of autophagy proteins involve in protein quality control. Here, we demonstrate that BAG3 regulates expression of Connexin 43, Cx43, one of the major proteins in gap junction structure which has a short half-life and rapid turnover and is involved in intercellular communication by gap junctions. Any pathological stress which impairs proper turnover of Cx43 and/or the state of its phosphorylation can adversely impact on myocardial cell behavior, thus leading to the development of cardiac disease and heart failure. Our results in primary neonatal rat ventricular cardiomyocytes show that any impairment of autophagy-lysosome pathway, either by inhibiting lysosomal activity or suppressing the level of BAG3, dysregulates proper turnover of Cx43. Inhibition of lysosomal activity leads to the accumulation of Cx43 aggregates and suppression of BAG3 significantly reduces turnover of Cx43. In addition, knock-down of BAG3 downregulates the levels of Cx43 by dysregulating its stability through a translational pathway. Under stress, expression of BAG3 impacts on the state of Cx43 phosphorylation and its degradation. Furthermore, we found co-localization of BAG3 with the cytoskeleton protein, tubulin, and depolymerization of tubulin leads to the accumulation of hypophosphorylated Cx43. These observations ascribe a novel function for BAG3 that involves control of quality of Cx43 under normal and stress conditions and potentially optimizing communication of cardiac muscle cells through gap junctions.

Introduction

Gap junctions are protein structures which permit metabolic and electrical coupling between two neighboring cardiomyocytes and mediate cell-to-cell communication. Each gap junction channel consists of two hemi-channels on the plasma membrane of two adjacent cells known as connexons. Connexons are formed by the assembly of hexameric complexes of connexin transmembrane proteins [Zhou et al., 2014]. In healthy heart, conduction of action potential through gap junctions maintains the heart's regular rhythm and contraction while under pathological condition, impairment of action potential propagation through myocardium results in arrhythmia and cardiovascular disease [Severs et al., 2004]. Among the members of the connexin protein family, connexin 43 (Cx43) is highly expressed in heart tissue and has a short half-life of between 1-5 hr [Saffitz et al., 2000]. Therefore, maintaining the homeostasis of Cx43 as a balance between its degradation and proper delivery of newly synthesized Cx43 to plasma membrane is of great importance for maintaining conduction of cardiac tissue and avoiding arrhythmia [Saffitz et al., 2000, Epifantseva et al., 2017].

Previous reports have described degradation of Cx43 through three main pathways: autophagy [Epifantseva et al., 2017], ubiquitin-proteasome [Leithe et al., 2004] and endo-lysosome [Gilleron et al., 2008]. Autophagy is an intracellular degradation mechanism which plays an important role in maintaining cardiac homeostasis by regulating cellular metabolism and energy balance [Lavandero et al., 2015]. In this process, damaged organelles and protein aggregates are engulfed within double-membrane vesicles, referred to as autophagosomes, and delivered for degradation and removal by lysosomes [Johansen et al., 2011]. The protective role of autophagy in the

76

heart under stress condition has been reported by several researchers [Su et al., 2016, Zhnag et al., 2016, Wu et al., 2017]. Recently, we reported that induction of autophagy in mice with myocardial ischemia/reperfusion injury significantly reduced infarct size and ameliorated heart function [Su et al., 2016]. Earlier studies demonstrated that autophagy is also involved in degradation of internalized gap junctions in cells overexpressing Cx43 [Fong et al., 2012]. However, the underlying mechanisms and key molecular players are poorly understood.

Among the various regulators of protein quality control (PQC), BAG3 has been reported to be a key regulator of the autophagy pathway in various cell types especially in the heart. BAG3 is a 575-amino acid protein which is highly expressed in cardiac and skeletal muscle [Knezevic et al., 2015]. BAG3 interacts with the ATPase domain of heat shock protein 70 (HSP70) through its BAG domain and regulates the function of the HSP70/HSC70 molecular chaperone to maintain protein homeostasis [Rosati et al., 2011]. BAG3 functions as an anti-apoptosis protein through binding with Bcl-2 and overexpression of BAG3 in cancer cells contributes to tumor resistance to chemotherapy [Liao et al., 2001]. Mutations of BAG3 impair Z-disc assembly and led to development of dilated cardiomyopathy [Feldman et al., 2014, Arimura et al., 2011, Franaszczyk et al., 2014]. BAG3 deficiency results in myofibrillar degeneration followed by development of lethal cardiomyopathy and death by 4 weeks of age [Homma et al., 2006]. While the role of BAG3 in quality control has been reported by several researchers, to our knowledge, there is no study describing the impact of BAG3 on gap junction quality control, either in basal or stress conditions. We hypothesized that BAG3 might be an important molecular player in regulating the life cycle of Cx43 and evaluated the role of BAG3 in maintaining Cx43 homeostasis.

In this study, we used primary cultures of neonatal cardiomyocytes and found that there was a significant reduction in Cx43 abundance as well as Cx43 flux in BAG3-suppressed cardiomyocytes. In addition, we found that suppression of BAG3 resulted in destabilization of Cx43. We also examined the impact of BAG3 on Cx43 degradation under starvation stress conditions and found that when BAG3 was knocked down, stress-induced degradation of Cx43 was significantly impaired. In addition, our results showed that BAG3 colocalized with the tubulin network and tubulin depolymerization led to significant accumulation of Cx43 within cardiomyocytes.

Experimental

Isolation of cardiomyocytes and culture conditions

All experiments were performed in accordance with the guidelines and regulations of the Temple University Institutional Animal Care and Use Committee. NRVCs were isolated from 1-2 day old Sprague-Dawley rats (Charles River) following the protocol described previously [Gupta et al., 2016]. Isolated cardiomyocytes were cultured in Dulbecco's modified Eagle's medium (DMEM, Life Technologies, Carlsbad, CA) supplemented with 2% fetal bovine serum (FBS, Denville Scientific Inc., Hollistion, MA) and 25 µg/ml gentamicin (Life Technologies).

Adenoviral transduction

NRVCs were transduced with Ad-siBAG3 (Vector Biolabs, Malvern, PA) in reduced volumes of FBS-free DMEM at 37°C for 2 hr. The medium was then replaced with DMEM with 2% FBS and 25 µg/ml gentamicin. As an internal control, cells were transduced with Ad-GFP (Vector Biolabs, Malvern, PA). Transduced cardiomyocytes were subjected to other treatments 3 or 5 days post transduction.

Western blot

NRVCs were washed with cold 1X PBS and lysed in RIPA buffer (25 mM Tris-HCl, 150 mM NaCl, 1% NP-40, 1% sodium deoxycholate, 0.1% SDS) supplemented with mammalian protease inhibitor cocktail (Sigma-Aldrich). After 30 min, cells were rotated at 4°C, they were spun down at 14000 rpm for 10 min and supernatants were kept as soluble fractions of cell lysates. In order to prepare insoluble fractions, lysis buffer insoluble pellets were washed with cold 1X PBS and dissolved in 2% (w/v) SDS for 30 min at room temperature (RT). Protein concentrations were determined using Bio-Rad Protein Assay Dye. Equal amounts of protein lysates were separated using 10% and 12% SDS polyacrylamide gels and transferred onto wet nitrocellulose membranes (LI-

COR) using Bio-Rad's Western blot system. Membranes were incubated for 3 hr with primary antibody (diluted 1:1000) and 1 hr with secondary antibody (diluted 1:10000) followed by washing with PBST containing 0.5% Tween 20 (1x, 5 min) and 1X PBS (3x, 5 min ea.) after each antibody incubation. The following antibodies were used: BAG3 (Proteintech, 10599-1-AP), LC3 (Sigma, L8918), Cx43 (Abcam, ab11370), α-Tubulin (Sigma, T6074), HSP70 (Santa Cruz, sc-24), Actinin (Sigma, A7732), AKT (Cell Signaling, 9272), PAKT (Cell signaling, 9271).

Immunocytochemistry

NRVCs were grown in 2-well chamber slides (Lab-Tek®), fixed with 4% paraformaldehyde (10 min, RT) and permeabilized with 0.5% Triton-X 100 (10 min, RT). Cells were then incubated with 0.1 M glycine (pH 3.5, 30 min, RT), blocked with 1% (w/v) bovine serum albumin solution containing 0.1% Tween 20 (30 min, RT) and labeled for 3 hr at RT with primary antibody (diluted 1:100) and then 1 hr at RT with Alexa Fluor® secondary antibody (diluted 1:200, Thermo Fisher Scientific, Eugene, OR). Cardiomyocytes were then mounted with DAPI-containing VECTASHIELD hard set (Vector Laboratories) and imaged using a Leica fluorescent microscope (Leica Microsystems, Deerfield, IL). The following antibodies were used: Cx43 (Abcam, ab11370), Actinin (Sigma, A7732), AKT (Cell Signaling, 9272), PAKT (Cell signaling, 9271), BAG3 (Proteintech, 10599-1-AP) and α-Tubulin (Sigma, T6074).

Co-Immunoprecipitation (Co-IP)

NRVCs were lysed in lysis buffer (20 mM Tris HCl pH 8, 137 mM NaCl, 10% glycerol, 1% Nonidet P-40 and 2 mM EDTA) and rotated with a specific antibody for BAG3 or normal rabbit serum (NRS) as control for 4 hr at 4°C. The resultant lysates were then rotated with protein A/G beads (Pierce) for 4 hr at 4°C followed by washing and analysis by western blotting.

Scrape-loading dye transfer

NRVCs were seeded in Lab-Tek® chamber slides and transduced with either Ad-control or Ad-siBAG3 for 3 days. Confluent cardiomyocytes were washed twice with HBSS medium and then scrape-loaded with 1.5 mg/mL sulforhodamine B (MP Biomedicals) followed by incubation at room temperature for 3 min. Cells were rinsed and fixed with PFA 4% at 4°C and imaged using Keyence BZ-X710 fluorescent microscope. Maximum dye transfer distance was quantified by taking two points in each image using Image J analysis.

Statistical analysis

Data are presented as mean ± SD. Student's *t*-test was utilized to calculate the significance of the differences between two groups. *P* values less than 0.05 was considered as statistically significant.

Results

Knock-down of BAG3 reduces lysosomal flux and protein levels of Cx43

As a first step, expression of Cx43 was analyzed in protein lysates of NRVCs by using an antibody against Cx43. Protein migration on SDS-PAGE gels resulted in triplet bands of phosphorylated Cx43 (P-Cx43) and non-phosphorylated Cx43 (NP-Cx43) around 40 kDa to 43 kDa which are indicative of its post-translational modifications and phosphorylation state (Figure S1A). In order to investigate whether Cx43 degradation in NRVCs occurs through lysosome, lysosomal activity was inhibited by treating the cardiomyocytes with 50 nM Bafilomycin A1 (BafA1) for 3 hr and the levels of autophagy markers, LC3 I and LC3 II, and Cx43 were analyzed by Western blot. BafA1 inhibits lysosomal acidification and blocks the fusion between autophagosome and lysosome by impairing the function of proton pumps in the lysosomal membrane [Mauvezin et al., 2015]. Data indicated that inhibition of lysosome resulted in the significant increase in the levels of LC3 I and LC3 II. Western blot data showed that the levels of phosphorylated (P-) and non-phosphorylated Cx43 (NP-Cx43) significantly increased as a result of lysosomal blockage (Figure 1A-D). We also investigated whether Cx43 degrades through the proteasome in cardiomyocytes. For this purpose, cells were treated for 12 hours with 5 µM MG132 and Cx43 levels were investigated. Western blot and quantification showed that only the levels of phosphorylated Cx43 significantly increased as a result of proteasome inhibition (Figure S1B-C). These findings were further confirmed by monitoring Cx43 localizations and morphology in control as well as cardiomyocytes treated with BafA1. Immunocytochemistry imaging indicated that Cx43 protein was highly expressed in plasma membrane of the primary cardiomyocytes. In the presence of BafA1, Cx43 aggregates were detected accumulated in the cytoplasm; suggesting that Cx43 degrades through lysosomal pathway (Figure 1E).

BAG3 functions with HSP70/HSC70 chaperone complex and regulates degradation of misfolded and damaged proteins through autophagy-lysosome pathway [Stürner et al., 2017]. BAG3's role in maintaining PQC has been investigated by several researchers but, to our knowledge, its role in the quality control of Cx43 has not been reported. To understand the role of BAG3 in the quality control of Cx43, NRVCs were knocked down for BAG3 using adenovirus transduction of siRNA to BAG3 for 3 and 5 days. Transduced cardiomyocytes were then treated with BafA1 and the levels of autophagy marker, LC3 II, P-Cx43 and NP-Cx43 were evaluated. Western blot data and quantification analysis of the soluble fractions showed that LC3 II levels significantly reduced in BAG3-suppressed cardiomyocytes compare to control cells. Furthermore, Cx43 levels significantly increased in the presence of BafA1 in control cells, but BafA1 treatment did not lead to significant increase in Cx43 levels in BAG3-suppressed NRVCs suggesting that knock-down of BAG3 has impaired lysosomal turnover of Cx43 (Figure 1F-I). Considering the notion that Cx43 is a membrane-spanning protein, we analyzed the insoluble fraction of cell lysates as well. Western blot data revealed that Cx43 protein levels significantly reduced in NRVCs knocked down for BAG3 (Figure 1J-L). We also investigated the effect of BAG3 suppression on proteasomal degradation of Cx43. For this purpose, transduced cardiomyocytes were treated with MG132 (5 µM, 12 hr) and the levels of Cx43 were investigated. Western blot data of the soluble and insoluble fractions and quantification showed that Cx43 proteasomal degradation was not affected by BAG3 suppression. (Figure S1D-G). α-tubulin served as a loading control for both soluble and insoluble fractions. Taken together, these results suggest that dysregulating the autophagy-lysosome pathway either by inhibiting the activity of lysosomal or suppressing BAG3 as a key molecular player in autophagy, impairs proper turnover of Cx43.
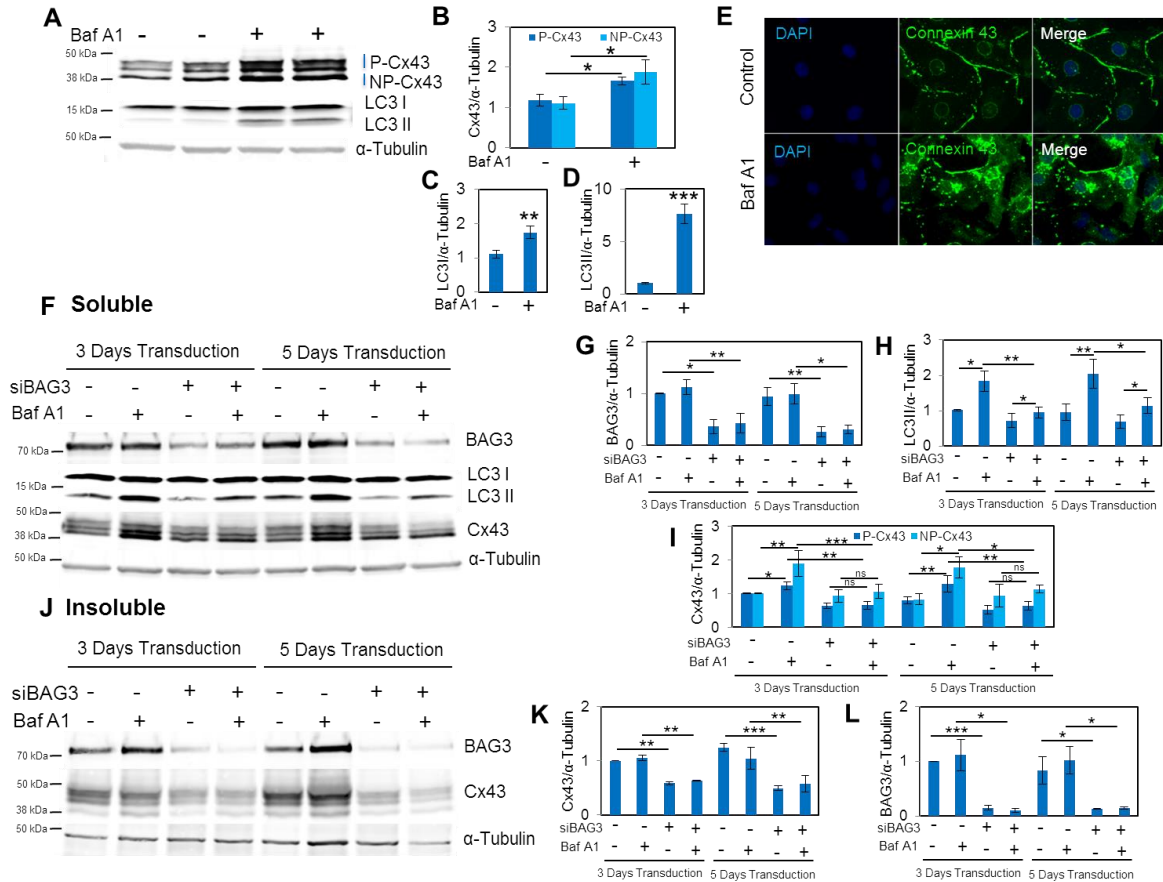
Figure 4.1. Cx43 degrades through autophagy-lysosome pathway and knock-down of BAG3 reduces protein levels of Cx43. (A-D) NRVCs were treated with the autophagy inhibitor BafA1 (50 nM, 3hr) and the levels of autophagy proteins, LC3 I and LC3 II, and Cx43 were measured and quantified. Western blot data showed that the levels of LC3 I, LC3 II and P-Cx43 and NP-Cx43 significantly elevated in the presence of BafA1. .*p<0.05; **p<0.01; ***p<0.001 (n=4). **(E)** Microscopic imaging using an antibody against Cx43 indicated that Cx43 is highly expressed in plasma membrane of NRVCs control cells. Internalized Cx43 aggregates were observed in NRVCs treated with lysosomal inhibitor BafA1 (50 nM, 3hr). NRVCs were transduced with either Ad-siBAG3 or Ad-control for 3 or 5 days in the presence or absence of BafA1 (50 nM, 3hr) and Cx43 levels were measured and quantified. **(F-I)** Western blot and quantifications of the soluble fractions of cell lysates indicated that autophagy flux of LC3 II, P-Cx43 and NP-Cx43 were significantly inhibited in NRVCs knocked down for BAG3.*p<0.05; **p<0.01, ***p<0.001 (n=3). **(J-L)** Western blot of the insoluble fractions of cell lysates indicating that Cx43 protein levels were significantly reduced in NRVCs knocked down for BAG3. **p<0.01; ***p<0.001 (n=3). α-Tubulin served as a loading control for both soluble and insoluble fractions.

BAG3 plays an important role in regulating stability of Cx43

Because we observed reduced levels of Cx43 in response to BAG3 knock-down and considering the role of BAG3 as a co-chaperone in protein stabilization [Fang et al., 2017], we next investigated whether BAG3 affects the stability of Cx43 through a translational pathway. To this end, transduced NRVCs were treated with the translation inhibitor, cycloheximide, for different time intervals and Cx43 levels were then evaluated by Western blot. Our data indicate that reduction of Cx43 protein at each time point was significantly higher in cardiomyocytes with BAG3 knocked down compared to control cells. At 6 hours post treatment with cycloheximide, the difference in Cx43 reduction between control and cardiomyocytes with BAG3 knocked down was insignificant. Furthermore, we investigated the effect of BAG3 suppression on translation of LC3 and found that LC3-II levels were significantly reduced in siBAG3-transduced NRVCs compare to control cells when cells were treated with cycloheximide (Figure 4.2A-D). The role of BAG3 in regulating mRNA translation of LC3-II was recently reported in HeLa cells and our data are consistent with those published previously [Rodriguez et al., 2016]. In addition, we also evaluated the protein levels of the BAG3 partner, HSP70, in control as well as BAG3-suppressed cardiomyocytes and did not detect any significant reduction in HSP70 levels as a result of cycloheximide treatment, either in control or BAG3-suppressed cardiomyocytes (Figure S4A-C). Taken together, our results suggest that BAG3 plays a key role in controlling the stability of Cx43 and LC3 II proteins in primary cardiomyocytes.
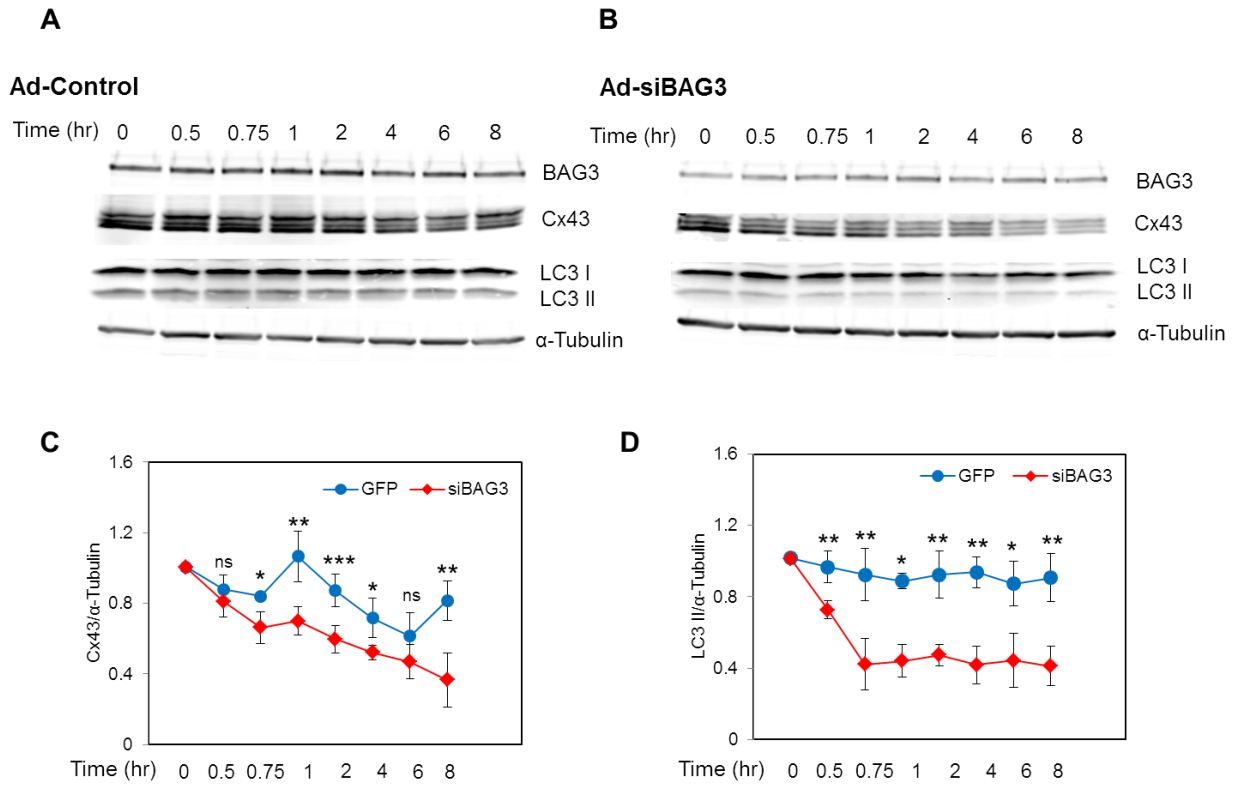
Figure 4.2. BAG3 plays a key role in regulating the stability of Cx43. (A-D) NRVCs were transduced with either Ad-siBAG3 or Ad-control for 3 days. Transduced NRVCs were then incubated with the mRNA translation inhibitor cycloheximide (10 µg/ml) for different time intervals (0, 30 min, 45 min, 1 hr, 2 hr, 4 hr, 6 hr and 8 hr) and the expression of autophagy marker LC3 II and Cx43 proteins were measured by Western blot. LC3-II and Cx43 levels for each condition (Ad-siBAG3 or Ad-control) at each time point were quantified and normalized to their levels at time zero. *$p<0.05$; **$p<0.01$; ***$p<0.001$ (n=5). α-Tubulin served as a loading control.

Cx43 dynamics under nutrient starvation

In order to explore the molecular mechanism underlying the turnover of Cx43 under pathological conditions, NRVCs were exposed to HBSS starvation medium and Cx43 expression and localization were investigated. Western blotting analysis of the soluble fraction of cell lysate indicated that starvation led to reduction in P-Cx43, while NP-Cx43 level increased over time. Quantification analysis revealed that 10 hours post starvation, there was a 55% and a 22% decrease in the levels of P-Cx43 and total Cx43, respectively. No significant change in the expression of BAG3 was found (Figure 4.3A-C). We also analyzed the insoluble fraction of cell lysate and found that consistent with data from the soluble fraction, P-Cx43 reduced and NP-Cx43 increased as a result of starvation. Previous studies have reported dephosphorylation [Beardslee et al., 2000] and autophagic degradation [Martins-Marques et al., 2015] of Cx43 during ischemic stress conditions. However, the precise pathways and key molecular players still remain unknown. Our results indicate that although dephosphorylation of Cx43 increased as a result of nutrient starvation, but 10 hours post starvation, total Cx43 expression exhibited 71% reduction suggesting that both degradation and dephosphorylation pathways are regulating the fate of Cx43 under stress condition (Figure 4.3D-F). Microscopic imaging revealed that Cx43 localized to the plasma membrane and perinucleus in control cells. In starved cardiomyocytes, the level of membrane-bound Cx43 was reduced and Cx43 aggregates were observed in the perinucleus (Figure 4.3G).

AKT has been reported to phosphorylate Cx43 on Ser373 [Park et al., 2007]. We then investigated the effect of HBSS starvation on protein levels of AKT and PAKT. Western blotting and microscopic analyses indicated that the levels of AKT and PAKT reduced as a result of HBSS starvation (Figure 4.3H-L). Taken together, these results indicate that

starvation leads to decrease in total levels of Cx43 as well as alteration in its phosphorylation state.
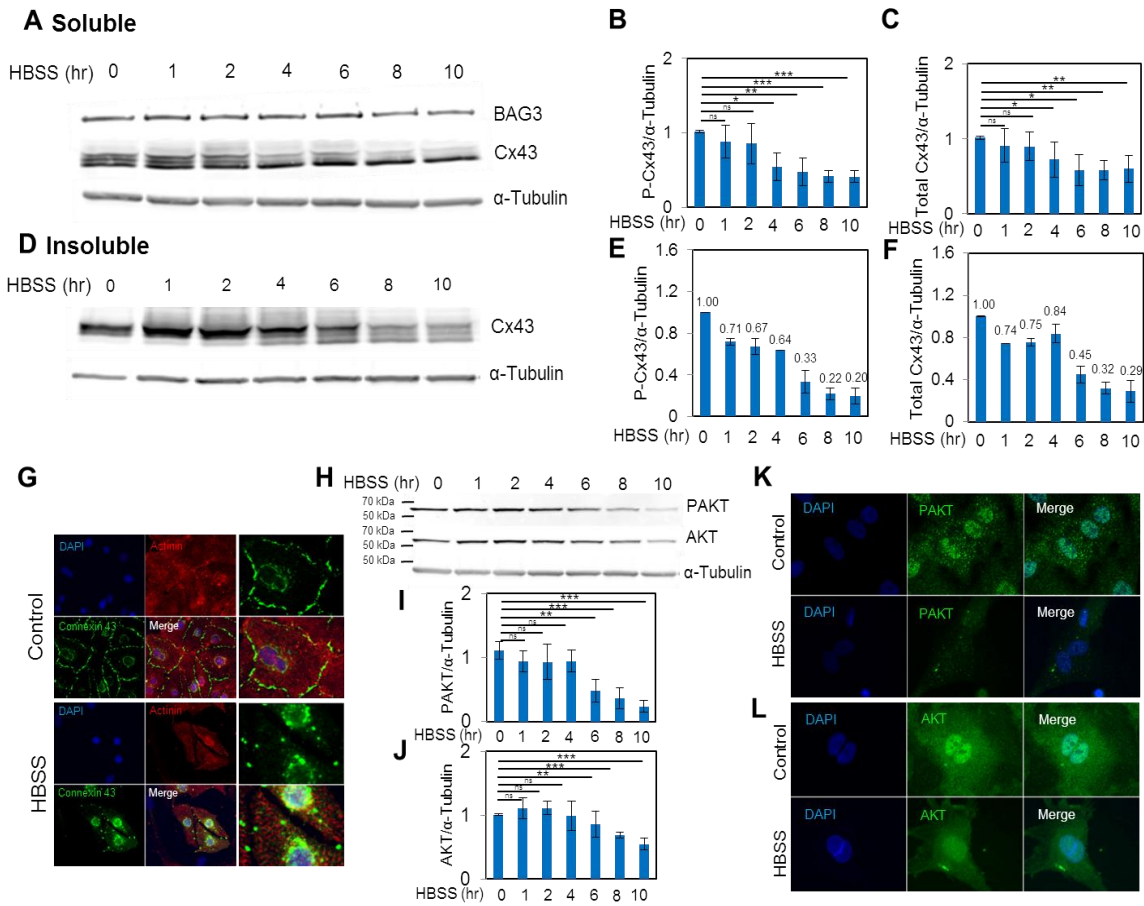
Figure 4.3. Alteration of Cx43 under conditions of nutrient starvation. NRVCs were starved in HBSS medium for different time intervals (0, 1, 2, 4, 6, 8 and 10 hr). **(A)** Protein levels of Cx43 were measured in soluble fractions of cell lysates by Western blot. The levels of **(B)** phosphorylated Cx43 and **(C)** total Cx43 in soluble fractions of cell lysates were quantified. *$p<0.05$; **$p<0.01$; ***$p<0.001$. (n=5). **(D)** Protein levels of Cx43 were measured in lysis buffer-insoluble fractions of cell lysates by Western blot. (n=3). The levels of **(E)** phosphorylated Cx43 and **(F)** total Cx43 in lysis buffer-insoluble fractions of cell lysates were quantified. (n=3). **(G)** NRVCs were starved for 8 hr in HBSS medium and Cx43 localization was monitored by immunocytochemistry. Microscopic imaging with antibodies to actinin and Cx43 indicated that under starvation, Cx43 levels reduced in plasma membrane while Cx43 localization increased in the perinucleus of cardiomyocytes. **(H)** Protein levels of PAKT and AKT were measure in soluble fractions of cell lysates by Western blot. The levels of **(I)** PAKT and **(J)** AKT in soluble fractions of cell lysates were quantified. **$p<0.01$; ***$p<0.001$. (n=4). NRVCs were starved for 8 hr in HBSS medium and **(K)** PAKT and **(L)** AKT localizations were monitored using immunofluorescence analysis. α-Tubulin served as a loading control for both the soluble and insoluble fractions.

BAG3 suppression impairs phosphorylation state and degradation of Cx43 under nutrient starvation

BAG3 has been reported to be a critical regulator of autophagy [Rosati et al., 2011]. In order to find out whether BAG3 plays a role in Cx43 degradation under pathological condition, NRVCs were transduced with either Ad-control or Ad-siBAG3 for 3 days. Transduced cardiomyocytes were then starved in HBSS medium for different time intervals of 2, 6 or 10 hours and Cx43 degradation was investigated by Western blot. We first evaluated the effect of BAG3 on autophagy activation by measuring the ratio of LC3-II/LC3-I. LC3-II is the lipidated form of LC3-I and is involved in autophagosome membrane fusion events during autophagy. The LC3-II/LC3-I ratio is indicative of autophagic activity and autophagosome formation. Analysis of the soluble fraction revealed that LC3-II/LC3-I ratio significantly increased in control cardiomyocytes at 6 and 10 hours after starvation, while no such increase was observed in BAG3-suppressed cardiomyocytes (Figure 4.4A-B). In addition, P-Cx43 levels significantly reduced 2, 6 and 10 hours after starvation in control cardiomyocytes while no significant reduction in P-Cx43 level was observed in Ad-siBAG3-transduced cardiomyocytes. We also investigated the levels of NP-Cx43 as a result of starvation and found that NP-Cx43 significantly upregulated in control cardiomyocytes while no significant increase in NP-Cx43 was detected in cardiomyocytes suppressed for BAG3 (Figure 4.4A-D). In addition, data from the lysis buffer-insoluble fraction indicate that 10 hr after starvation, there was a 58% reduction in P-Cx43 in control cardiomyocytes and it a 30% reduction in cells with BAG3 knocked down; suggesting that BAG3 suppression interferes with Cx43 degradation under stress (Figure 4.4E-F). Considering the role of AKT in Cx43 phosphorylation, we then investigated the levels of PAKT and AKT in control as well as BAG3-knocked down cardiomyocytes under starvation. Data indicate that 10 hours after starvation, there was 79% reduction in PAKT level in control cells; while it reached to

50% in BAG3-knocked down cells. Furthermore 10 hours after starvation, AKT level significantly reduced by 48% in control cells; while no significant reduction was detected in AKT level in cardiomyocytes with BAG3 suppression (Figure 4.4G-I). Collectively, these data suggest that BAG3 plays an important role in regulating quality of Cx43, either degradation or phosphorylation state, under stress condition.
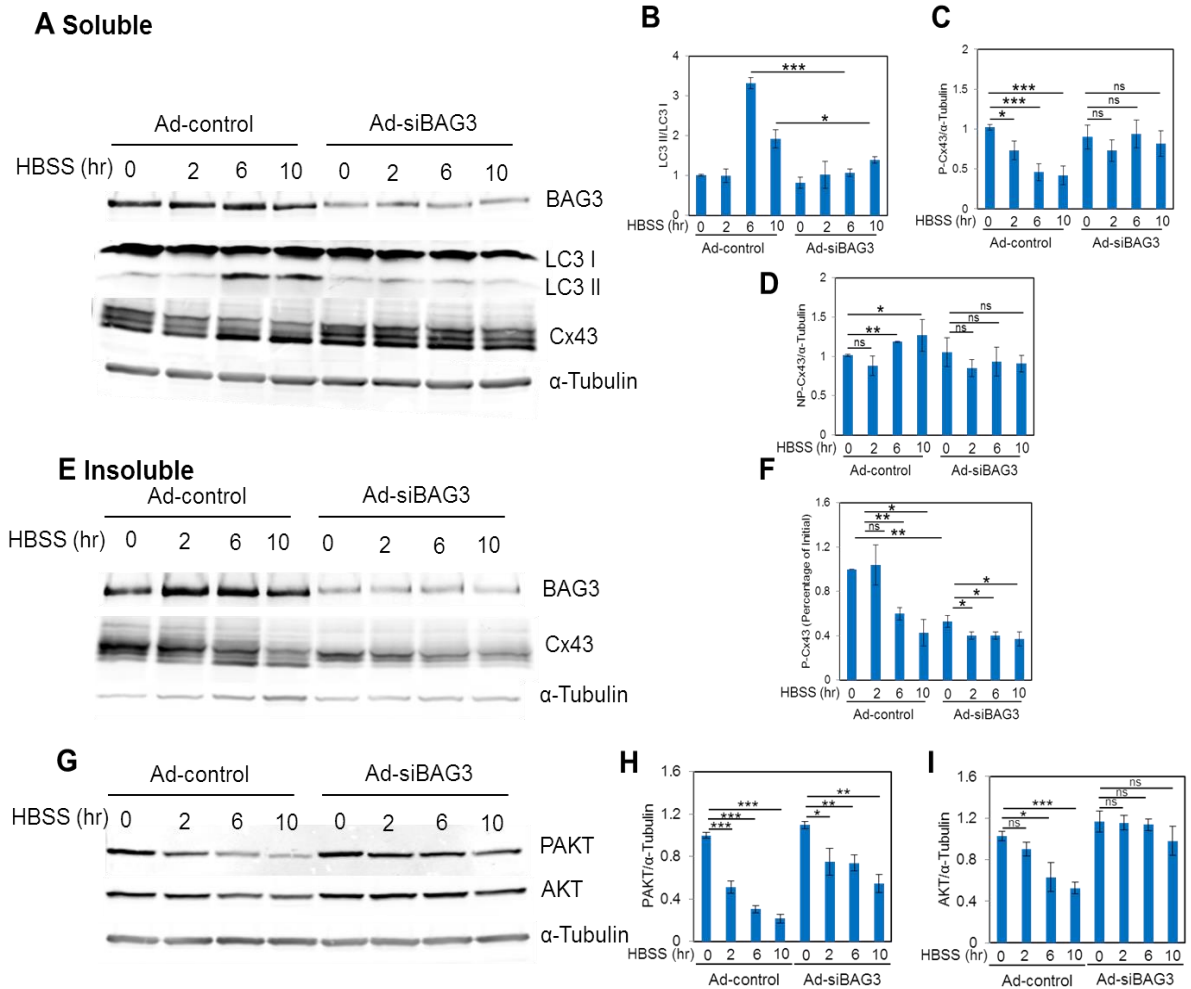
Figure 4.4. Knock-down of BAG3 impairs Cx43 dynamics under starvation stress condition. NRVCs were transduced with either Ad-siBAG3 or Ad-control for 3 days and then cells were starved in HBSS medium for 2, 6 or 10 hr. **(A)** The levels of the autophagy markers, LC3-II and LC3-I, Cx43 and BAG3 were measured in soluble fractions of cell lysates by Western blot. **(B)** The levels of LC3-II/LC3-I in soluble fractions of cell lysates were quantified based on the data shown in (A). *$p<0.05$; ***$p<0.001$. (n=3). **(C)** The levels of phosphorylated Cx43 in soluble fractions of cell lysates were quantified based on the data shown in (A). *$p<0.05$; ***$p<0.001$. (n=5). **(D)** The levels of non-phosphorylated Cx43 in soluble fractions of cell lysates were quantified based on the data shown in (A). *$p<0.05$; **$p<0.01$. (n=5). **(E)** The levels of BAG3 and Cx43 in lysis buffer-insoluble fractions of cell lysates were measured. **(F)** The levels of phosphorylated Cx43 in lysis buffer-insoluble fractions of cell lysates were quantified based on the data shown in (E). *$p<0.05$; **$p<0.01$ (n=3). **(G)** The levels of PAKT and AKT were measured in soluble fractions of cell lysates by Western blot. **(H)** The levels of PAKT in soluble fractions of cell lysates were quantified based on the data shown in (G). *$p<0.05$; **$p<0.01$; ***$p<0.001$ (n=3). **(I)** The levels of AKT in soluble fractions of cell lysates were quantified based on the data shown in (G). *$p<0.05$; ***$p<0.001$ (n=3). α-Tubulin served as a loading control for both soluble and insoluble fractions. α-Tubulin served as a loading control for both soluble and insoluble fractions.

Tubulin deplymerization dysregulates Cx43

BAG3 transports protein aggregates to lysosomes for removal through autophagy pathway by interacting with microtubules [Gamerdinger et al., 2011]. Next, we performed a series of experiments to explore the importance of tubulin in regulating the Cx43 turnover. Microscopic imaging using antibodies against BAG3 and α-Tubulin indicated that BAG3 colocalized with the tubulin network in primary cardiomyocytes (Figure 4.5A). Co-IP by using an antibody to pull down BAG3 protein indicated that BAG3 interacts with tubulin network in NRVCs (Figure 4.5B). We also investigated the localization of Cx43 and tubulin and found that Cx43 was surrounded by the tubulin network in the perinucleus (Figure 4.5C). We further investigated the impact of tubulin on Cx43 protein homeostasis by impairing the assembly of microtubules using vinblastine. NRVCs were treated with 5, 10 or 25 μM vinblastine for 12 hours and the level of Cx43 protein was investigated in both the soluble and lysis buffer-insoluble fractions. Data indicate that the levels of NP-Cx43 significantly increased in response to 10 and 25 μM concentrations of vinblastine. In addition, we found that NP-Cx43 bands were upregulated in insoluble fractions as a result of vinblastine treatment (Figure 4.5D-F). Immunofluorescence analysis indicated that transport of Cx43 to plasma membrane inhibited and Cx43 accumulated in cellular cytoplasm as a result of microtubule depolymerization (Figure 4.5G). In addition, accumulation of BAG3 aggregates were observed in vinblastine-treated cardiomyocytes (Figure 4.5H). These data suggest that BAG3 and tubulin are two important regulators of Cx43 in cardiomyocytes.
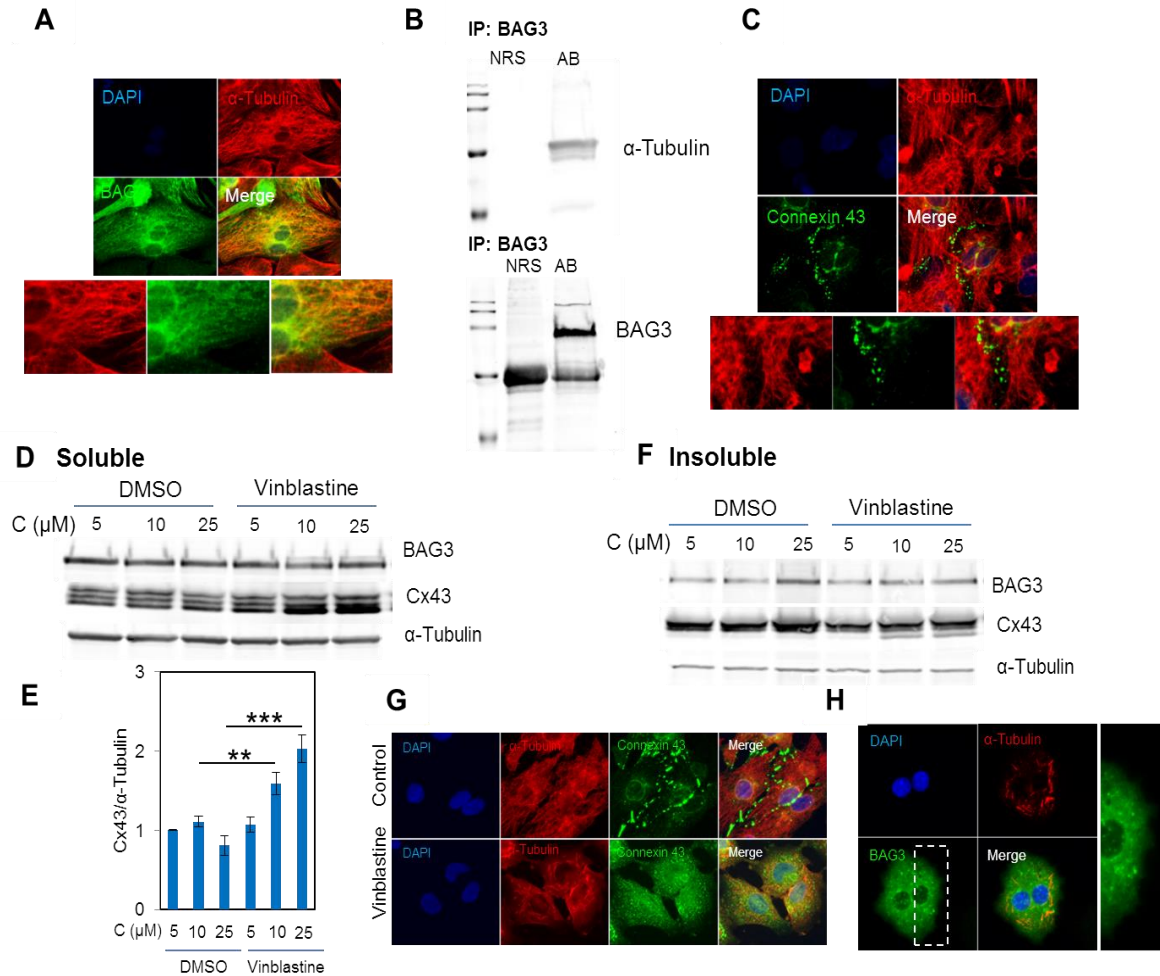
Figure 4.5. BAG3 colocalizes with the tubulin network and tubulin depolymerization dysregulates Cx43. (A) Immunocytochemistry labeling using antibodies against α-tubulin and BAG3 proteins showed that BAG3 colocalized with α-tubulin cytoskeleton network. **(B)** Co-IP results by pulling down BAG3 protein showed that BAG3 interacts with tubulin network. **(C)** Immunocytochemistry labeling by using antibodies against α-tubulin and Cx43 proteins showed that Cx43 colocalized with α-tubulin in the perinucleus. NRVCs were treated for 12 hr with 5, 10 and 25 µM microtubule depolymerizing agent, vinblastine. **(D)** The levels of BAG3 and Cx43 proteins were measured in soluble fractions of cell lysates by Western blot. **(E)** The levels of total Cx43 protein were quantified in soluble fractions of cell lysates based on the data shown in (D). ******$p<0.01$; *******$p<0.001$. (n=3). **(F)** The levels of BAG3 and Cx43 proteins were measured in lysis buffer-insoluble fractions of cell lysates. α-Tubulin served as a loading control for both soluble and insoluble fractions. **(G)** Immunocytochemistry labeling by using antibodies against α-tubulin and Cx43 proteins showed that Cx43 accumulated in cellular cytoplasm as a result of vinblastine treatment. **(H)** Immunocytochemisty labeling by using antibodies against α-tubulin and BAG3 showed that BAG3 aggregates accumulated in cellular cytoplasm as a result of vinblastine treatment.

BAG3 suppression impairs gap junction function

To determine whether BAG3 suppression impacts the function of gap junction in cardiomyocytes, we measured transfer distance of low molecular weight dye, sulforhodamine B, by using scrape-loading technique. For this purpose, several scratches were made in confluent culture of transduced cardiomyocytes using surgical scalpel. NRVCs were then incubated with sulforhodamine B dye followed by imaging. Image J analysis indicated that dye transfer distance significantly reduced as a result of BAG3 suppression; suggesting that BAG3 may impact intercellular communication of cardiomyocytes by impairing the quality of gap junction protein, Cx43 (Figure 4.6A-B).
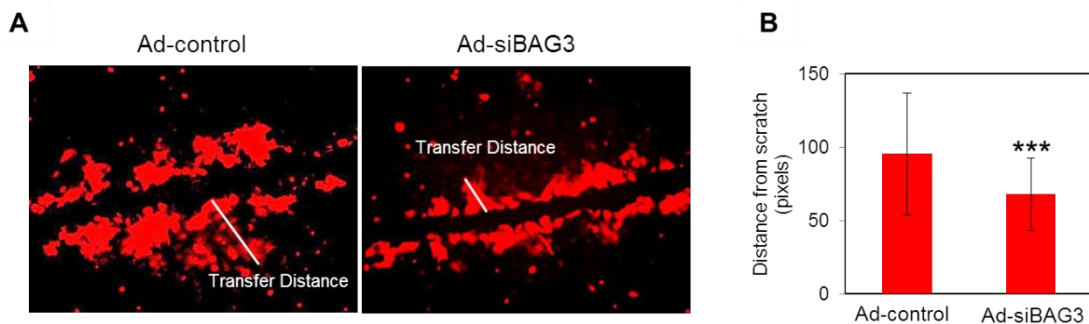
Figure 4.6. Knock down of BAG3 impairs gap junction-mediated dye transfer. (A) NRVCs were transduced with either Ad-siBAG3 or Ad-control. 3 days post transduction, confluent cardiomyocytes were scape loaded with sulforhodamine B dye followed by imaging using fluorescent microscope. **(B)** Image J quantification indicated that dye transfer distance was significantly less in BAG3-suppressed cardiomyocytes compare to that in control cells. ***$p<0.001$ (n=56)

Discussion

Gap junctions propagate action potentials through the myocardium and maintain cardiac rhythm by connecting the plasma membrane of cardiomyocytes [Severs et al., 2004]. Cx43 is highly expressed in cardiomyocytes and has a very dynamic turnover [Epifantseva et al., 2017]. Therefore, exploring the key molecular players which regulate quality control of Cx43 is of great importance for understanding proper heart function. In this manuscript, we have identified the importance of BAG3 in regulating the fate of Cx43 under normal as well as stress conditions in primary cultures of neonatal cardiomyocytes using different experimental approaches. Co-chaperone BAG3 interacts with the HSP70/HSC70 chaperone complex through its BAG domain [Stürner et al., 2017]. Molecular chaperones interact with unfolded polypeptides and assist protein folding and stability. Impairment of chaperone function dysregulates protein homeostasis and results in the formation of protein aggregates and disease development [Hartl et al., 2011]. Mutations of BAG3 dysregulate the function of the HSP70/HSC70 chaperone complex and impair protein homeostasis leading to accumulation of protein aggregates and development of cardiomyopathy [Fang et al., 2017]. Our data indicate that Cx43 protein expression was downregulated as a result of BAG3 knock-down. By inhibiting translation, we found that stability of Cx43 protein significantly reduced in BAG3-suppressed cardiomyocytes compared to control cells. Whether BAG3 directly impacts on Cx43 stability or the absence of BAG3 destabilizes Cx43 by impairing the chaperone activity of heat shock proteins remains in question. Interestingly, a recent study showed that deletion of a member of heat shock protein family, HSPB7, resulted in Cx43 reduction in mice followed by impairment of cardiac electrical conduction and development of heart failure [Liao et al., 2018].

The role of BAG3 in protein quality control in cardiomyocytes has been reported previously [Knezevic et al., 2015]. However, to our knowledge, there is no report describing the role of BAG3 in gap junction quality control. Recent studies have showed that BAG3 impacts autophagosome formation and autophagy flux by regulating LC3 lipidation through a translational mechanism [Rodriguez et al., 2016]. Autophagy is a catabolic process which recovers essential amino acids and sustains cellular energy balance by degrading unnecessary components during nutrient starvation [Johansen et al., 2011]. We found that when lysosomal activity was inhibited by BafA1, both P- and NP-Cx43 levels significantly increased and Cx43 aggregates accumulated in the cytoplasm. When BAG3 was suppressed using adenovirus transduction of BAG3 siRNA, autophagic flux of Cx43 was inhibited. Considering the rapid turnover of Cx43 in heart, impairment of Cx43 flux adversely affects cell-to-cell communication in cardiac tissue and contributes toward arrhythmia and heart failure [Saffitz et al., 2000].

When cardiomyocytes were subjected to starvation, dephosphorylation of Cx43 occurred while total Cx43 level reduced. Immunofuorescence labeling indicated that Cx43 aggregates localized to the perinucleus as a result of starvation. It was previously reported that Cx43 degrades through autophagy pathway during ischemia [Martins-Marques et al., 2015]. BAG3 plays a protective role under cardiac stress conditions by activating autophagy [Tahrir et al., 2017]. Therefore, we next investigated the effect of BAG3-mediated autophagy on the fate of Cx43 under stress conditions. Western blot data of the levels of autophagy markers, LC3-I and LC3-II, indicated that autophagosome formation was significantly higher in control cells compared to cardiomyocytes with BAG3-knocked down. We then found that Cx43 degradation was significantly impaired in BAG3-suppressed cardiomyocytes. In addition, our data indicate that knock down of BAG3 significantly impaired Cx43 dephosphorylation. During

ischemia, protein phosphatases interact with Cx43 and cause its dephosphorylation [Ai et al., 2005]. However, further experiments are required to explore the effect of BAG3 on the activity of phosphotases and the phosphorylation state of Cx43.

Microtubules interact directly with Cx43 and control its trafficking and translocation into gap junction structure [Giepmans et al., 2001]. In addition, it has been reported that BAG3 interacts with microtubule-motor dynein and delivers misfolded proteins into aggresomes for further degradation and elimination by autophagy. Aggresome formation was impaired when microtubules were depolymerized [Gamerdinger et al., 2011]. We found that BAG3 colocalized with tubulin in NRVCs and tubulin disassembly resulted in alteration of Cx43 as NP-Cx43 was significantly accumulated. Accumulation of nonphosphorylated Cx43 within gap junctions is associated with arrhythmogenesis and heart failure [Beardslee et al., 2000]. These data suggest that BAG3 and tubulin are important regulators of Cx43 in primary cardiomycyotes (Figure 4.7).
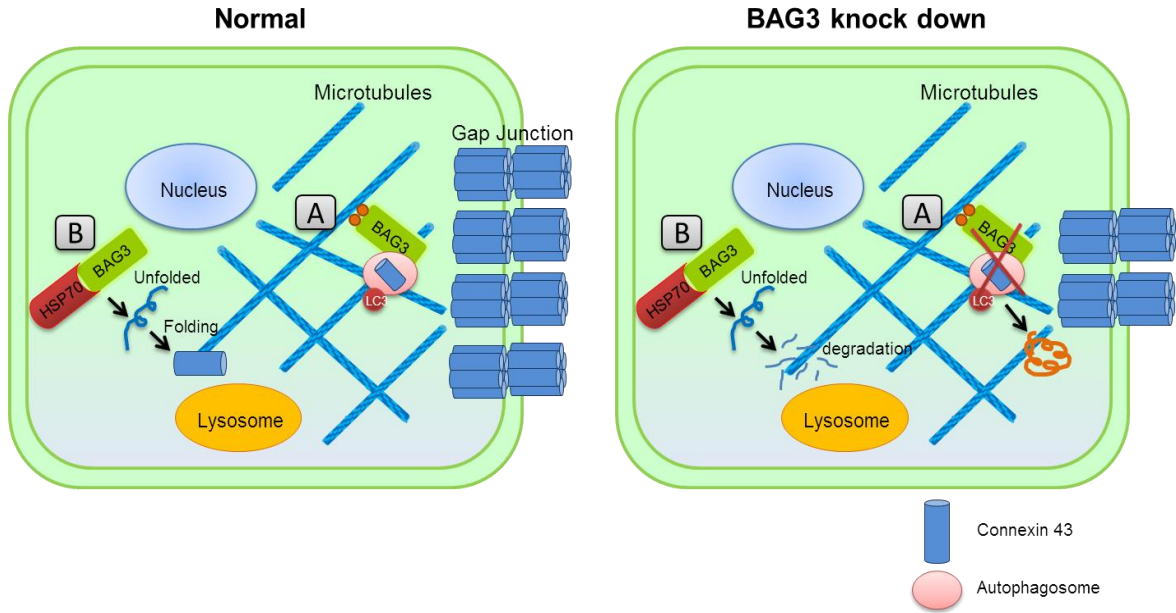
Figure 4.7. Schematic model representing the role of BAG3 in quality control as well as stability of Cx43 protein. (A) BAG3 through association with microtubules delivers misfolded and damaged proteins for further degradation and removal through autophagy-lysosome pathway. Impair of autophagic degradation of proteins in the absence of BAG3, results in the accumulation of insoluble aggregates. **(B)** BAG3 functions as a co-chaperone of HSP70/HSC70 chaperone complex and plays an important role in protein stabilization. BAG3 suppression results in the destabilization of Cx43; leading to Cx43 degradation and reduction in Cx43 level.

5. Supplementary Figures
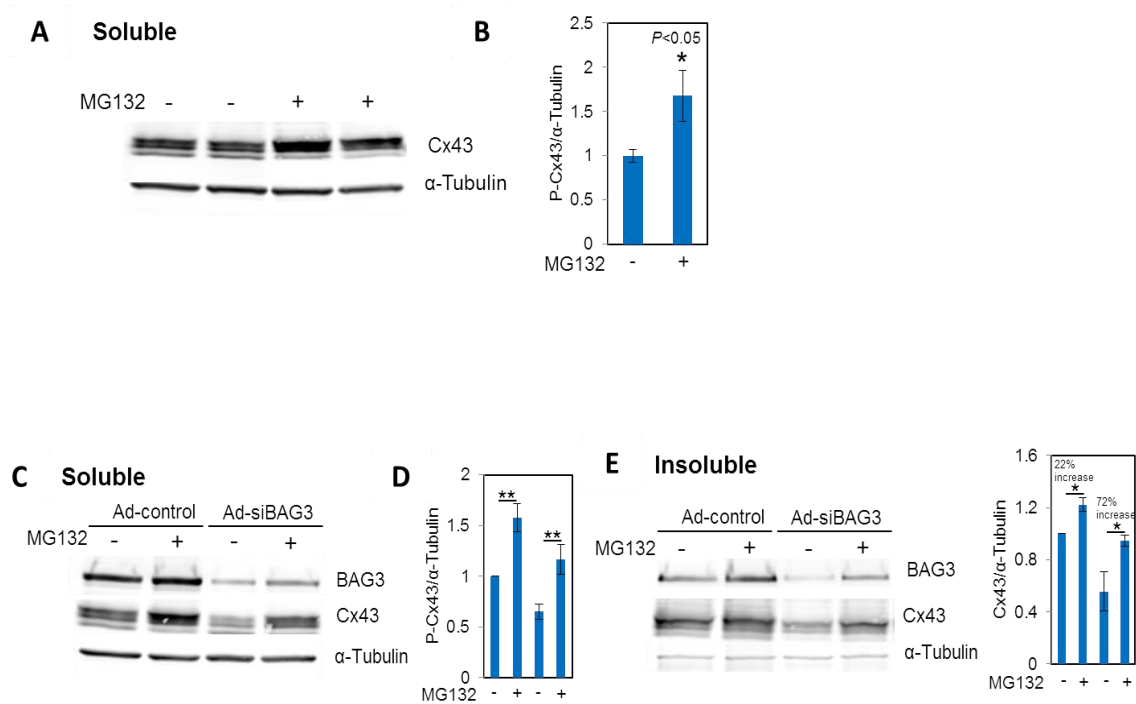
Figure S3. Cx43 degrades through ubiquitin-proteasome pathway in cardiomyocytes. (A) NRVCs were treated for 12 hr with 5 µM proteasome inhibitor, MG132, and the levels of Cx43 were measured by Western blot. **(B)** The levels of phosphorylated Cx43 were quantified based on the data shown in (A). *$p<0.05$ (n=4). NRVCs were transduced with either Ad-control or Ad-siBAG3 for 3 days and then treated with MG132 (5 µM, 12 hr). **(C)** The levels of BAG3 and Cx43 were measured in soluble fractions of cell lysates by Western blot. **(D)** The levels of phosphorylated Cx43 were quantified based on the data shown in (C). **$p<0.01$. (n=4). **(E)** The levels of BAG3 and Cx43 were measured in insoluble fractions of cell lysates by Western blot.

A

Ad-Control

Time (hr)	0	0.5	0.75	1	2	4	6	8	
	—	—	—	—	—	—	—	—	HSP70
	—	—	—	—	—	—	—	—	α-Tubulin

B

Ad-siBAG3

Time (hr)	0	0.5	0.75	1	2	4	6	8	
	—	—	—	—	—	—	—	—	HSP70
	—	—	—	—	—	—	—	—	α-Tubulin

C
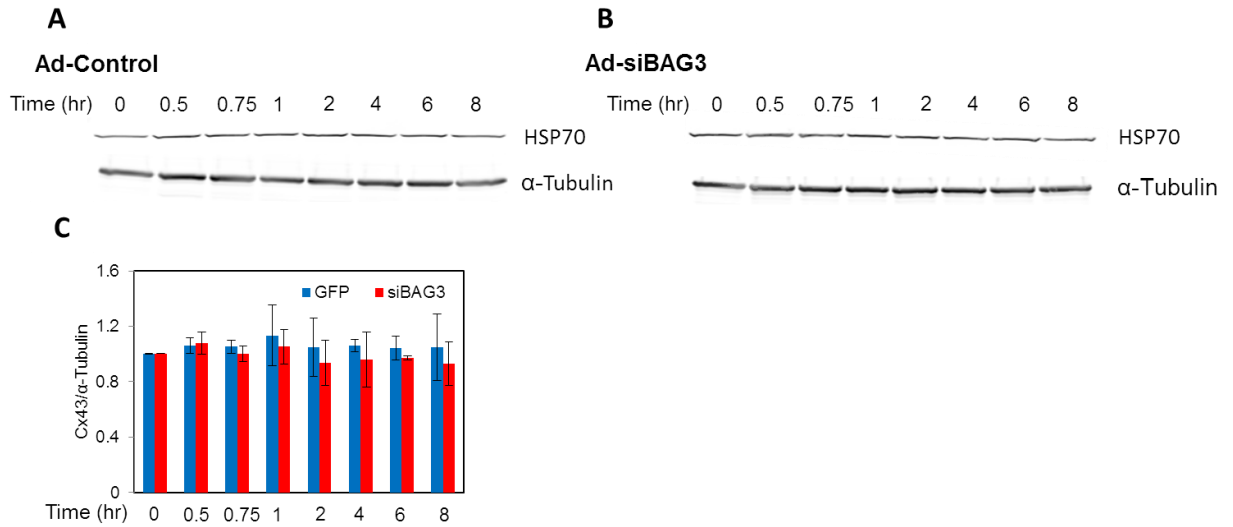
Figure S4. Stability of HSP70. (A, B) NRVCs were transduced with either Ad-siBAG3 or Ad-control for 3 days. Transduced NRVCs were then incubated with the mRNA translation inhibitor cycloheximide (10 µg/mL) for different time intervals (0, 30 min, 45 min, 1hr, 2hr, 4hr, 6hr and 8hr). The levels of HSP70 in each condition (Ad-siBAG3 or Ad-control) were measured by Western blot. **(C)** HSP70 levels for each condition (Ad-siBAG3 or Ad-control) at each time point were quantified and normalized to their levels at time zero. α-Tubulin served as a loading control.

100

CHAPTER 5

BAG3 SUPPRESSION IMPAIRS ELECTRICAL ACTIVITY OF CARDIOMYOCYTES

Abstract

Gap junctions (GJs) are intercellular channels which connect plasma membrane of two adjacent cardiomyocytes to propagate action potentials (APs) generated by ion channels throughout the myocardium; therefore, they play an important role in maintaining cardiac synchronous beating and rhythm. Impair of GJ coupling results in electrical conduction abnormalities and has been associated with arrhythmogenesis. Recently, we have demonstrated that bcl2-associated athanogene 3 (BAG3) plays an important role in regulating the quality of connexin 43 (Cx43), the most abundantly expressed GJ protein in ventricles, in neonatal cardiomyocytes. BAG3 is an anti-apoptotic protein whose mutations have been implicated in the pathogenesis of cardiac complications such as dilated cardiomyopathy. Herein we have used an *in vitro* model of neonatal rat ventricular cardiomyocytes (NRVCs) to investigate whether dysregulation of GJ quality via BAG3 suppression impacts cardiomyocyte electrical activity. For this purpose, electrical activities of control and BAG3-suppressed NRVCs were recorded using microelectrode array (MEA) system and important electrophysiological components such as signal propagation pattern and conduction velocity were extracted from the complex signal recordings. Our data indicated that impair of GJ quality via BAG3 suppression attenuated electrophysiological activity of neonatal cardiomyocytes. Furthermore, considering the notion that GJ proteins are located in both plasma membrane and mitochondria of cardiomyocytes, we investigated mitochondrial bioenergetics change as a result of GJ inhibition and found that impair of GJ activity significantly dysregulated mitochondrial membrane potential and calcium homeostasis. Taken together, our results

demonstrate that Cx43 alterations dysregulate electrophysiological activities as well as mitochondrial bioenergetics in neonatal cardiomyocytes.

Introduction

Electrical potential change as a result of ion movement across plasma membrane between inside and outside of the cell is known as action potential (AP) [Grant et al., 2009]. APs are initiated by ion channels and propagated throughout the myocardium via the action of GJs [Epifantseva et al., 2018]. To this end, excitatory currents generated by ion channels spread through intercellular GJs to depolarize adjacent cardiomyocytes [Grant et al., 2009]. Electrical activity of the heart is assessed by means of various techniques such as electrocardiogram (ECG), patch-clamping and microelectrode array (MEA); in which ECG measures electrical activity of atria and ventricles, patch-clamping measures AP from a single cell and MEA measures extracellular ion currents known as field potentials (FPs) [Navarrete et al., 2012]. Monitoring the intra- and extracellular electrical activity of cardiac cells and precise determination of electrophysiological parameters are essential as alterations in electrophysiological parameters are indicative of myocardial abnormalities and arrhythmia [Sameni et al., 2010]. For example, ion channel mutations which cause dysregulation of ventricular repolarization lead to prolongation of QT and development of long-QT syndrome [Schwartz et al., 2009, Grant et al., 2009].

GJs are vital components for cardiac AP propagation as they permit direct communication between neighboring cardiomyocytes. Impair of GJ activity under cardiac stress conditions results in cardiac conduction abnormalities and has been implicated in the pathogenesis of arrhythmia [Epifantseva et al., 2018]. Each adult cardiomyocyte is

coupled to ~ 11 adjacent cells via GJs to ensure anisotropic electrical conduction in the myocardium [Rohr et al., 2004]. Therefore, modulation of intercellular coupling via GJs has become a promising target for the action of anti-arrhythmic drugs [Grant et al., 2009]. Among various techniques to measure cardiac electrical activity, MEA screening mapping technique is a high resolution and non-invasive method which has been widely used for drug screening purposes in pharmacological studies to identify cardiotoxic drugs [Navarrete et al., 2012]. Precise measurement and analysis of MEA-derived FP recordings give rise to a better understanding of electrophysiology of cardiac cells; as FP parameters correlate with those measured by ECG or patch-clamping. For example, FP duration (FPD) correlates with AP duration (APD) measured by patch-clamping and QT intervals measured by ECG [Navarrete et al., 2012].

BAG3 is an anti-apoptotic protein composed of 575 amino acids and is highly expressed in cardiac and skeletal muscles [Myers et al., 2018]. BAG3 deficiency in mice led to muscle degeneration and lethal cardiomyopathy followed by death by 4 weeks of age [Homma et al., 2006]. Several research studies have reported BAG3 as a key regulator of protein quality control in the heart [Myers et al., 2018]. Recently, we have demonstrated that BAG3 suppression impaired the quality of GJ protein, Cx43, by enhancing its degradation. Connexin proteins are the main constituents of GJ hemichannels and Cx43 is the most abundantly expressed isoform of connexin family in the structure of GJs in ventricular cardiomyocytes [Boengler et al., 2018]. Role of connexin proteins in cardiac electrical conduction has been reported previously [Vaidya et al., 2001]. Cx40 is present in atria and His-purkinje system [Tse et al., 2015] and deficiency of Cx40 resulted in dysregulation of intercellular coupling and led to electrical conduction failure in mouse hearts [Tamaddon et al., 2000]. Dysregulation of Cx43 resulted in cell-to-cell uncoupling and was associated with arrhythmogenesis [Vaidya et

al., 2001]. Cx43 also plays an important role in heart remodeling during cardiac development and Cx43 deficiency led to ventricular malformation and early neonatal death in mice [Reaume et al., 1995]. Furthermore, Cx43 alteration and remodeling under ischemia/reperfusion has been associated with arrhythmia and infarction [Schulz et al., 2015]. Considering the role of Cx43 in cardiac electrical activity, we have evaluated the impact of BAG3 suppression on electrophysiological activity of primary neonatal cardiomyocytes.

Herein we have used an *in vitro* culture of spontaneously beating neonatal cardiomyocytes to study the impact of BAG3 attenuation on electrical signal generation and progression in monolayer culture of cardiomyocytes. Acquired data were analyzed using custom-designed MATLAB algorithms and important electrophysiological parameters such as spike frequency, spike amplitude and signal conduction velocity were extracted. Furthermore, considering the notion that Cx43 resides on both the plasma membrane and mitochondria, the impact of Cx43 inhibition on mitochondrial bioenergetics was investigated as well.

Experimental

Isolation and culture of neonatal cardiomyocytes

All animal protocols used within this study were approved by the Institutional Animal Care and Use Committee at Temple University. NRVCs were isolated from 2-3 day old Harlan Sprague-Dawley rats (Charles River) using the protocol previously described [Gupta et al., 2016]. Isolated cardiomyocytes were plated on EmbyoMax® 0.1% Gelatin solution (Millipore)-coated plates in minimum essential medium alpha (MEMα, Life Technologies) with 10% fetal bovine serum (FBS, Denville Scientific Inc., Hollistion, MA). 24 hours post seeding, the medium was replaced with Dulbecco's minimal essential medium (DMEM, Life Technologies, Carlsbad, CA) supplemented with 2% FBS and 25 µg/mL gentamicin (Life Technologies).

Adenovirus transduction

24 hours after isolation, NRVCs were transduced with either Ad-control (Vector Biolabs) or Ad-siBAG3 (Vector Biolabs) in reduced volumes of FBS-free DMEM for 2 hours. The transduction medium was then replaced with DMEM supplemented with 2% FBS and 25 µg/mL gentamicin.

MEA recording

NRVCs were plated at a density of 1000 cells/mm^2 on MEA glass arrays (Multichannel Systems, Germany) pre-coated with EmbyoMax® 0.1% Gelatin solution (Millipore) and were allowed to adjust for 48 hr. Each MEA plate consists of 60 titanium nitrate (TiN) electrodes with diameter of 30 µm embedded in the bottom of the dish and positioned in a rectangular grid. Two days post seeding, extracellular recordings of untreated cardiomyocytes were performed as initial conditions using MEA-1060 system (Multichannel Systems, Germany). Then afterwards, cardiomyocytes were either transduced with Adenovirus or subjected to various GJ inhibitors such as carbenoxolone

(CBX, Sigma) and ioxynil-octanoate (Iox, abcam). Extracellular recordings were performed at the sampling frequency of 2 kHz using MC_Rack software which generates data in the format of mcd. Then by using MC_Data Tool, data were converted to ASCII format for further analysis by MATLAB®. Cardiomyocytes were maintained in an incubator at 37°C supplied with 5% CO_2 throughout the duration of experiments.

Measurement of mitochondrial calcium uptake and membrane potential ($\Delta\Psi_m$)

NRVCs were treated with GJ inhibitors, CBX (100 μM) and Iox (10 μM), for 1 hr and mitochondrial calcium uptake and $\Delta\Psi_m$ were measured following the protocol described previously [Tomar et al., 2016]. Trypsinized cardiomyocytes were bathed in an intracellular-like medium (120 mM KCl, 10 mM NaCl, 1 mM KH_2PO_4, 20 mM Hepes-Tris, pH 7.2 and 2 μM thapsigargin) and permeabilized with digitonin (40 μg/ml). The permeabilized cardiomyocytes were treated with bath Ca^{2+} indicator Fura2FF (1 μM) and $\Delta\Psi_m$ indicator JC-1 (800 nM) and extramitochondrial Ca^{2+} ($[Ca^{2+}]_{out}$) clearance and $\Delta\Psi_m$ were simultaneously measured in the presence of 10 μM Ca^{2+} pulses using multiwavelength excitation dual-wavelength emission fluorimeter (Delta RAM, PTI).

Western blotting

Cells were washed with cold 1X PBS and scraped into RIPA lysis buffer (25 mM Tris-HCl, 150 mM NaCl, 1% NP-40, 1% sodium deoxycholate, 0.1% SDS) supplemented with protease inhibitor. Cell lysates were rotated for 30 min and centrifuged at 14000 rpm for 10 min. Protein concentrations in supernatant were determined using Bio-Rad protein assay (Bio-Rad). Equal amounts of protein lysates were loaded onto 10% and 12% SDS-polyacrylamide gels followed by gel electrophoresis to separate protein bands based on their molecular weight. Gels were transferred onto nitrocellulose membranes (LI-COR) and blocked in LI-COR blocking solution for 1 hr at RT. After blocking,

membranes were probed with primary and secondary antibodies and scanned with Odyssey® CLx Imaging System (LI-COR).

Statistical analysis

Student's t-test was used to calculate the statistical differences between two independent groups. p values less than 0.05 were considered as statistically significant.

Results

Suppression of BAG3 dysregulates electrical activity of cardiomyocytes

NRVCs were plated onto MEA plates and allowed to settle for 48 hr. Extracellular electrical activities from spontaneously beating NRVCs were recorded as initial conditions (day zero, D0). Then afterwards, cells were transduced with adenovirus and electrophysiological activities were recorded over time via MEA (D1, D2 and D3) and reported as Local Field Potentials (LFPs). Each recording was carried out for 10 min. As a first step to analyze data, signals obtained from MEA recordings were filtered by a low-pass filter to enhance signal-to-noise ratio by attenuating the electrical signals with frequency higher than cutoff frequency (f_c). In order to determine signal f_c, Fast Fourier Transform (FFT) was applied to decompose the time-based signal into its constituent frequencies. The resultant transformation represented the signal in frequency domain in which Y-axis corresponds to signal intensity and X-axis corresponds to signal frequency (Figure 5.1A). Typically the background noise of the system determined from the reference electrode was about 12 µV (Figure 5.1B). Each spike in FP recordings is characterized by a biphasic peak with positive and negative potentials. We then calculated spike frequency as the number of spikes divided by the time difference between the first and last spikes of each electrode. Our results indicated that adenovirus transduction enhanced spike frequency 1 day post transduction. Then over time, BAG3 suppression led to higher extent attenuation of spike frequency compared to control cardiomyocytes. 3 days post transduction, firing frequency was 1.7-fold higher in control cells compare to their initial frequency; while it reduced by 63% compare to initial frequency in BAG3-suppressed cardiomyocytes. We also calculated spike amplitude as the voltage difference between positive and negative values of each spike. Data indicated that signal amplitudes in control and BAG3-suppressed cardiomyocytes significantly reduced 3 days post transduction. The averages of spike frequencies and

amplitudes from 60 electrodes belonging to 3 independent experiments were plotted for each condition. In control cells, increase in signal frequency requires higher energy demand which may contribute to signal amplitude suppression. However, data from MEA recordings indicated that both signal frequency and amplitude reduced in BAG3-suppressed cardiomyocytes 3 days pot transduction. Furthermore, electrical activity of some of the electrodes completely suppressed as a result of BAG3 knock down which were not considered in amplitude calculations (Figure 5.1C-E).
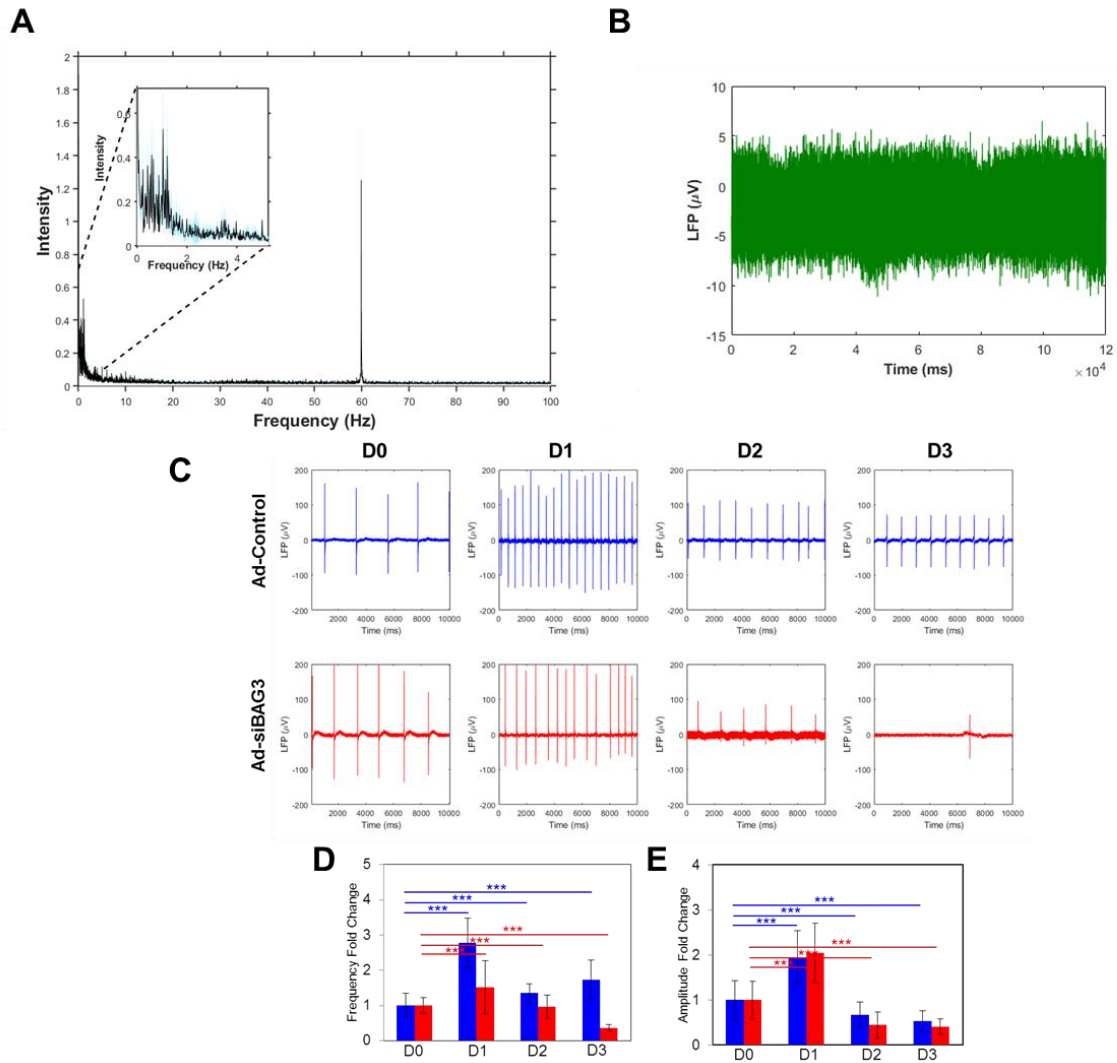
Figure 5.1. BAG3 suppression attenuated electrophysiological activity of cardiomyocytes. **(A)** By applying Fast Fourier Transform to the signals recorded by MEA, Cutoff frequency was determined as 60 Hz. **(B)** Background noise of the recording system was determined to be approximately 12 µV. **(C)** Electrical activities of NRVCs were recorded as initial conditions (D0). Cells were then transduced with either Ad-control or Ad-siBAG3 and extracellular FPs were recorded via MEA over time (D1, D2 and D3). **(D)** The impact of BAG3 suppression on spike frequencies was quantified based on the data presented in (A). **(E)** The impact of BAG3 suppression on spike amplitudes was quantified based on the data presented in (A). ***p<0.001. (n=3).

In order to determine the spiking activity of the monolayer culture of cardiomyocytes simultaneously recorded by 60 electrodes, spike raster plots for control and BAG3-suppressed cardiomyocytes were created over time. For this purpose, a MATLAB algorithm was designed to read the electrical trace and leave a dot by detecting any spike at each time point. Figure 5.2 shows two dimensional (2D) spike occurrence representing the activity of 60 electrodes over 10 seconds of reading time. Y-axis corresponds to the electrode number and X-axis corresponds to time. Spike activation at initial condition (D0) indicated similar patterns for both conditions; while BAG3 suppression led to dysregulation of spike activity over time as the number of spikes reduced and irregular spontaneous activity increased as a result of BAG3 reduction. We then magnified spike occurrence within 1000 ms of recording and found that spontaneous firing pattern and spike timing were dysregulated as a result of BAG3 suppression over time. Data analysis indicated that 3 days post transduction, regular activity of the monolayer culture of cardiomyocytes dysregulated as a result of BAG3 knock down. Furthermore, BAG3 suppression led to alteration in signal wave shape 3 days post transduction (Figure 5.3A-B).
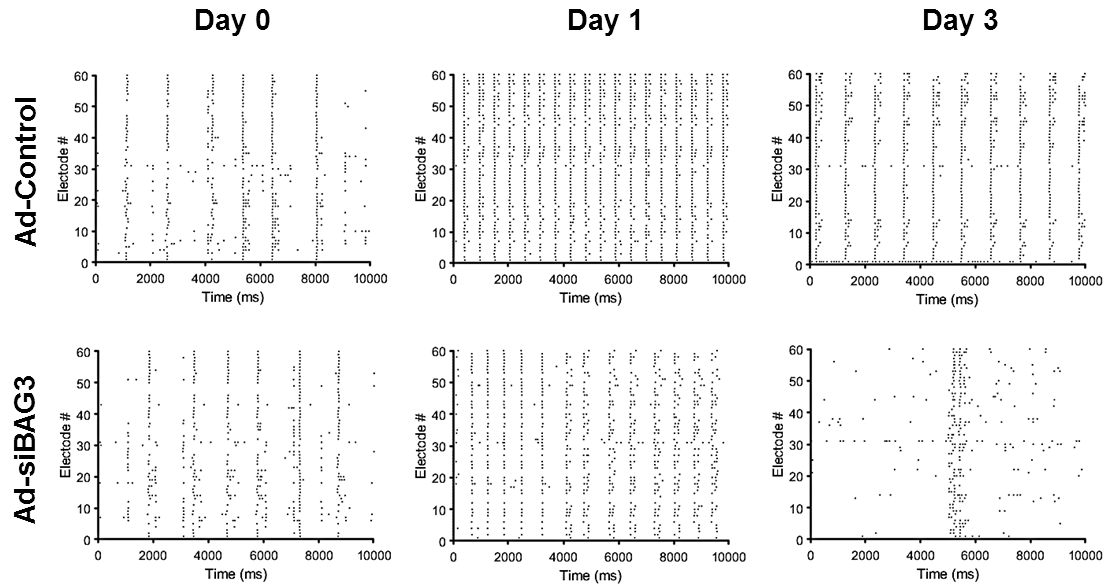
Figure 5.2. Spike rasters depicting simultaneous activity of 60 electrodes in control and BAG3-suppressed cardiomyocytes within 10,000 ms of recording. Data indicate that the number of firing and spiking irregularity reduced as a result of BAG3 suppression in cardiomyocytes.
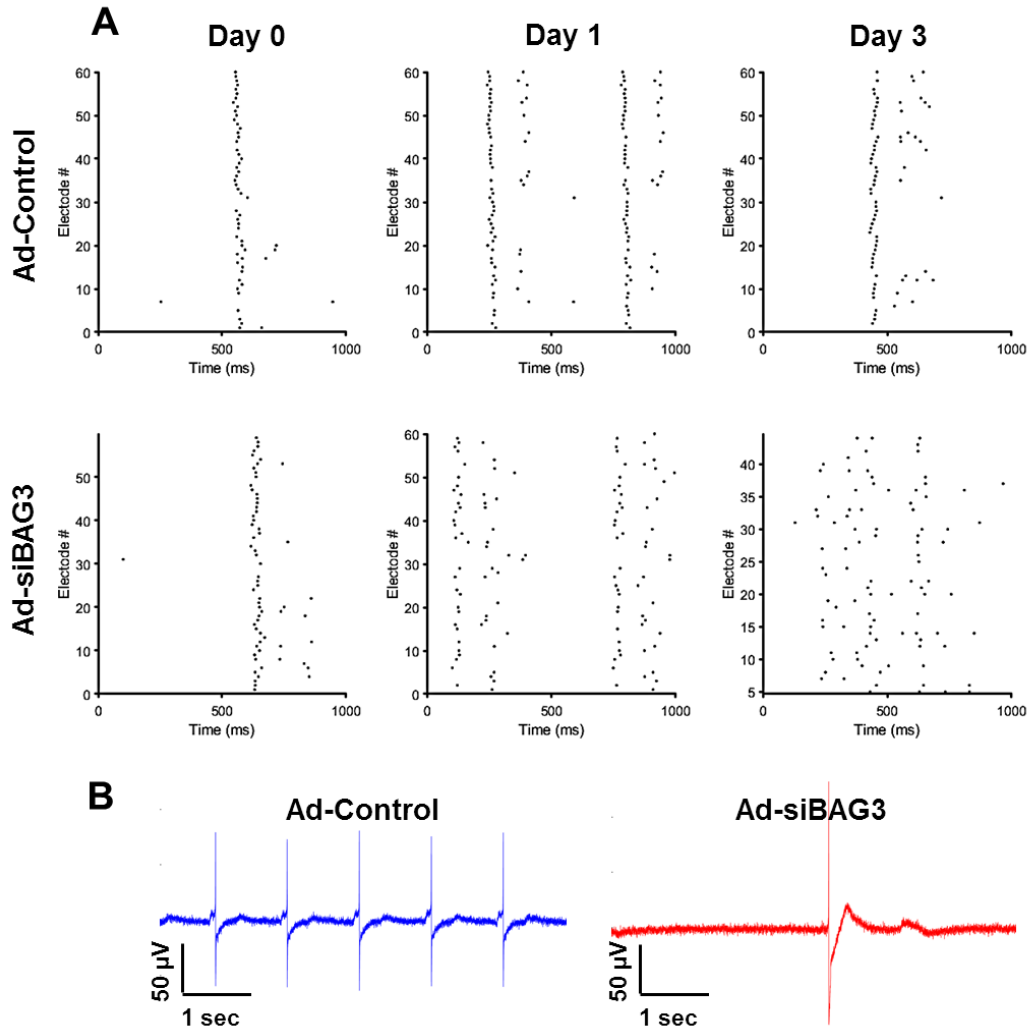
Figure 5.3. Spike rasters depicting simultaneous activity of 60 electrodes in control and BAG3-suppressed cardiomyocytes within 1000 ms of recording. (A) Data indicate that regular activity of 60 electrodes embedded all over the culture reduced as a result of BAG3 suppression. **(B)** BAG3 suppression altered signal wave shape 3 days post transduction.

By knowing the activation time of each electrode from raster plots, we then plotted color-coded activation maps to exhibit the effect of BAG3 suppression on electrical signal initiation and propagation within the culture of spontaneously beating cardiomyocytes. For this aim, an 8-by-8 grid representing the activation time of 60 electrodes arranged throughout the monolayer culture was plotted. Each segment of the grid indicates local activation time of each electrode. Activation maps for initial conditions indicated earlier activation locations (yellow regions) within the matrix followed by impulse spread toward the remaining regions (red regions). 3 days post transduction, activation maps indicated faster signal spread in control cells compared to their initial condition, while areas with delayed activation (red regions) increased as a result of BAG3 suppression. In control culture, total activation time of 60 electrodes reduced from 58.27 ± 12.36 ms to 43.78 ± 11.23 ms by the day of 3 post transduction; while activation time increased from 47.52 ± 13.84 ms to 160.97 ± 63.58 ms as a result of BAG3 suppression (Figure 5.4A-B).
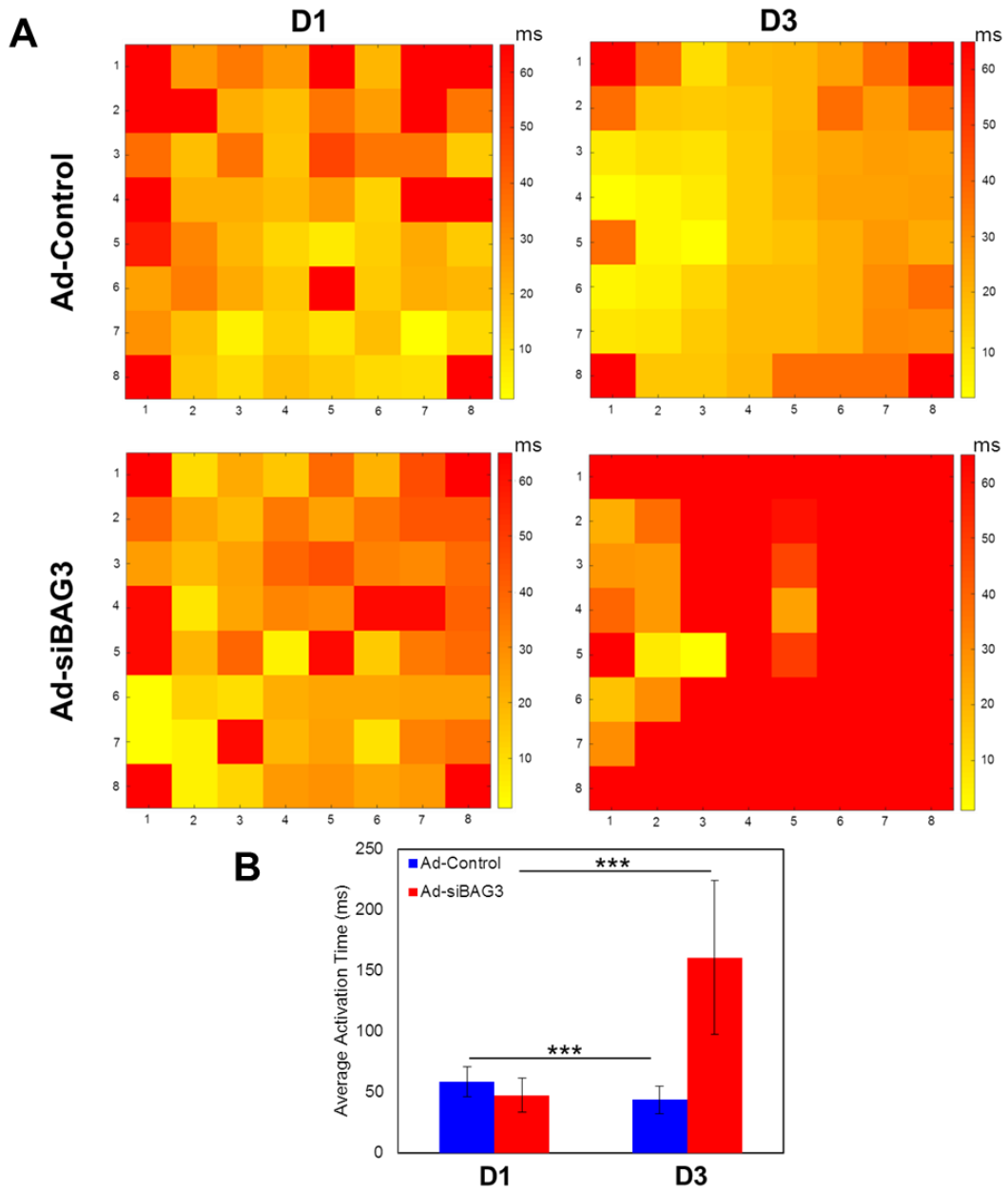
Figure 5.4. BAG3 suppression slows down activation of electrodes and impulse progression throughout the culture. (A) BAG3 suppression alters electrical activation pattern of electrodes within the monolayer culture of neonatal cardiomyocytes 3 days post transduction. Color scale bar depicts regions with earliest (yellow) and latest (red) electrical activation (0 to 60 ms). **(B)** BAG3 suppression significantly reduced impulse propagation throughout the culture. ***p<0.001 (n=3).

Next, we hypothesized that dysregulation of Cx43 protein mediated by BAG3 suppression may alter signal conduction velocity (CV). CV is the speed at which electrical impulse is transmitted among the electrodes throughout the monolayer culture of spontaneously beating cardiomyocytes. In order to calculate signal CV, first correlation coefficient between each pair of electrodes (E_i and E_j, i,j=1:60) was assessed in MATLAB environment. Linear correlation coefficient between electrodes i and j is determined using the equation below:

$$Correlation\ coefficient\ (Ei, Ej) = \frac{Cov(E_i, E_j)}{\sqrt{Var(E_i)Var(E_j)}}$$

Var (E_i,E_j) denotes variance and *Cov (E_i,E_j)* denotes covariance between electrodes i and j.

Correlation coefficient varies from -1 to +1. Correlation coefficient of 0 indicates no correlation between two electrodes. Correlation coefficient of +1 indicates perfect relationship, positive correlation, and correlation coefficient of -1 indicates negative correlation between two electrodes (Figure 5.5).
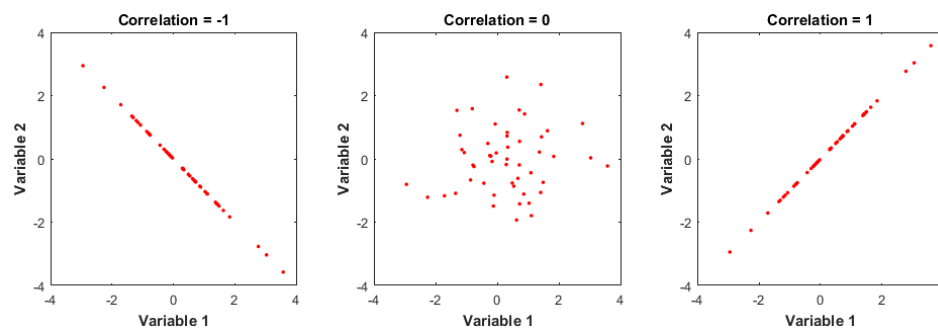
Figure 5.5. Linear correlation between variable 1 and variable 2. Correlation coefficients of +1 or -1 represent a positive or negative dependence between two variables, respectively. Correlation coefficient of 0 represents no dependence between two variables.

We then represented the results in a symmetrical 60x60 matrix in which each element exhibits the extent of correlation between each pair of electrodes. In this representative matrix, green indicates no correlation (correlation coefficient 0) and red indicates high correlation (correlation coefficient +1) between two electrodes. Data analysis indicated that 3 days post transduction, two distinct clusters of beating cardiomyocyte populations, which were highly correlated within each cluster and were not correlated with each other, were found in BAG3-suppressed cardiomyocytes. However, there was only one cluster of highly correlated electrodes 3 days post transduction in control cells. This observation suggests the important role of BAG3 in maintaining the cardiac tissue as a single contracting unit whose deficiency exerts detrimental effects on the cardiac tissue integrity and function (Figure 5.6).
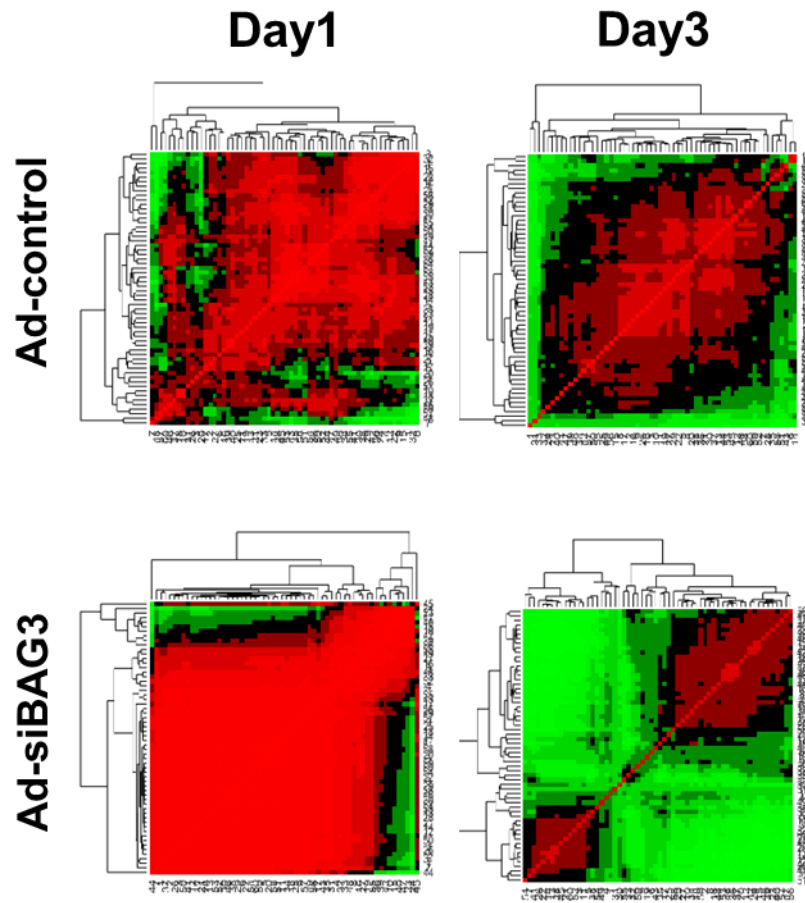
Figure 5.6. Correlation matrices representing the impact of BAG3 suppression on coordinated activity of primary cardiomyocytes. Hierarchical clustering of MEA recording-based correlation matrices for primary neonatal cardiomyocytes reveals that control cardiomyocytes (top row) exhibit one single cluster, while BAG3 suppression (bottom row) results in the formation of two distinct clusters of cardiomyocyte 3 days post transduction.

Local signal CV between electrode i and j, $V_{i,j}$, is calculated by dividing the distance between two electrodes ($\Delta l_{i,j}$) by their activation time distance ($\Delta t_{i,j}$) and mean CV for electrode i (V_i) is calculated using the equation below (Figure 5.7):

$$V_{i,j} = \frac{\Delta l_{i,j}}{\left|\Delta t_{i,j}\right|}, \quad V_i = \frac{\sum_{j=1, j\neq i}^{60} Vi,j}{n-1}$$

n denotes the number of electrodes.

The overall signal CV is calculated as an average signal velocities calculated for 60 electrodes:

$$\text{Signal CV} = \frac{\sum_{i=1}^{60} Vi}{60}$$
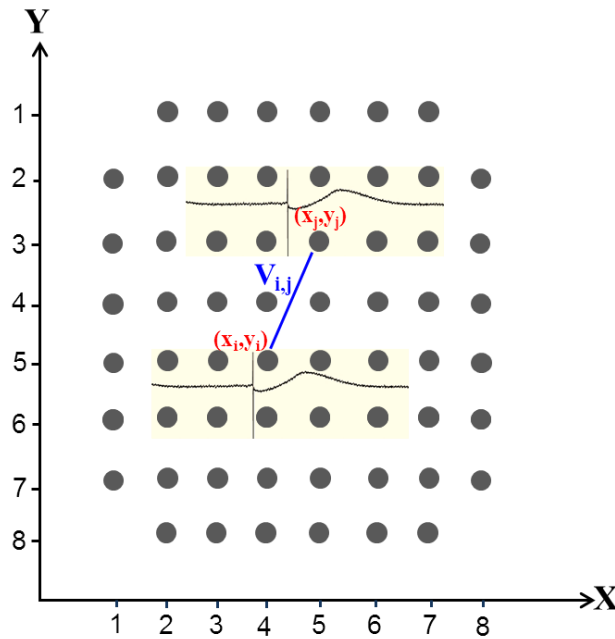
Figure 5.7. Impulse transmission among the electrodes in monolayer culture of cardiomyocytes. Conduction velocity ($V_{i,j}$) between electrodes i and j is calculated by diving the distance between two electrodes by the time of signal propagation.

Figure 5.8A exhibits average impulse CV calculated based on the data recorded by 60 electrodes embedded throughout the culture of spontaneously beating cardiomyocytes within 60 seconds of recording. CV was determined for control and BAG3-suppressed cardiomyocytes from initial condition (D0, no transduction) until 3 days post transduction (D3). We then calculated average CV_{max} for each culture and found that in control cells CV_{max} significantly was reduced by 8% from 36.1±5.6 cm/s on D0 to 33.28±2.6 cm/s on D3, while in BAG3-suppressed cardiomyocytes CV_{max} significantly reduced by 42% from 34.0±1.52 cm/s on D0 to 20.01±1.89 cm/s on D3 (Figure 5.8B).
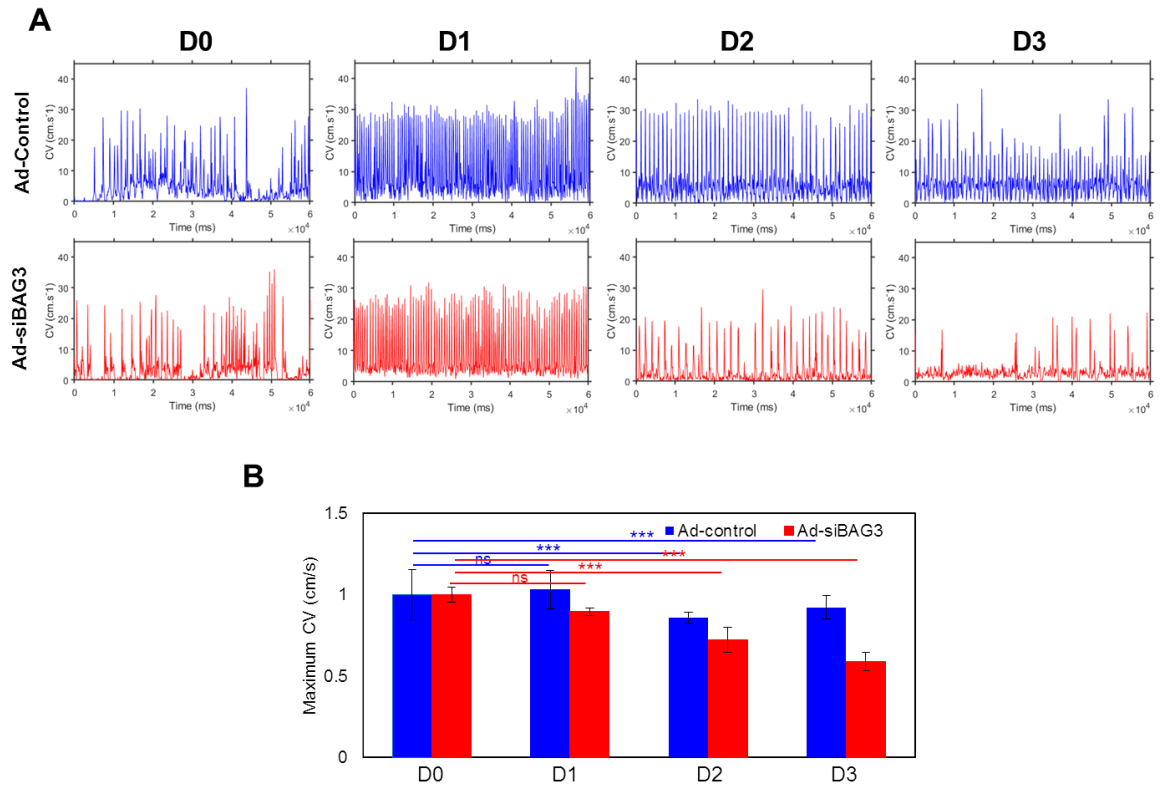
Figure 5.8. Suppression of BAG3 resulted in signal CV reduction in the culture of neonatal cardiomyocytes. (A) Electrophysiological activities of cardiomyocytes were recorded at initial condition (D0, no transduction) until 3 days post transduction (D3) for control and BAG3-suppressed cardiomyocytes. CVs were then calculated and represented within 60 seconds of recording. **(B)** CV_{max} was calculated based on the data presented in (A) and results showed that CV_{max} reduced by 8% in control cells while BAG3 suppression resulted in 42% reduction of CV_{max} 3 days post transduction. ***p<0.001 (n=3).

Inhibition of gap junction dysregulates electrical activity of cardiomyocytes

In another experiment, cultured NRVCs were treated with GJ inhibitors, CBX (100 µM) and Iox (10 µM), for different time intervals (1 to 8 hr) and the level of GJ protein, Cx43, was evaluated using western blotting and immunofluorescence staining. CBX was dissolved in water to make a stock concentration of 25 mM and Iox was prepared with a stock concentration of 200 mM in EtOH. Western blotting and immunofluorescence data indicated that Iox treatment led to significant reduction in Cx43 level (Figure 5.9A-E); while Cx43 level did not change as a result of CBX treatment (Data are not shown).

Extracellular recordings of untreated cardiomyocytes were performed before any treatments as initial conditions. Cells were then administrated with GJ inhibitors, Iox and CBX, and signals were recorded over time. Electrical signals were recorded immediately to minimize residual drug effects. Each recording was carried out for 10 min and cells were maintained in an incubator at 37°C perfused with 5% CO_2 during the experiments. Data indicated that CBX administration led to arrhythmic spiking with significant increase in FP frequency and reduction in amplitude within the culture. Total firing frequency increased to 147% of baseline while firing amplitude reduced to 53 % of baseline amplitude as a result of CBX administration 10 min post treatment. Furthermore, Iox treatment also led to alteration in cardiac spiking as spike frequency increased to 14% of baseline and spike amplitude reduced to 88 % of baseline as a result of Iox administration 10 min post treatment. The onset of responses with both CBX and Iox were very quick and immediately after drug administration arrhythmic responses were observed. Increase in signal frequency lasted until the end of 1 hr recording and complete cessation of spontaneous electrical activity was observed by longer time treatment (Figure 5.10A-F).
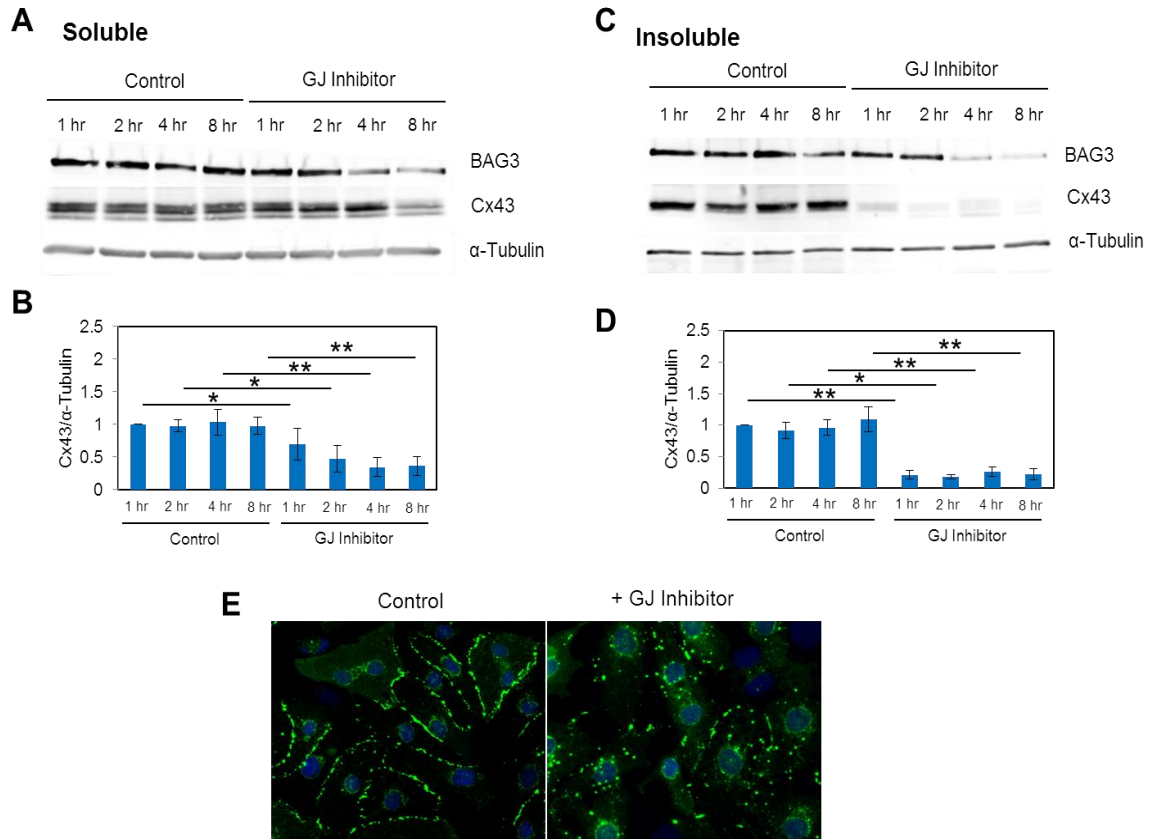
Figure 5.9. GJ inhibitor treatment led to Cx43 degradation in neonatal cardiomyocytes. NRVCs were subjected to Iox treatment (10 µM) for different time intervals of 1, 2, 4, and 8 hr and Cx43 levels were measured via western blotting and quantified in **(A,B)** soluble and **(C,D)** insoluble fractions of cell lysates. **(E)** NRVCs were treated with 10 µM Iox for 1 hr and Cx43 protein was observed via immunofluorescence staining. *$p<0.05$; **$p<0.01$ (n=3).
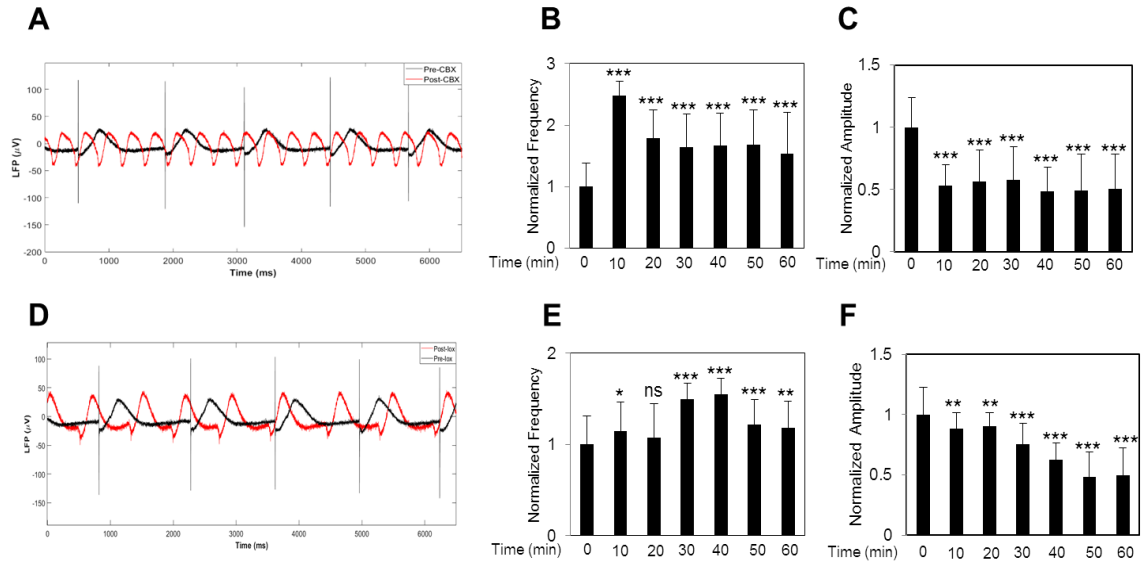
Figure 5.10. Inhibition of GJ activity dysregulates electrical activity of cardiomyocytes. (A) NRVCs were treated with CBX (100 µM) and extracellular FPs were recorded via MEA over time (0, 10, 20, 30, 40, 50 and 60 min). **(B)** FP frequencies were quantified based on the data presented in (A). **(C)** FP amplitudes were quantified based on the data presented in (B). **(D)** NRVCs were treated with Iox (10 µM) and extracellular FPs were recorded via MEA over time (0, 10, 20, 30, 40, 50 and 60 min). **(E)** FP frequencies were quantified based on the data presented in (D). **(F)** FP amplitudes were quantified based on the data presented in (D).

Inhibition of GJ activity dysregulates mitochondrial membrane potential and calcium uptake

GJ protein, Cx43, has been reported to be present in both plasma membrane and mitochondria of cardiomyocytes [Boengler et al., 2005]. In order to evaluate whether GJ proteins function as key regulators of mitochondrial bioenergetics, NRVCs were treated with GJ inhibitors, CBX (100 µM) and Iox (10 µM), and mitochondrial bioenergetics such as membrane potential and calcium uptake were evaluated 1 hr post treatment. Data indicated that inhibition of GJ led to significant reduction in mitochondrial membrane potential and impair of mitochondrial calcium uptake (Figure 5.11A-D).
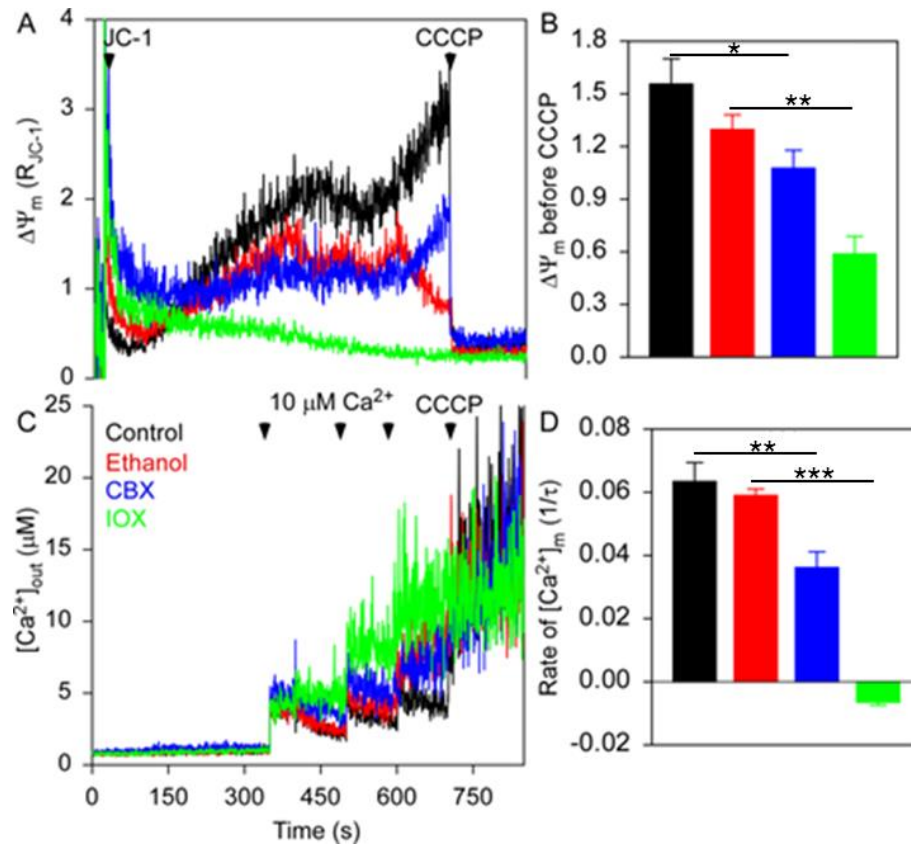
Figure 5.11. Inhibition of GJ activity dysregulates mitochondrial bioenergetics. (A) NRVCs were treated with GJ inhibitors, CBX (100 μM) and Iox (10 μM), for 1 hr and mitochondrial membrane potentials were measured. **(B)** Mitochondrial membrane potential quantifications were based on the data presented in (A). **(C)** NRVCs were treated with GJ inhibitors, CBX (100 μM) and Iox (10 μM), for 1 hr and mitochondrial calcium uptake was measured. **(D)** Mitochondrial calcium uptake quantifications were based on the data presented in (A). *$p<0.05$; **$p<0.01$; ***$p<0.001$ (n=3).

Discussion

GJs are 0.1-5 µM long structures located on cellular plasma membrane which permit passage of ion messengers and maintain chemical and electrical coupling of cardiac cells [Solan et al., 2014]. GJs are important determinants of impulse propagation in cardiac tissue and alterations in GJ coupling impair impulse conduction velocity between cardiomyocytes which contributes toward development of arrhythmias [Rohr et al., 2004]. Cardiac arrhythmia is important cause of cardiovascular morbidity in the United States [Tse et al., 2015]. Furthermore, GJ alterations have been observed in the failing human hearts [Kostin et al., 2003]. Therefore, understanding the mechanisms underlying the role of GJs in cardiac impulse propagation is pivotal toward discovering the mechanisms underlying heart failure. Among the proteins in the structure of GJs, Cx43 is a major GJ protein which is highly expressed in the heart and rapidly propagates AP between cardiac myocytes; therefore plays an important role in synchronization of cardiac contraction and heart beat [Epifantseva et al., 2018]. Cx43 is expressed in both atria and ventricles and is highly dynamic with rapid turnover and short half-life of 1-3 hr in the heart. Cx43 truncations lead to alterations in GJ permeability and changes in cardiac electrophysiological properties [Solan et al., 2014]. Recently we have reported that BAG3, a key regulator of autophagy in cardiac cells, significantly impacts the quality of Cx43 and impairs the function of GJ in neonatal cardiomyocytes. In this study, we have used a non-invasive MEA method to monitor and analyze the effect of BAG3 suppression on the electrophysiological activity of cardiomyocytes over time. For this purpose, NRVCs were transduced with adenovirus and extracellular electrical activities were recorded over a period of 1-3 days post transduction and analyzed to extract important electrophysiological components.

Considering limited regenerative capacity of adult myocardium, targeted differentiation of stem cells toward cardiac phenotypes have attracted attention for cardiac repair purposes post myocardial infarction [Kehat et al., 2004]. However, cardiac cells derived from human embryonic or pluripotent stem cells have been reported to be immature with lower cardiac function in terms of contractility and electrical signal conduction [Feinberg et al., 2013]. Considering cost, low-yield isolation and ethical issues associated with adult cardiomyocytes [Ehler et al., 2013], in this study we have used an *in vitro* model of primary neonatal cardiomyocytes and recorded spontaneously evoked extracellular electrical activity utilizing MEA system. MEA has been widely used for drug screening purposes to recognize cardiotoxic drugs which have proarrhythmic potential [Jans et al., 2017]. Each MEA plate is a 60-electrode configuration which records extracellular ion currents generated by populations of spontaneously beating cardiomyocytes known as FPs. Manual analysis of large amount of raw data generated by MEA is difficult. In this regard, applications such as MultiElec could be run independently of MATLAB License [Georgiadis et al., 2015]; however, they do not offer flexibility for further modifications. Therefore, development of custom-designed MATLAB scripts which could precisely estimate electrophysiological parameters are of great importance toward precise interpretation of cardiomyocyte behavior.

Previously we reported that BAG3 suppression significantly reduced Cx43 protein levels by increasing its degradation. Cx43 dysregulation has been associated with conduction abnormalities and arrhythmogenesis [Poelzing et al., 2004]. Cx43 deficiency in mice model resulted in death by 2 month of age [Gutstein et al., 2000]. Enhancement of Cx43 improved ventricular conduction velocity and protected against ventricular arrhythmias in Langendorff-perfused isolated rabbit hearts under stress condition [Hsieh et al., 2016].

MEA recordings revealed that BAG3 suppression led to dysregulation of the electrophysiological activity of neonatal cardiomyocytes.

Spike raster plots indicate population events underlying each spike occurrence. Raster plots of the transduced cells, either Ad-control or Ad-siBAG3, indicated an increase in the number of spikes one day post transduction; however, a noticeable reduction in the number of spikes was observed as a result of BAG3 suppression over time. Furthermore, data exhibited that BAG3 suppression led to alterations in spike distribution and spike timing among the electrodes; suggesting that the number of random firings increased within the culture as a result of BAG3 reduction. Beat frequency correlates with heart beat obtained from ECG and we observed spike frequency reduced as a result of BAG3 suppression. We have previously demonstrated BAG3 as a promising target for heart failure treatment as overexpression of BAG3 improved cardiac function in mice post myocardial infarction [Knezevic et al., 2016]. In order to further evaluate changes in the population-wide activity of cardiomyocytes as a result of BAG3 attenuation, color-coded activation maps were plotted to indicate simultaneous electrical activity of 60 electrodes within the culture. Data indicated that BAG3 suppression altered signal progression and activation pattern throughout the monolayer culture; such that areas with delayed activation and dysregulated spike firing increased as a result of BAG3 knock down.

Further analysis of MEA-recorded signals revealed that impulse CV determined as the ratio of distance traveled by impulse to the time distance between electrodes activation significantly reduced from 34.01±1.5 cm/s to 20.01±1.89 cm/s as a result of BAG3 suppression 3 days post transduction. Electrical signal for each heartbeat is initiated in sinoatrial (SA) node positioned in the wall of the right atrium. The excitatory signal then propagates throughout the atria and ventricles to depolarize them (systole) followed by

repolarization (diastole) [Sameni et al., 2011]. AP conduction is anisotropic which spreads 3 to 8 times faster in longitudinal direction parallel with myocardial fiber axis - compared to transverse direction in the heart [Tse et al., 2015, Grant et al., 2009, Peters et al., 1998]; as conduction properties change at different directions within the myocardium [Peters et al., 1998]. Longitudinal CV was determined as 66 cm/s and 22 cm/s in adult and neonatal rat ventricles respectively [Nygren et al., 2003, Papadaki et al., 2001]. Ion channels and GJs are important determinants of AP conduction in the heart and their mutations contribute toward arrhythmogenesis [Tse et al., 2015, Grant et al., 2009]. Cx43 localizes at the intercalated disks where mechanical and electrical coupling occurs in the structure of ventricular GJs between adjacent cardiomyocytes [Schulz et al., 2015, Tse et al., 2015] and Cx43 alterations are associated with alterations in ventricular CV [Peters et al., 1998]. Sodium ion channels are also located in intercalated disks and co-localize with GJs in adult myocytes [Tse et al., 2015]. BAG3 was demonstrated to co-localize with Na^+-K^+-ATPase in adult mouse left ventricular myocytes [Feldman et al., 2016]; therefore, dysregulation of Cx43 and ion channel activity as a result of BAG3 deficiency may contribute toward conductance disturbance.

In addition to the role of Cx43 in intercellular communication, previous studies reported that Cx43 is also localized in the inner mitochondrial membrane of myocardium. Under ischemic preconditioning, Cx43 translocated to mitochondria and played a cardioprotective role which was independent of Cx43 role in cell-to-cell communication [Boengler et al., 2005]. Furthermore, dysregulation of calcium homeostasis has been reported in failing myocardium [Tse et al., 2015]. However, the precise mechanism through which translocation of Cx43 to mitochondria plays a protective role remains under question. Our data indicated that inhibition of GJ activity led to dysregulation of electrophysiological activity of NRVCs as signal amplitude reduced and signal frequency

increased when cells were treated with GJ inhibitors. Furthermore, our data indicated that inhibition of GJ activity resulted in significant reduction in mitochondrial calcium uptake as well as mitochondrial membrane potential in neonatal cardiomyocytes. Taken together, our data suggest that impair of GJ activity results in dysregulation of cell-to-cell communication and mitochondrial bioenergetics in neonatal cardiomyocytes.

CHAPTER 6

CONCLUSIONS AND FUTURE WORK PLANS

Conclusions for specific aim 1:

This aim indicates that HIV-1 Tat significantly impacts mitochondrial function in NRVCs leading to significant ROS accumulation, respiration impairment and ATP reduction. Tat impairs calcium signaling and electrophysiological activity of cardiomyocytes and induces apoptosis. In addition, Tat interferes with autophagy initiation as well as proper degradation of autophagic proteins especially under stress conditions. We propose that regulation of autophagy might be a promising target to reduce HIV toxicity in cardiac cells.

Future work plans for specific aim 1:

Considering the notion that direct infection of cardiomyocytes by HIV-1 in the heart remains under question, it would be of great importance to evaluate the mitochondrial function in cardiomyocytes maintained in the conditioned media obtained from HIV-1-infected endothelial cells or fibroblasts. This experiment will present a better model of disease condition in which cardiomyocytes uptake HIV-1-encoded proteins secreted by the neighboring cells.

Conclusions for specific aim 2:

This aim uses NRVCs to demonstrate a new pathway for the clearance of dysfunctional mitochondria in which BAG3 regulates both endogenous and exogenous expression of Parkin. BAG3 and Parkin are both recruited to the mitochondria upon depolarization. BAG3 knock-down reduced autophagy flux and impaired the clearance of defective mitochondria which led to the higher levels of toxicity within the cells and subsequent cell death. Proteasome inhibition suggested BAG3's crucial role in activating the autophagy process along with other autophagy proteins such as HSP70 and p62. Taken together, our observations demonstrate that BAG3 may be a promising target for the treatment of heart failure and other myofbrillar myopathies.

Future work plans for specific aim 2:

Further mechanistic studies are needed to determine the mechanism through which BAG3 and Parkin function, whether Parkin ubiquitination signaling is essential for BAG3 recruitment, and whether BAG3 works upstream of Parkin. Moreover, the role of BAG3 as a key factor in mitophagy regulation in adult cardiomyocytes remains to be demonstrated. Additionally, in order to better mimic the stress condition in case of myocardial infarction, further studies are needed to investigate the role of BAG3 in mitochondrial quality control under ischemia-reperfusion injury both *in vitro* and *in vivo*.

Conclusions for specific aim 3:

In this aim, we have reported the impact of BAG3 on regulating the stability of gap junction protein Cx43. Considering the dynamic structure of gap junctions, its quality control is of great importance in cardiac synchronous contraction. We found that there was a significant reduction in Cx43 abundance and autophagic flux when cardiomyocytes were knocked down for BAG3. In addition, the stability of Cx43 protein was significantly reduced in BAG3-suppressed cardiomyocytes. Taken together, our findings suggest that BAG3 plays an important role in modulating the fate of Cx43 and enhancing BAG3 levels under stress conditions and might be a promising target to improve heart function.

Future work plans for specific aim 3:

Whether BAG3 directly impacts Cx43 quality or impair of BAG3 partner, heat shock protein chaperone complex, as a result of BAG3 suppression may impact Cx43 quality remains to be determined. In addition, the impact of BAG3 suppression on Cx43 quality in adult cardiomyocytes under normal and ischemia-reperfusion conditions remains to be determined.

Conclusions for specific aim 4:

Precise characterization of electrical activity of primary cardiomyocytes gives rise to a powerful model for better understanding of mechanisms underlying cardiac synchronization as well as precise electrophysiological assessment of engineered myocardium. Recently we reported that BAG3 suppression led to alterations in cardiac major GJ protein, Cx43, in neonatal cardiomyocytes. Considering the notion that GJ impairments are associated with cardiac conduction abnormalities and arrhythmias, the goal of this study was to characterize electrophysiological consequences of BAG3 suppression such as impulse propagation pattern and conduction velocity in NRVCs. Data indicated that knock down of BAG3 resulted in significant alterations in electrical activity of primary cardiomyocytes.

Future work plans for specific aim 4:

Monolayer culture of cardiomyocytes demonstrated here, proposes a two dimensional model with isotropic electrical signal propagation which lacks various electrical phenomena occurring in the complex heart tissue such as cardiomyocyte-fibroblast coupling; resulting in anisotropic propagation in which conduction speed differs in different directions within the myocardium. Therefore, improving the culture methods to obtain co-culture of cardiomyocytes and fibroblasts as well as considering the impact of extracellular matrix could enhance the model and improve the clinical translation of obtained results.

Peer-reviewed publications

1. **Tahrir FG,** Knezevic T, Gupta MK, Gordon J, Cheung JY, Feldman AM, Khalili K. Evidence for the role of BAG3 in mitochondrial quality control in cardiomyocytes. Journal of cellular physiology. 2017 Apr 1;232(4):797-805.

2. **Tahrir FG,** Shanmughapriya S, Ahooyi TM, Knezevic T, Gupta MK, Kontos CD, McClung JM, Madesh M, Gordon J, Feldman AM, Cheung JY, Khalili K. Dysregulation of Mitochondrial Bioenergetics and Quality Control by HIV-1 Tat in Cardiomyocytes. Journal of cellular physiology. 2018 Feb 1.

3. Gupta MK, **Tahrir FG,** Knezevic T, White MK, Gordon J, Cheung JY, Khalili K, Feldman AM. GRP78 Interacting Partner Bag5 Responds to ER Stress and Protects Cardiomyocytes From ER Stress-Induced Apoptosis. Journal of cellular biochemistry. 2016 Aug 1;117(8):1813-21.

4. Su F, Myers VD, Knezevic T, Wang J, Gao E, Madesh M, **Tahrir FG,** Gupta MK, Gordon J, Rabinowitz J, Ramsey FV, Tilley DG, Khalili K, Cheung JY, Feldman AM. Bcl-2–associated athanogene 3 protects the heart from ischemia/reperfusion injury. JCI insight. 2016 Nov 17;1(19).

5. Myers VD, McClung JM, Wang J, **Tahrir FG,** Gupta MK, Gordon J, Kontos CH, Khalili K, Cheung JY, Feldman AM. The Multifunctional Protein BAG3: A Novel Therapeutic Target in Cardiovascular Disease. JACC: Basic to Translational Science. 2018 Feb 28;3(1):122-31.

6. Myers VD, Tomar D, Madesh M, Wang J, Song J, Zhang XQ, Gupta MK, **Tahrir FG,** Gordon J, McClung JM, Kontos CD. Haplo-insufficiency of Bcl2-associated Athanogene 3 in Mice Results in Progressive Left Ventricular Dysfunction, β-Adrenergic Insensitivity and Increased Apoptosis. Journal of cellular physiology. 2018 Jan 11.

7. **Tahrir FG,** Gupta MK, Myers VD, Gordon J, Cheung YJ, Feldman AM, Khalili K. Role of BAG3 in Quality of Gap Junction Protein, Connexin 43, in Cardiomyocytes. Submitted.

8. Cheung JY, Gordon J, Wang JF, Song J, Zhang XQ, Prado FJ, Shanmughapriya S, Rajan S, Tomar D, **Tahrir FG,** Gupta MK, Kontos CD, McClug JM, Klotman PE, Madesh M, Khalili K, Feldman AM. Mitochondrial Dysfunction in HIV-1 Transgenic Mouse Cardiac Myocytes. Submitted.

9. **Tahrir FG,** Khalili K. Mitochondrial Quality Control in Cardiac Cells; A Review of Mechanisms and Role in Cardiac Disease. Under Preparation.

10. **Tahrir FG,** Ahooyi TM, Khalili K. Suppression of BAG3 Impairs Electrophysiological Activity of Cardiomyocytes. Under preparation.

REFERENCES

Ai X, Pogwizd SM. Connexin 43 downregulation and dephosphorylation in nonischemic heart failure is associated with enhanced colocalized protein phosphatase type 2A. Circulation research. 2005 Jan 7;96(1):54-63.

Arimura T, Ishikawa T, Nunoda S, Kawai S, Kimura A. Dilated cardiomyopathy- associated BAG3 mutations impair Z- disc assembly and enhance sensitivity to apoptosis in cardiomyocytes. Human mutation. 2011 Dec 1;32(12):1481-91.

Ashrafi G, Schwarz TL. The pathways of mitophagy for quality control and clearance of mitochondria. Cell death and differentiation. 2013 Jan;20(1):31.

Andres AM, Tucker KC, Thomas A, Taylor DJ, Sengstock D, Jahania SM, Dabir R, Pourpirali S, Brown JA, Westbrook DG, Ballinger SW. Mitophagy and mitochondrial biogenesis in atrial tissue of patients undergoing heart surgery with cardiopulmonary bypass. JCI insight. 2017 Feb 23;2(4).

Barbaro G. Cardiovascular manifestations of HIV infection. Circulation. 2002 Sep 10;106(11):1420-5.

Barodia SK, Creed RB, Goldberg MS. Parkin and PINK1 functions in oxidative stress and neurodegeneration. Brain research bulletin. 2017 Jul 1;133:51-9.

Beardslee MA, Lerner DL, Tadros PN, Laing JG, Beyer EC, Yamada KA, Kléber AG, Schuessler RB, Saffitz JE. Dephosphorylation and intracellular redistribution of ventricular connexin43 during electrical uncoupling induced by ischemia. Circulation research. 2000 Oct 13;87(8):656-62.

Behl C. BAG3 and friends: co-chaperones in selective autophagy during aging and disease. Autophagy. 2011 Jul 1;7(7):795-8.

Berthiaume JM, Kurdys JG, Muntean DM, Rosca MG. Mitochondrial NAD+/NADH Redox State and Diabetic Cardiomyopathy. Antioxidants & redox signaling. 2017 Dec 11.

Bhandari P, Song M, Chen Y, Burelle Y, Dorn GW. Mitochondrial Contagion Induced by Parkin Deficiency in Drosophila Hearts and Its Containment by Suppressing MitofusinNovelty and Significance. Circulation research. 2014 Jan 17;114(2):257-65.

Billia F, Hauck L, Konecny F, Rao V, Shen J, Mak TW. PTEN-inducible kinase 1 (PINK1)/Park6 is indispensable for normal heart function. Proceedings of the National Academy of Sciences. 2011 Jun 7;108(23):9572-7.

Boengler K, Dodoni G, Rodriguez-Sinovas A, Cabestrero A, Ruiz-Meana M, Gres P, Konietzka I, Lopez-Iglesias C, Garcia-Dorado D, Di Lisa F, Heusch G. Connexin 43 in cardiomyocyte mitochondria and its increase by ischemic preconditioning. Cardiovascular research. 2005 Aug 1;67(2):234-44.

Boengler K, Schulz R. Connexins in Cardiac Ischemia. Current Opinion in Physiology. 2018 Feb 22.

Bragoszewski P, Turek M, Chacinska A. Control of mitochondrial biogenesis and function by the ubiquitin–proteasome system. Open biology. 2017 Apr 1;7(4):170007.

Brunelle JK, Letai A. Control of mitochondrial apoptosis by the Bcl-2 family. Journal of cell science. 2009 Feb 15;122(4):437-41.

Bruno AP, De Simone FI, Iorio V, De Marco M, Khalili K, Sariyer IK, Capunzo M, Nori SL, Rosati A. HIV-1 Tat protein induces glial cell autophagy through enhancement of BAG3 protein levels. Cell cycle. 2014 Dec 1;13(23):3640-4.

Cao DJ, Lavandero S, Hill JA. Parkin gone wild: Unbridled ubiquitination. Circulation research. 2015 July,117(4):311-313

Carey AN, Sypek EI, Singh HD, Kaufman MJ, McLaughlin JP. Expression of HIV-Tat protein is associated with learning and memory deficits in the mouse. Behavioural brain research. 2012 Apr 1;229(1):48-56.

Chan NC, Salazar AM, Pham AH, Sweredoski MJ, Kolawa NJ, Graham RL, Hess S, Chan DC. Broad activation of the ubiquitin–proteasome system by Parkin is critical for mitophagy. Human molecular genetics. 2011 Feb 4;20(9):1726-37.

Chen Y, Dorn GW. PINK1-phosphorylated mitofusin 2 is a Parkin receptor for culling damaged mitochondria. Science. 2013 Apr 26;340(6131):471-5.

Chen Y, Liu Y, Dorn GW. Mitochondrial Fusion is Essential for Organelle Function and Cardiac HomeostasisNovelty and Significance. Circulation research. 2011 Dec 9;109(12):1327-31.

Cheung JY, Gordon J, Wang J, Song J, Zhang XQ, Tilley DG, Gao E, Koch WJ, Rabinowitz J, Klotman PE, Khalili K. Cardiac Dysfunction in HIV-1 Transgenic Mouse: Role of Stress and BAG3. Clinical and translational science. 2015 Aug 1;8(4):305-10.

Chistiakov DA, Shkurat TP, Melnichenko AA, Grechko AV, Orekhov AN. The role of mitochondrial dysfunction in cardiovascular disease: a brief review. Annals of medicine. 2018 Feb 17;50(2):121-7.

Ciechanover A. Intracellular protein degradation: from a vague idea thru the lysosome and the ubiquitin-proteasome system and onto human diseases and drug targeting. Best Practice & Research Clinical Haematology. 2017 Dec 1;30(4):341-55.

Disatnik MH, Ferreira JC, Campos JC, Gomes KS, Dourado PM, Qi X, Mochly-Rosen D. Acute inhibition of excessive mitochondrial fission after myocardial infarction prevents long-term cardiac dysfunction. Journal of the American Heart Association. 2013 Oct 10;2(5):e000461.

Doenst T, Nguyen TD, Abel ED. Cardiac metabolism in heart failure: implications beyond ATP production. Circulation research. 2013 Aug 30;113(6):709-24.

Domingo P, Suarez-Lozano I, Teira R, Lozano F, Terrón A, Viciana P, González J, Galindo MJ, Geijo P, Vergara A, Cosín J. Dyslipidemia and cardiovascular disease risk factor management in HIV-1-infected subjects treated with HAART in the Spanish VACH cohort. The open AIDS journal. 2008;2:26.

Dorn GW, Vega RB, Kelly DP. Mitochondrial biogenesis and dynamics in the developing and diseased heart. Genes & development. 2015 Oct 1;29(19):1981-91.

Dorn GW, Clark CF, Eschenbacher WH, Kang MY, Engelhard JT, Warner SJ, Matkovich SJ, Jowdy CC. MARF and Opa1 Control Mitochondrial and Cardiac Function in DrosophilaNovelty and Significance. Circulation research. 2011 Jan 7;108(1):12-7.

Drummond GR, Selemidis S, Griendling KK, Sobey CG. Combating oxidative stress in vascular disease: NADPH oxidases as therapeutic targets. Nature reviews Drug discovery. 2011 Jun;10(6):453.

Duan M, Yao H, Hu G, Chen X, Lund AK, Buch S. HIV Tat induces expression of ICAM-1 in HUVECs: implications for miR-221/-222 in HIV-associated cardiomyopathy. PloS one. 2013 Mar 28;8(3):e60170.

Dutta D, Xu J, Kim JS, Dunn Jr WA, Leeuwenburgh C. Upregulated autophagy protects cardiomyocytes from oxidative stress-induced toxicity. Autophagy. 2013 Mar 7;9(3):328-44.

Ehler E, Moore-Morris T, Lange S. Isolation and culture of neonatal mouse cardiomyocytes. Journal of visualized experiments: JoVE. 2013(79).

Engberding N, Spiekermann S, Schaefer A, Heineke A, Wiencke A, Müller M, Fuchs M, Hilfiker-Kleiner D, Hornig B, Drexler H, Landmesser U. Allopurinol attenuates left ventricular remodeling and dysfunction after experimental myocardial infarction: a new action for an old drug?. Circulation. 2004 Oct 12;110(15):2175-9.

Epifantseva I, Shaw RM. Intracellular trafficking pathways of Cx43 gap junction channels. Biochimica et Biophysica Acta (BBA)-Biomembranes. 2018 Jan 31;1860(1):40-7.

Espert L, Denizot M, Grimaldi M, Robert-Hebmann V, Gay B, Varbanov M, Codogno P, Biard-Piechaczyk M. Autophagy is involved in T cell death after binding of HIV-1 envelope proteins to CXCR4. The Journal of clinical investigation. 2006 Aug 1;116(8):2161-72.

Eugenin EA, Morgello S, Klotman ME, Mosoian A, Lento PA, Berman JW, Schecter AD. Human immunodeficiency virus (HIV) infects human arterial smooth muscle cells in vivo and in vitro: implications for the pathogenesis of HIV-mediated vascular disease. The American journal of pathology. 2008 Apr 1;172(4):1100-11.

Falk MM, Kells RM, Berthoud VM. Degradation of connexins and gap junctions. FEBS letters. 2014 Apr 17;588(8):1221-9.

Fang Q, Kan H, Lewis W, Chen F, Sharma P, Finkel MS. Dilated cardiomyopathy in transgenic mice expressing HIV Tat. Cardiovascular toxicology. 2009 Mar 1;9(1):39-45.

Fang X, Bogomolovas J, Wu T, Zhang W, Liu C, Veevers J, Stroud MJ, Zhang Z, Ma X, Mu Y, Lao DH. Loss-of-function mutations in co-chaperone BAG3 destabilize small HSPs and cause cardiomyopathy. The Journal of Clinical Investigation. 2017 Aug 1;127(8):3189-200.

Feinberg AW, Ripplinger CM, Van Der Meer P, Sheehy SP, Domian I, Chien KR, Parker KK. Functional differences in engineered myocardium from embryonic stem cell-derived versus neonatal cardiomyocytes. Stem cell reports. 2013 Nov 19;1(5):387-96.

Feldman AM, Begay RL, Knezevic T, Myers VD, Slavov DB, Zhu W, Gowan K, Graw SL, Jones KL, Tilley DG, Coleman RC. Decreased levels of BAG3 in a family with a rare variant and in idiopathic dilated cardiomyopathy. Journal of cellular physiology. 2014 Nov 1;229(11):1697-702.

Feldman AM, Gordon J, Wang J, Song J, Zhang XQ, Myers VD, Tilley DG, Gao E, Hoffman NE, Tomar D, Madesh M. BAG3 regulates contractility and Ca2+ homeostasis in adult mouse ventricular myocytes. Journal of molecular and cellular cardiology. 2016 Mar 1;92:10-20.

Fiala M, Polik W, Qiao JH, Lossinsky AS, Alce T, Tran K, Yang W, Roos KP, Arthos J. HIV-1 induces cardiomyopathy by cardiomyocyte invasion and gp120, Tat, and cytokine apoptotic signaling. Cardiovascular toxicology. 2004 Jun 1;4(2):97-107.

Fields J, Dumaop W, Elueteri S, Campos S, Serger E, Trejo M, Kosberg K, Adame A, Spencer B, Rockenstein E, He JJ. HIV-1 Tat alters neuronal autophagy by modulating autophagosome fusion to the lysosome: implications for HIV-associated neurocognitive disorders. Journal of Neuroscience. 2015 Feb 4;35(5):1921-38.

Fimia GM, Kroemer G, Piacentini M. Molecular mechanisms of selective autophagy. Cell death and differentiation 2013;20:1.

Fong JT, Kells RM, Gumpert AM, Marzillier JY, Davidson MW, Falk MM. Internalized gap junctions are degraded by autophagy. Autophagy. 2012 May 13;8(5):794-811.

Franaszczyk M, Bilinska ZT, Sobieszczańska-Małek M, Michalak E, Sleszycka J, Sioma A, Małek ŁA, Kaczmarska D, Walczak E, Włodarski P, Hutnik Ł. The BAG3 gene variants in Polish patients with dilated cardiomyopathy: four novel mutations and a genotype-phenotype correlation. Journal of translational medicine. 2014 Dec;12(1):192.

Fulda S. Shifting the balance of mitochondrial apoptosis: therapeutic perspectives. Frontiers in oncology. 2012 Oct 8;2:121.

Gamerdinger M, Kaya AM, Wolfrum U, Clement AM, Behl C. BAG3 mediates chaperone-based aggresome-targeting and selective autophagy of misfolded proteins. EMBO reports. 2011 Feb 1;12(2):149-56.

Gaudesius G, Miragoli M, Thomas SP, Rohr S. Coupling of cardiac electrical activity over extended distances by fibroblasts of cardiac origin. Circulation research. 2003 Sep 5;93(5):421-8.

Gegg ME, Schapira AH. PINK1-parkin-dependent mitophagy involves ubiquitination of mitofusins 1 and 2: implications for Parkinson disease pathogenesis. Autophagy. 2011 Feb 1;7(2):243-5.

Georgiadis V, Stephanou A, Townsend PA, Jackson TR. MultiElec: A MATLAB based application for MEA data analysis. PloS one. 2015 Jun 15;10(6):e0129389.

Giepmans BN, Verlaan I, Hengeveld T, Janssen H, Calafat J, Falk MM, Moolenaar WH. Gap junction protein connexin-43 interacts directly with microtubules. Current Biology. 2001 Sep 4;11(17):1364-8.

Gilleron J, Fiorini C, Carette D, Avondet C, Falk MM, Segretain D, Pointis G. Molecular reorganization of Cx43, Zo-1 and Src complexes during the endocytosis of gap junction plaques in response to a non-genomic carcinogen. J Cell Sci. 2008 Dec 15;121(24):4069-78.

Gong G, Song M, Csordas G, Kelly DP, Matkovich SJ, Dorn GW. Parkin-mediated mitophagy directs perinatal cardiac metabolic maturation in mice. Science. 2015 Dec 4;350(6265):aad2459.

Goldberg GS, Valiunas V, Brink PR. Selective permeability of gap junction channels. Biochimica et Biophysica Acta (BBA)-Biomembranes. 2004 Mar 23;1662(1-2):96-101.

Griffiths EJ, Rutter GA. Mitochondrial calcium as a key regulator of mitochondrial ATP production in mammalian cells. Biochimica et Biophysica Acta (BBA)-Bioenergetics. 2009 Nov 1;1787(11):1324-33.

Grant AO. Cardiac ion channels. Circulation: Arrhythmia and Electrophysiology. 2009 Apr 1;2(2):185-94.

Große L, Wurm CA, Brüser C, Neumann D, Jans DC, Jakobs S. Bax assembles into large ring-like structures remodeling the mitochondrial outer membrane in apoptosis. The EMBO journal. 2016 Feb 15;35(4):402-13.

Gupta MK, Tahrir FG, Knezevic T, White MK, Gordon J, Cheung JY, Khalili K, Feldman AM. GRP78 Interacting Partner Bag5 Responds to ER Stress and Protects Cardiomyocytes From ER Stress-Induced Apoptosis. Journal of cellular biochemistry. 2016 Aug 1;117(8):1813-21.

Gustafsson ÅB, Gottlieb RA. Autophagy in ischemic heart disease. Circulation research. 2009 Jan 30;104(2):150-8.

Gutstein DE, Morley GE, Tamaddon H, Vaidya D, Schneider MD, Chen J, Chien KR, Stuhlmann H, Fishman GI. Conduction slowing and sudden arrhythmic death in mice with cardiac-restricted inactivation of connexin43. Circulation research. 2001 Feb 16;88(3):333-9.

Hammerling BC, Gustafsson ÅB. Mitochondrial quality control in the myocardium: cooperation between protein degradation and mitophagy. Journal of molecular and cellular cardiology. 2014 Oct 1;75:122-30.

Hartl FU, Bracher A, Hayer-Hartl M. Molecular chaperones in protein folding and proteostasis. Nature. 2011 Jul;475(7356):324.

Hsieh YC, Lin JC, Hung CY, Li CH, Lin SF, Yeh HI, Huang JL, Lo CP, Haugan K, Larsen BD, Wu TJ. Gap junction modifier rotigaptide decreases the susceptibility to ventricular arrhythmia by enhancing conduction velocity and suppressing discordant alternans during therapeutic hypothermia in isolated rabbit hearts. Heart Rhythm. 2016 Jan 1;13(1):251-61.

Hedhli N, Lizano P, Hong C, Fritzky LF, Dhar SK, Liu H, Tian Y, Gao S, Madura K, Vatner SF, Depre C. Proteasome inhibition decreases cardiac remodeling after initiation of pressure overload. American Journal of Physiology-Heart and Circulatory Physiology. 2008 Oct;295(4):H1385-93.

Hill BG, Dranka BP, Zou L, Chatham JC, Darley-Usmar VM. Importance of the bioenergetic reserve capacity in response to cardiomyocyte stress induced by 4-hydroxynonenal. Biochemical Journal. 2009 Nov 15;424(1):99-107.

Hishiya A, Kitazawa T, Takayama S. BAG3 and Hsc70 Interact With Actin Capping Protein CapZ to Maintain Myofibrillar Integrity Under Mechanical StressNovelty and Significance. Circulation research. 2010 Nov 12;107(10):1220-31.

Holmgren D, Wahlander H, Eriksson BO, Oldfors A, Holme E, Tulinius M. Cardiomyopathy in children with mitochondrial disease: Clinical course and cardiological findings. European heart journal. 2003 Feb 1;24(3):280-8.

Homma S, Iwasaki M, Shelton GD, Engvall E, Reed JC, Takayama S. BAG3 deficiency results in fulminant myopathy and early lethality. The American journal of pathology. 2006 Sep 1;169(3):761-73.

Ikeda Y, Shirakabe A, Brady C, Zablocki D, Ohishi M, Sadoshima J. Molecular mechanisms mediating mitochondrial dynamics and mitophagy and their functional roles in the cardiovascular system. Journal of molecular and cellular cardiology. 2015 Jan 1;78:116-22.

Jackson S, Schaefer J, Meinhardt M, Reichmann H. Mitochondrial abnormalities in the myofibrillar myopathies. European journal of neurology. 2015 Nov 1;22(11):1429-35.

Jang S, Lewis TS, Powers C, Khuchua Z, Baines CP, Wipf P, Javadov S. Elucidating mitochondrial electron transport chain supercomplexes in the heart during ischemia–reperfusion. Antioxidants & redox signaling. 2017 Jul 1;27(1):57-69.

Jans D, Callewaert G, Krylychkina O, Hoffman L, Gullo F, Prodanov D, Braeken D. Action potential-based MEA platform for in vitro screening of drug-induced cardiotoxicity using human iPSCs and rat neonatal myocytes. Journal of pharmacological and toxicological methods. 2017 Sep 1;87:48-52.

Jeang KT, Xiao H, Rich EA. Multifaceted activities of the HIV-1 transactivator of transcription, Tat. Journal of Biological Chemistry. 1999 Oct 8;274(41):28837-40.

Jin Q, Li R, Hu N, Xin T, Zhu P, Hu S, Ma S, Zhu H, Ren J, Zhou H. DUSP1 alleviates cardiac ischemia/reperfusion injury by suppressing the Mff-required mitochondrial fission and Bnip3-related mitophagy via the JNK pathways. Redox biology. 2018 Apr 1;14:576-87.

Jonckheere AI, Smeitink JA, Rodenburg RJ. Mitochondrial ATP synthase: architecture, function and pathology. Journal of inherited metabolic disease. 2012 Mar 1;35(2):211-25.

Johansen T, Lamark T. Selective autophagy mediated by autophagic adapter proteins. Autophagy. 2011 Mar 1;7(3):279-96.

Kageyama Y, Hoshijima M, Seo K, Bedja D, Sysa-Shah P, Andrabi SA, Chen W, Höke A, Dawson VL, Dawson TM, Gabrielson K. Parkin-independent mitophagy requires Drp1 and maintains the integrity of mammalian heart and brain. The EMBO journal. 2014 Dec 1;33(23):2798-813.

Kane LA, Lazarou M, Fogel AI, Li Y, Yamano K, Sarraf SA, Banerjee S, Youle RJ. PINK1 phosphorylates ubiquitin to activate Parkin E3 ubiquitin ligase activity. J Cell Biol. 2014 Apr 21:jcb-201402104.

Kang PT, Chen CL, Lin P, Chilian WM, Chen YR. Impairment of pH gradient and membrane potential mediates redox dysfunction in the mitochondria of the post-ischemic heart. Basic research in cardiology. 2017 Jul 1;112(4):36.

Kazlauskaite A, Kondapalli C, Gourlay R, Campbell DG, Ritorto MS, Hofmann K, Alessi DR, Knebel A, Trost M, Muqit MM. Parkin is activated by PINK1-dependent phosphorylation of ubiquitin at Ser65. Biochemical Journal. 2014 May 15;460(1):127-41.

Kehat I, Khimovich L, Caspi O, Gepstein A, Shofti R, Arbel G, Huber I, Satin J, Itskovitz-Eldor J, Gepstein L. Electromechanical integration of cardiomyocytes derived from human embryonic stem cells. Nature biotechnology. 2004 Oct;22(10):1282.

Kim NC, Tresse E, Kolaitis RM, Molliex A, Thomas RE, Alami NH, Wang B, Joshi A, Smith RB, Ritson GP, Winborn BJ. VCP is essential for mitochondrial quality control by PINK1/Parkin and this function is impaired by VCP mutations. Neuron. 2013 Apr 10;78(1):65-80.

Knezevic T, Myers VD, Gordon J, Tilley DG, Sharp TE, Wang J, Khalili K, Cheung JY, Feldman AM. BAG3: a new player in the heart failure paradigm. Heart failure reviews. 2015 Jul 1;20(4):423-34.

Knezevic T, Myers VD, Su F, Wang J, Song J, Zhang XQ, Gao E, Gao G, Madesh M, Gupta MK, Gordon J. Adeno-Associated Virus Serotype 9–Driven Expression of BAG3 Improves Left Ventricular Function in Murine Hearts With Left Ventricular Dysfunction Secondary to a Myocardial Infarction. JACC: Basic to Translational Science. 2016 Dec 1;1(7):647-56.

Koene S, Smeitink J. Metabolic manipulators: a well founded strategy to combat mitochondrial dysfunction. Journal of inherited metabolic disease. 2011 Apr 1;34(2):315-25.

Koene S, Smeitink J. Mitochondrial medicine: entering the era of treatment. Journal of internal medicine. 2009 Feb 1;265(2):193-209.

Kostin S, Rieger M, Dammer S, Hein S, Richter M, Klövekorn WP, Bauer EP, Schaper J. Gap junction remodeling and altered connexin43 expression in the failing human heart. InCardiac Cell Biology 2003 (pp. 135-144). Springer, Boston, MA.

Koyano F, Okatsu K, Kosako H, Tamura Y, Go E, Kimura M, Kimura Y, Tsuchiya H, Yoshihara H, Hirokawa T, Endo T. Ubiquitin is phosphorylated by PINK1 to activate parkin. Nature. 2014 Jun;510(7503):162.

Kubli DA, Zhang X, Lee Y, Hanna RA, Quinsay MN, Nguyen CK, Jimenez R, Petrosyan S, Murphy AN, Gustafsson ÅB. Parkin protein deficiency exacerbates cardiac injury and reduces survival following myocardial infarction. Journal of Biological Chemistry. 2013 Jan 11;288(2):915-26.

Kuzmicic J, del Campo A, López-Crisosto C, Morales PE, Pennanen C, Bravo-Sagua R, Hechenleitner J, Zepeda R, Castro PF, Verdejo HE, Parra V. Mitochondrial dynamics: a potential new therapeutic target for heart failure. Revista Española de Cardiología (English Edition). 2011 Oct 1;64(10):916-23.

Kyei GB, Dinkins C, Davis AS, Roberts E, Singh SB, Dong C, Wu L, Kominami E, Ueno T, Yamamoto A, Federico M. Autophagy pathway intersects with HIV-1 biosynthesis and regulates viral yields in macrophages. The Journal of cell biology. 2009 Jul 27;186(2):255-68.

Lazarou M, Sliter DA, Kane LA, Sarraf SA, Wang C, Burman JL, Sideris DP, Fogel AI, Youle RJ. The ubiquitin kinase PINK1 recruits autophagy receptors to induce mitophagy. Nature. 2015 Aug;524(7565):309.

Lavandero S, Chiong M, Rothermel BA, Hill JA. Autophagy in cardiovascular biology. The Journal of clinical investigation. 2015 Jan 2;125(1):55-64.

Lee JY, Nagano Y, Taylor JP, Lim KL, Yao TP. Disease-causing mutations in parkin impair mitochondrial ubiquitination, aggregation, and HDAC6-dependent mitophagy. The Journal of cell biology. 2010 May 10:jcb-201001039.

Leithe E, Rivedal E. Epidermal growth factor regulates ubiquitination, internalization and proteasome-dependent degradation of connexin43. J Cell Sci. 2004 Mar 1;117(7):1211-20.

Lesnefsky EJ, Chen Q, Tandler B, Hoppel CL. Mitochondrial dysfunction and myocardial ischemia-reperfusion: implications for novel therapies. Annual review of pharmacology and toxicology. 2017 Jan 6;57:535-65.

Li S, Zhang HY, Wang T, Meng X, Zong ZH, Kong DH, Wang HQ, Du ZX. BAG3 promoted starvation-induced apoptosis of thyroid cancer cells via attenuation of autophagy. The Journal of Clinical Endocrinology & Metabolism. 2014 Nov 1;99(11):E2298-307.

Liao Q, Ozawa F, Friess H, Zimmermann A, Takayama S, Reed JC, Kleeff J, Büchler MW. The anti-apoptotic protein BAG-3 is overexpressed in pancreatic cancer and induced by heat stress in pancreatic cancer cell lines. FEBS letters. 2001 Aug 17;503(2-3):151-7.

Liao WC, Juo LY, Shih YL, Chen YH, Yan YT. HSPB7 prevents cardiac conduction system defect through maintaining intercalated disc integrity. PLoS genetics. 2017 Aug 21;13(8):e1006984.

Liu BQ, Du ZX, Zong ZH, Li C, Li N, Zhang Q, Kong DH, Wang HQ. BAG3-dependent noncanonical autophagy induced by proteasome inhibition in HepG2 cells. Autophagy. 2013 Jun 6;9(6):905-16.

Liu L, Feng D, Chen G, Chen M, Zheng Q, Song P, Ma Q, Zhu C, Wang R, Qi W, Huang L. Mitochondrial outer-membrane protein FUNDC1 mediates hypoxia-induced mitophagy in mammalian cells. Nature cell biology. 2012 Feb;14(2):177.

Liu X, Ye B, Miller S, Yuan H, Zhang H, Tian L, Nie J, Imae R, Arai H, Li Y, Cheng Z. Ablation of ALCAT1 mitigates hypertrophic cardiomyopathy through effects on oxidative stress and mitophagy. Molecular and cellular biology. 2012 Nov 1;32(21):4493-504.

Li J, Horak KM, Su H, Sanbe A, Robbins J, Wang X. Enhancement of proteasomal function protects against cardiac proteinopathy and ischemia/reperfusion injury in mice. The Journal of clinical investigation. 2011 Aug 15;121(9).

Logan A, Pell VR, Shaffer KJ, Evans C, Stanley NJ, Robb EL, Prime TA, Chouchani ET, Cochemé HM, Fearnley IM, Vidoni S. Assessing the mitochondrial membrane potential in cells and in vivo using targeted click chemistry and mass spectrometry. Cell metabolism. 2016 Feb 9;23(2):379-85.

Luongo TS, Lambert JP, Yuan A, Zhang X, Gross P, Song J, Shanmughapriya S, Gao E, Jain M, Houser SR, Koch WJ. The mitochondrial calcium uniporter matches energetic supply with cardiac workload during stress and modulates permeability transition. Cell reports. 2015 Jul 7;12(1):23-34.

Ma LL, Ma X, Kong FJ, Guo JJ, Shi HT, Zhu JB, Zou YZ, Ge JB. Mammalian target of rapamycin inhibition attenuates myocardial ischaemia–reperfusion injury in hypertrophic heart. Journal of cellular and molecular medicine. 2018 Jan 4.

Maldarelli F, Sato H, Berthold E, Orenstein J, Martin MA. Rapid induction of apoptosis by cell-to-cell transmission of human immunodeficiency virus type 1. Journal of virology. 1995 Oct 1;69(10):6457-65.

Manga P, McCutcheon K, Tsabedze N, Vachiat A, Zachariah D. HIV and nonischemic heart disease. Journal of the American College of Cardiology. 2017 Jan 3;69(1):83-91.

Maron BJ, Towbin JA, Thiene G, Antzelevitch C, Corrado D, Arnett D, Moss AJ, Seidman CE, Young JB. Contemporary definitions and classification of the cardiomyopathies: an American heart

association scientific statement from the council on clinical cardiology, heart failure and transplantation committee; quality of care and outcomes research and functional genomics and translational biology interdisciplinary working groups; and council on epidemiology and prevention. Circulation. 2006 Apr 11;113(14):1807-16.

Martins-Marques T, Catarino S, Zuzarte M, Marques C, Matafome P, Pereira P, Girão H. Ischaemia-induced autophagy leads to degradation of gap junction protein connexin43 in cardiomyocytes. Biochemical Journal. 2015 Apr 15;467(2):231-45.

Matsuda N, Tanaka K. Cell biology: Tagged tags engage disposal. Nature. 2015 Aug;524(7565):294.

Mauvezin C, Neufeld TP. Bafilomycin A1 disrupts autophagic flux by inhibiting both V-ATPase-dependent acidification and Ca-P60A/SERCA-dependent autophagosome-lysosome fusion. Autophagy. 2015 Aug 3;11(8):1437-8.

Maulik SK, Kumar S. Oxidative stress and cardiac hypertrophy: a review. Toxicology mechanisms and methods. 2012 Jun 1;22(5):359-66.

McCORMACK JG, DENTON RM. The activation of isocitrate dehydrogenase (NAD+) by Ca2+ within intact uncoupled rat brown adipose tissue mitochondria incubated in the presence and absence of albumin. Biochemical Society Transactions 1980;8:339.

McWilliams TG, Prescott AR, Montava-Garriga L, Ball G, Singh F, Barini E, Muqit MM, Brooks SP, Ganley IG. Basal Mitophagy Occurs Independently of PINK1 in Mouse Tissues of High Metabolic Demand. Cell metabolism. 2018 Jan 11.

Milan E, Perini T, Resnati M, Orfanelli U, Oliva L, Raimondi A, Cascio P, Bachi A, Marcatti M, Ciceri F, Cenci S. A plastic SQSTM1/p62-dependent autophagic reserve maintains proteostasis and determines proteasome inhibitor susceptibility in multiple myeloma cells. Autophagy. 2015 Jul 3;11(7):1161-78.

Minoia M, Boncoraglio A, Vinet J, Morelli FF, Brunsting JF, Poletti A, Krom S, Reits E, Kampinga HH, Carra S. BAG3 induces the sequestration of proteasomal clients into cytoplasmic puncta: implications for a proteasome-to-autophagy switch. Autophagy. 2014 Sep 19;10(9):1603-21.

Myers VD, McClung JM, Wang J, Tahrir FG, Gupta MK, Gordon J, Kontos CH, Khalili K, Cheung JY, Feldman AM. The Multifunctional Protein BAG3: A Novel Therapeutic Target in Cardiovascular Disease. JACC: Basic to Translational Science. 2018 Feb 28;3(1):122-31.

Nakai A, Yamaguchi O, Takeda T, Higuchi Y, Hikoso S, Taniike M, Omiya S, Mizote I, Matsumura Y, Asahi M, Nishida K. The role of autophagy in cardiomyocytes in the basal state and in response to hemodynamic stress. Nature medicine. 2007 May;13(5):619.

Narendra D, Tanaka A, Suen DF, Youle RJ. Parkin is recruited selectively to impaired mitochondria and promotes their autophagy. The Journal of cell biology. 2008 Dec 1;183(5):795-803.

Narendra DP, Youle RJ. Targeting mitochondrial dysfunction: role for PINK1 and Parkin in mitochondrial quality control. Antioxidants & redox signaling. 2011 May 15;14(10):1929-38.

Nath A, Steiner J. Synaptodendritic injury with HIV-Tat protein: what is the therapeutic target?. Experimental neurology. 2014 Jan;251:112.

Navarrete EG, Liang P, Lan F, Sanchez-Freire V, Simmons C, Gong T, Sharma A, Burridge PW, Patlolla B, Lee AS, Wu H. Screening drug-induced arrhythmia using human induced pluripotent stem cell–derived cardiomyocytes and low-impedance microelectrode arrays. Circulation. 2013 Sep 10;128(11 suppl 1):S3-13.

Nygren A, Kondo C, Clark RB, Giles WR. Voltage-sensitive dye mapping in Langendorff-perfused rat hearts. American Journal of Physiology-Heart and Circulatory Physiology. 2003 Mar 1;284(3):H892-902.

Neary MT, Ng KE, Ludtmann MH, Hall AR, Piotrowska I, Ong SB, Hausenloy DJ, Mohun TJ, Abramov AY, Breckenridge RA. Hypoxia signaling controls postnatal changes in cardiac mitochondrial morphology and function. Journal of molecular and cellular cardiology. 2014 Sep 1;74:340-52.

Niemann B, Schwarzer M, Rohrbach S. Heart and Mitochondria: Pathophysiology and Implications for Cardiac Surgeons. The Thoracic and cardiovascular surgeon. 2017 Dec 19.

Nishida K, Otsu K. Sterile inflammation and degradation systems in heart failure. Circulation Journal. 2017 Apr 25;81(5):622-8.

Norman JP, Perry SW, Kasischke KA, Volsky DJ, Gelbard HA. HIV-1 trans activator of transcription protein elicits mitochondrial hyperpolarization and respiratory deficit, with dysregulation of complex IV and nicotinamide adenine dinucleotide homeostasis in cortical neurons. The Journal of Immunology. 2007 Jan 15;178(2):869-76.

Ong SB, Subrayan S, Lim SY, Yellon DM, Davidson SM, Hausenloy DJ. Inhibiting mitochondrial fission protects the heart against ischemia/reperfusion injury. Circulation. 2010 May 11;121(18):2012-22.

Ong SB, Kalkhoran SB, Hernández-Reséndiz S, Samangouei P, Ong SG, Hausenloy DJ. Mitochondrial-Shaping Proteins in Cardiac Health and Disease–the Long and the Short of It!. Cardiovascular drugs and therapy. 2017 Feb 1;31(1):87-107.

Padman BS, Bach M, Lucarelli G, Prescott M, Ramm G. The protonophore CCCP interferes with lysosomal degradation of autophagic cargo in yeast and mammalian cells. Autophagy. 2013 Nov 3;9(11):1862-75.

Pankiv S, Clausen TH, Lamark T, Brech A, Bruun JA, Outzen H, Øvervatn A, Bjørkøy G, Johansen T. p62/SQSTM1 binds directly to Atg8/LC3 to facilitate degradation of ubiquitinated protein aggregates by autophagy. Journal of biological chemistry. 2007 Aug 17;282(33):24131-45.

Papadaki M, Bursac N, Langer R, Merok J, Vunjak-Novakovic G, Freed LE. Tissue engineering of functional cardiac muscle: molecular, structural, and electrophysiological studies. American Journal of Physiology-Heart and Circulatory Physiology. 2001 Jan 1;280(1):H168-78.

Papanicolaou KN, Kikuchi R, Ngoh GA, Coughlan KA, Dominguez I, Stanley WC, Walsh K. Mitofusins 1 and 2 are essential for postnatal metabolic remodeling in heart. Circulation research. 2012 Jan 1:CIRCRESAHA-112.

Park DJ, Wallick CJ, Martyn KD, Lau AF, Jin C, Warn-Cramer BJ. Akt phosphorylates Connexin43 on Ser373, a "mode-1" binding site for 14-3-3. Cell communication & adhesion. 2007 Jan 1;14(5):211-26.

Parihar P, Parihar MS. Metabolic enzymes dysregulation in heart failure: the prospective therapy. Heart failure reviews. 2017 Jan 1;22(1):109-21.

Perry SW, Norman JP, Barbieri J, Brown EB, Gelbard HA. Mitochondrial membrane potential probes and the proton gradient: a practical usage guide. Biotechniques. 2011 Feb;50(2):98.

Perry SW, Norman JP, Litzburg A, Zhang D, Dewhurst S, Gelbard HA. HIV-1 transactivator of transcription protein induces mitochondrial hyperpolarization and synaptic stress leading to apoptosis. The Journal of Immunology. 2005 Apr 1;174(7):4333-44.

Peters NS, Wit AL. Myocardial architecture and ventricular arrhythmogenesis. Circulation. 1998 May 5;97(17):1746-54.

Piquereau J, Godin R, Deschênes S, Bessi VL, Mofarrahi M, Hussain SN, Burelle Y. Protective role of PARK2/Parkin in sepsis-induced cardiac contractile and mitochondrial dysfunction. Autophagy. 2013 Nov 3;9(11):1837-51.

Poelzing S, Rosenbaum DS. Altered connexin43 expression produces arrhythmia substrate in heart failure. American Journal of Physiology-Heart and Circulatory Physiology. 2004 Oct;287(4):H1762-70.

Predmore JM, Wang P, Davis F, Bartolone S, Westfall MV, Dyke DB, Pagani F, Powell SR, Day SM. Ubiquitin proteasome dysfunction in human hypertrophic and dilated cardiomyopathies. Circulation. 2010 Mar 2;121(8):997-1004.

Pye J, Ardeshirpour F, McCain A, Bellinger DA, Merricks E, Adams J, Elliott PJ, Pien C, Fischer TH, Baldwin Jr AS, Nichols TC. Proteasome inhibition ablates activation of NF-κB in myocardial reperfusion and reduces reperfusion injury. American Journal of Physiology-Heart and Circulatory Physiology. 2003 Mar 1;284(3):H919-26.

Qiao H, Ren H, Du H, Zhang M, Xiong X, Lv R. Liraglutide repairs the infarcted heart: The role of the SIRT1/Parkin/mitophagy pathway. Molecular medicine reports. 2018 Jan 2.

Quintana MT, Parry TL, He J, Yates CC, Sidorova TN, Murray KT, Bain JR, Newgard CB, Muehlbauer MJ, Eaton SC, Hishiya A. Cardiomyocyte-specific human Bcl2-associated anthanogene 3 P209L expression induces mitochondrial fragmentation, Bcl2-associated anthanogene 3 haploinsufficiency, and activates p38 signaling. The American journal of pathology. 2016 Aug 1;186(8):1989-2007.

Reaume AG, de Sousa PA, Kulkarni S, Langille BL, Zhu D, Davies TC, Juneja SC, Kidder GM, Rossant J. Cardiac malformation in neonatal mice lacking connexin43. Science. 1995 Mar 24;267(5205):1831-4.

Rodríguez-Mora S, Mateos E, Moran M, Martín MÁ, López JA, Calvo E, Terrón MC, Luque D, Muriaux D, Alcamí J, Coiras M. Intracellular expression of Tat alters mitochondrial functions in T cells: a potential mechanism to understand mitochondrial damage during HIV-1 replication. Retrovirology. 2015 Dec;12(1):78.

Rodríguez AE, López-Crisosto C, Peña-Oyarzún D, Salas D, Parra V, Quiroga C, Morawe T, Chiong M, Behl C, Lavandero S. BAG3 regulates total MAP1LC3B protein levels through a translational but not transcriptional mechanism. Autophagy. 2016 Feb 1;12(2):287-96.

Rohr S. Role of gap junctions in the propagation of the cardiac action potential. Cardiovascular research. 2004 May 1;62(2):309-22.

Rosati A, Graziano V, De Laurenzi V, Pascale M, Turco MC. BAG3: a multifaceted protein that regulates major cell pathways. Cell death & disease. 2011 Apr;2(4):e141.

Rosca MG, Hoppel CL. Mitochondrial dysfunction in heart failure. Heart failure reviews. 2013 Sep 1;18(5):607-22.

Russell RC, Yuan HX, Guan KL. Autophagy regulation by nutrient signaling. Cell research. 2014 Jan;24(1):42.

Saffitz JE, Laing JG, Yamada KA. Connexin expression and turnover: implications for cardiac excitability. Circulation research. 2000 Apr 14;86(7):723-8.

Sagnier S, Daussy CF, Borel S, Robert-Hebmann V, Faure M, Blanchet FP, Beaumelle B, Biard-Piechaczyk M, Espert L. Autophagy restricts HIV-1 infection by selectively degrading Tat in CD4+ T lymphocytes. Journal of virology. 2015 Jan 1;89(1):615-25.

Sameni R, Clifford GD. A review of fetal ECG signal processing; issues and promising directions. The open pacing, electrophysiology & therapy journal. 2010 Jan 1;3:4.

Schänzer A, Rupp S, Gräf S, Zengeler D, Jux C, Akintürk H, Gulatz L, Mazhari N, Acker T, Van Coster R, Garvalov BK. Dysregulated autophagy in restrictive cardiomyopathy due to Pro209Leu mutation in BAG3. Molecular genetics and metabolism. 2018 Mar 1;123(3):388-99.

Scherz-Shouval R, Elazar Z. ROS, mitochondria and the regulation of autophagy. Trends in cell biology. 2007 Sep 1;17(9):422-7.

Schulz R, Görge PM, Görbe A, Ferdinandy P, Lampe PD, Leybaert L. Connexin 43 is an emerging therapeutic target in ischemia/reperfusion injury, cardioprotection and neuroprotection. Pharmacology & therapeutics. 2015 Sep 1;153:90-106.

Schwartz PJ, Stramba-Badiale M, Crotti L, Pedrazzini M, Besana A, Bosi G, Gabbarini F, Goulene K, Insolia R, Mannarino S, Mosca F. Prevalence of the congenital long-QT syndrome. Circulation. 2009 Nov 3;120(18):1761-7.

Sepuri NB, Angireddy R, Srinivasan S, Guha M, Spear J, Lu B, Anandatheerthavarada HK, Suzuki CK, Avadhani NG. Mitochondrial LON protease-dependent degradation of cytochrome c oxidase subunits under hypoxia and myocardial ischemia. Biochimica et Biophysica Acta (BBA)-Bioenergetics. 2017 Jul 1;1858(7):519-28.

Severs NJ, Coppen SR, Dupont E, Yeh HI, Ko YS, Matsushita T. Gap junction alterations in human cardiac disease. Cardiovascular research. 2004 May 1;62(2):368-77.

Sharp WW, Beiser DG, Fang YH, Han M, Piao L, Varughese J, Archer SL. Inhibition of the Mitochondrial Fission Protein Drp1 Improves Survival in a Murine Cardiac Arrest Model. Critical care medicine. 2015 Feb;43(2):e38.

Sharp WW, Fang YH, Han M, Zhang HJ, Hong Z, Banathy A, Morrow E, Ryan JJ, Archer SL. Dynamin-related protein 1 (Drp1)-mediated diastolic dysfunction in myocardial ischemia-reperfusion injury:

therapeutic benefits of Drp1 inhibition to reduce mitochondrial fission. The FASEB Journal. 2014 Jan 1;28(1):316-26.

Shirakabe A, Zhai P, Ikeda Y, Saito T, Maejima Y, Hsu CP, Nomura M, Egashira K, Levine B, Sadoshima J. Drp1-dependent mitochondrial autophagy plays a protective role against pressure-overload-induced mitochondrial dysfunction and heart failure. Circulation. 2016 Feb 25:CIRCULATIONAHA-115.

Siddall HK, Yellon DM, Ong SB, Mukherjee UA, Burke N, Hall AR, Angelova PR, Ludtmann MH, Deas E, Davidson SM, Mocanu MM. Loss of PINK1 increases the heart's vulnerability to ischemia-reperfusion injury. PloS one. 2013 Apr 29;8(4):e62400.

Singh IN, El-Hage N, Campbell ME, Lutz SE, Knapp PE, Nath A, Hauser KF. Differential involvement of p38 and JNK MAP kinases in HIV-1 Tat and gp120-induced apoptosis and neurite degeneration in striatal neurons. Neuroscience. 2005 Jan 1;135(3):781-90.

Solan JL, Lampe PD. Specific Cx43 phosphorylation events regulate gap junction turnover in vivo. FEBS letters. 2014 Apr 17;588(8):1423-9.

Song M, Gong G, Burelle Y, Gustafsson ÅB, Kitsis RN, Matkovich SJ, Dorn GW. Interdependence of Parkin-mediated mitophagy and mitochondrial fission in adult mouse hearts. Circulation research. 2015 Jun 2:CIRCRESAHA-115.

Song M, Mihara K, Chen Y, Scorrano L, Dorn GW. Mitochondrial fission and fusion factors reciprocally orchestrate mitophagic culling in mouse hearts and cultured fibroblasts. Cell metabolism. 2015 Feb 3;21(2):273-85.

Song M, Chen Y, Gong G, Murphy E, Rabinovitch PS, Dorn GW. Super-Suppression of Mitochondrial Reactive Oxygen Species Signaling Impairs Compensatory Autophagy in Primary Mitophagic CardiomyopathyNovelty and Significance. Circulation research. 2014 Jul 18;115(3):348-53.

Sterky FH, Lee S, Wibom R, Olson L, Larsson NG. Impaired mitochondrial transport and Parkin-independent degeneration of respiratory chain-deficient dopamine neurons in vivo. Proceedings of the National Academy of Sciences. 2011 Aug 2;108(31):12937-42.

Stürner E, Behl C. The role of the multifunctional BAG3 protein in cellular protein quality control and in disease. Frontiers in molecular neuroscience. 2017 Jun 21;10:177.

Su F, Myers VD, Knezevic T, Wang J, Gao E, Madesh M, Tahrir FG, Gupta MK, Gordon J, Rabinowitz J, Ramsey FV. Bcl-2–associated athanogene 3 protects the heart from ischemia/reperfusion injury. JCI insight. 2016 Nov 17;1(19).

Sugamura K, Keaney Jr JF. Reactive oxygen species in cardiovascular disease. Free Radical Biology and Medicine. 2011 Sep 1;51(5):978-92.

Tahrir FG, Shanmughapriya S, Ahooyi TM, Knezevic T, Gupta MK, Kontos CD, McClung JM, Madesh M, Gordon J, Feldman AM, Cheung JY. Dysregulation of Mitochondrial Bioenergetics and Quality Control by HIV-1 Tat in Cardiomyocytes. Journal of cellular physiology. 2018 Feb 1.

Tahrir FG, Knezevic T, Gupta MK, Gordon J, Cheung JY, Feldman AM, Khalili K. Evidence for the role of BAG3 in mitochondrial quality control in cardiomyocytes. Journal of cellular physiology. 2017 Apr 1;232(4):797-805.

Tamaddon HS, Vaidya D, Simon AM, Paul DL, Jalife J, Morley GE. High-resolution optical mapping of the right bundle branch in connexin40 knockout mice reveals slow conduction in the specialized conduction system. Circulation research. 2000 Nov 10;87(10):929-36.

Tian L, Neuber-Hess M, Mewburn J, Dasgupta A, Dunham-Snary K, Wu D, Chen KH, Hong Z, Sharp WW, Kutty S, Archer SL. Ischemia-induced Drp1 and Fis1-mediated mitochondrial fission and right ventricular dysfunction in pulmonary hypertension. Journal of Molecular Medicine. 2017 Apr 1;95(4):381-93.

Tomar D, Dong Z, Shanmughapriya S, Koch DA, Thomas T, Hoffman NE, Timbalia SA, Goldman SJ, Breves SL, Corally DP, Nemani N. MCUR1 is a scaffold factor for the MCU complex function and promotes mitochondrial bioenergetics. Cell reports. 2016 May 24;15(8):1673-85.

Truban D, Hou X, Caulfield TR, Fiesel FC, Springer W. PINK1, parkin, and mitochondrial quality control: what can we learn about Parkinson's disease pathobiology?. Journal of Parkinson's disease. 2017 Jan 1;7(1):13-29.

Tse G, Yeo JM. Conduction abnormalities and ventricular arrhythmogenesis: the roles of sodium channels and gap junctions. IJC Heart & Vasculature. 2015 Dec 7;9:75-82.

Twu C, Liu NQ, Popik W, Bukrinsky M, Sayre J, Roberts J, Rania S, Bramhandam V, Roos KP, MacLellan WR, Fiala M. Cardiomyocytes undergo apoptosis in human immunodeficiency virus cardiomyopathy through mitochondrion-and death receptor-controlled pathways. Proceedings of the National Academy of Sciences. 2002 Oct 29;99(22):14386-91.

Van Grol J, Subauste C, Andrade RM, Fujinaga K, Nelson J, Subauste CS. HIV-1 inhibits autophagy in bystander macrophage/monocytic cells through Src-Akt and STAT3. PloS one. 2010 Jul 22;5(7):e11733.

Vaidya D, Tamaddon HS, Lo CW, Taffet SM, Delmar M, Morley GE, Jalife J. Null mutation of connexin43 causes slow propagation of ventricular activation in the late stages of mouse embryonic development. Circulation research. 2001 Jun 8;88(11):1196-202.

Vincent AE, Grady JP, Rocha MC, Alston CL, Rygiel KA, Barresi R, Taylor RW, Turnbull DM. Mitochondrial dysfunction in myofibrillar myopathy. Neuromuscular Disorders. 2016 Oct 1;26(10):691-701.

Vincow ES, Merrihew G, Thomas RE, Shulman NJ, Beyer RP, MacCoss MJ, Pallanck LJ. The PINK1–Parkin pathway promotes both mitophagy and selective respiratory chain turnover in vivo. Proceedings of the National Academy of Sciences. 2013 Apr 16;110(16):6400-5.

Vives-Bauza C, Zhou C, Huang Y, Cui M, de Vries RL, Kim J, May J, Tocilescu MA, Liu W, Ko HS, Magrané J. PINK1-dependent recruitment of Parkin to mitochondria in mitophagy. Proceedings of the National Academy of Sciences. 2010 Jan 5;107(1):378-83.

Wang H, Song P, Du L, Tian W, Yue W, Liu M, Li D, Wang B, Zhu Y, Cao C, Zhou J. Parkin ubiquitinates Drp1 for proteasome-dependent degradation implication of dysregulated mitochondrial dynamics in parkinson disease. Journal of Biological Chemistry. 2011 Apr 1;286(13):11649-58.

Wang B, Nie J, Wu L, Hu Y, Wen Z, Dong L, Zou MH, Chen C, Wang DW. AMPKα2 Protects Against the Development of Heart Failure by Enhancing Mitophagy via PINK1 Phosphorylation. Circulation research. 2017 Dec 28:CIRCRESAHA-117.

Watanabe Y, Tanaka M. p62/SQSTM1 in autophagic clearance of a non-ubiquitylated substrate. J Cell Sci. 2011 Aug 15;124(16):2692-701.

Wattin M, Gaweda L, Muller P, Baritaud M, Scholtes C, Lozano C, Gieseler K, Kretz-Remy C. Modulation of Protein Quality Control and Proteasome to Autophagy Switch in Immortalized Myoblasts from Duchenne Muscular Dystrophy Patients. International journal of molecular sciences. 2018 Jan 7;19(1):178.

Wild P, Dikic I. Mitochondria get a Parkin'ticket. nature cell biology. 2010 Feb;12(2):104.

Wu P, Yuan X, Li F, Zhang J, Zhu W, Wei M, Li J, Wang X. Myocardial upregulation of cathepsin D by ischemic heart disease promotes autophagic flux and protects against cardiac remodeling and heart failure. Circulation: Heart Failure. 2017 Jul 1;10(7):e004044.

Yoshii SR, Kishi C, Ishihara N, Mizushima N. Parkin mediates proteasome-dependent protein degradation and rupture of the outer mitochondrial membrane. Journal of Biological Chemistry. 2011 Jun 3;286(22):19630-40.

Yuan Y, Zheng Y, Zhang X, Chen Y, Wu X, Wu J, Shen Z, Jiang L, Wang L, Yang W, Luo J. BNIP3L/NIX-mediated mitophagy protects against ischemic brain injury independent of PARK2. Autophagy. 2017 Oct 3;13(10):1754-66.

Zhang W, Siraj S, Zhang R, Chen Q. Mitophagy receptor FUNDC1 regulates mitochondrial homeostasis and protects the heart from I/R injury. Autophagy. 2017 Jun 3;13(6):1080-1.

Zhang H, Liu B, Li T, Zhu Y, Luo G, Jiang Y, Tang F, Jian Z, Xiao Y. AMPK activation serves a critical role in mitochondria quality control via modulating mitophagy in the heart under chronic hypoxia. International journal of molecular medicine. 2018 Jan 1;41(1):69-76.

Zhang W, Ren H, Xu C, Zhu C, Wu H, Liu D, Wang J, Liu L, Li W, Ma Q, Du L. Hypoxic mitophagy regulates mitochondrial quality and platelet activation and determines severity of I/R heart injury. Elife. 2016;5.

Zhang W, Chen C, Wang J, Liu L, He Y, Chen Q. Mitophagy in cardiomyocytes and in platelets: a major mechanism of cardioprotection against ischemia/reperfusion injury. Physiology. 2018 Feb 7;33(2):86-98.

Zhang J, He Z, Xiao W, Na Q, Wu T, Su K, Cui X. Overexpression of BAG3 attenuates hypoxia-induced cardiomyocyte apoptosis by inducing autophagy. Cellular Physiology and Biochemistry. 2016;39(2):491-500.

Zhou H, Zhang Y, Hu S, Shi C, Zhu P, Ma Q, Jin Q, Cao F, Tian F, Chen Y. Melatonin protects cardiac microvasculature against ischemia/reperfusion injury via suppression of mitochondrial fission-VDAC1-HK2-mPTP-mitophagy axis. Journal of pineal research. 2017 Aug 1.

Zhou H, Li D, Zhu P, Hu S, Hu N, Ma S, Zhang Y, Han T, Ren J, Cao F, Chen Y. Melatonin suppresses platelet activation and function against cardiac ischemia/reperfusion injury via PPARγ/FUNDC1/mitophagy pathways. Journal of pineal research. 2017 Nov 1.

Zhou JZ, Jiang JX. Gap junction and hemichannel-independent actions of connexins on cell and tissue functions–An update. FEBS letters. 2014 Apr 17;588(8):1186-92.

Zhou H, Zhu P, Guo J, Hu N, Wang S, Li D, Hu S, Ren J, Cao F, Chen Y. Ripk3 induces mitochondrial apoptosis via inhibition of FUNDC1 mitophagy in cardiac IR injury. Redox biology. 2017 Oct 1;13:498-507.